

Regulation and enzymatic properties of renal cytochrome P450 isoforms

Dissertation

zur Erlangung des akademischen Grades des
Doktors der Naturwissenschaften (Dr.rer.nat)

eingereicht im
Fachbereich Biologie, Chemie, Pharmazie
der Freien Universität Berlin

vorgelegt von

Marija Marković
aus Belgrad

August, 2007

*1. Gutachter: Prof. Dr. Volker A. Erdmann,
Institute for Chemistry / Biochemistry, Free University,
Berlin*

*2. Gutachter: Prof. Dr.Dr. Santosh Nigam,
Charité – University Medical Center Berlin, Campus Benjamin
Franklin*

Defence took place in Berlin on 18.11.2008

Acknowledgements

It was a long way from the point I started my PhD studies till now and there were a lot of people who kindly helped me with their experimental experience and personal advice. Here I would like to thank all of them.

First of all, I am very grateful to Prof. Nigam for giving me the opportunity to do my Ph.D. studies in his group and in the group of his collaborative partner, Dr. Schunck, MDC Berlin. I would like to thank Dr. Schunck for introducing me into the world of cytochrome P450 enzymes and his co-workers for collaboration and help. Moreover, special thanks also to Prof. Luft and Dr. Müller for the fruitful collaboration in the animal experiments. Last but not least, I am very grateful to Prof. Erdmann for being the first referent for defending my thesis at the Faculty for Biology, Chemistry and Pharmacy of the Free University, Berlin.

I would also like to take this occasion to thank all the other colleagues who accompanied my studies with their specific advice and technical help. In particular, personal thanks go to Eduardo, Cosima, Micha, Christel and Ramona. For me it was also especially important that all of them were very patient and helpful in my never-ending process of learning german.

I would not be here where I am now without help of my parents. They enabled my education, and together with my brother and sister encouraged me and supported me when it was the toughest. I am very happy that I can thank (in alphabetical order) Aleksandra, Branislav, Darko, Jasmina, Jeca, Jelena, Maja, Milka, Nevena and Smiljana for being my friends. At the end I want thank Christoph for being at the right time at the right place.

Table of contents

Summary	V
Zusammenfassung	VIII
Abbreviations	XI
1. Introduction	1
1.1 Cytochrome P450 enzymes	1
1.1.1. Function and mechanism of CYP catalyzed reactions.....	1
1.1.2 Distribution of CYPs and their substrate specificity.....	3
1.1.3 CYP-dependent AA metabolism	4
1.1.4 CYP2C-dependent biosynthesis of EETs	7
1.1.4.1 Human CYP2C isoforms	8
1.1.4.2 Rat CYP2C isoforms	10
1.1.5 CYP4A/4F dependent biosynthesis of HETEs.....	11
1.1.5.1 Human CYP4A/4F isoforms.....	11
1.1.5.2 Rat CYP4A isoforms	12
1.1.5.3 Mouse Cyp4a isoforms.....	12
1.1.6 Biological activities of EETs and HETEs	13
1.1.7 Alterations in CYP-dependent AA metabolism in animal models of hypertension.....	15
1.2 ω -3 polyunsaturated fatty acids	19
1.2.1 ω -3 and ω -6 fatty acids as essential nutrients.....	19
1.2.2 ω -3 fatty acids as bioactive mediators.....	22
1.2.2.1 Beneficial effects of fish oil fatty acids	22
1.2.2.2 Possible ways of actions of fish oil fatty acids.....	23
1.3. Objectives and specific aims	24
2. Material and methods	26
2.1. Cloning of CYPs and preparation of recombinant baculovirus	26
2.1.1 Cloning of CYP cDNAs into the donor plasmid pFASTBac I.....	26
2.1.2 Preparation of recombinant bacmids	30
2.1.2.1 Generation of recombinant bacmids in <i>E. coli</i> DH10Bac	30
2.1.2.2 Isolation and preparation of recombinant bacmids.....	31

2.1.2.3 Analysis of recombinant bacmid.....	32
2.1.2.4 Transfection of insect cells.....	33
2.1.2.5 Harvesting and amplification of recombinant baculovirus	34
2.2 Heterologous expression of CYP enzymes in the baculovirus / Sf9 insect cell system.....	35
2.2.1 Culturing of insect Sf9 cells	35
2.2.2 Expression of CYP Sf9-insect cells	35
2.2.3 Co-expression of CYP and hCPR enzymes in Sf9-insect cells.....	36
2.2.4 Determination of CYP concentration.....	36
2.2.5 NADPH-CYP reductase activity determination.....	37
2.2.6 Sf9 microsomes preparation	38
2.2.7 Determination of protein concentration	39
2.2.8 Western blot analysis	39
2.3 Metabolism of fatty acids by recombinant CYP enzymes	42
2.3.1 CYP-dependent metabolism of fatty acids	42
2.3.2 RP-HPLC separation of CYP-dependent AA, EPA, DPA and DHA metabolites	43
2.3.3 Separation of EPA, DPA and DHA epoxy-regioisomers by NP-HPLC.....	44
2.3.4 Separation of 17,18-EETeTr enantiomers by chiral HPLC	44
2.4. Experiments with hypertensive rats	45
2.4.1 Experimental animals	45
2.4.2 Renal microsomal preparation	45
2.4.3 Renal microsomal metabolism.....	46
2.4.4 Statistical analysis	46
3. Results.....	47
3.1 Regulation of renal AA-metabolism in a rat model of angiotensin II- induced hypertension and end-organ damage.....	47
3.1.1 Effects of fenofibrate on mortality, blood pressure and renal damage	47
3.1.2 Effects of fenofibrate on CYP-dependent AA metabolism under pathological conditions.....	49
3.1.2.1 Fenofibrate treatment strongly increases renal AA-epoxygenase but no AA-hydroxylase activity in dTGR.....	49

3.1.2.2. <i>CYP2C23 is the major AA-epoxygenase in the kidney of dTGR and fenofibrate-treated dTGR</i>	52
3.1.2.3 <i>Renal protein expression of CYP2C23 is increased by fenofibrate treatment</i>	53
3.1.3 <i>Effects of fenofibrate on CYP dependent AA metabolism under physiological conditions</i>	55
3.1.4 <i>Effect of fenofibrate on the generation of secondary AA metabolites</i>	57
3.1.4.1 <i>Fenofibrate strongly induces secondary product formation</i>	57
3.1.4.2 <i>HEET production from both 20-HETE and 11,12-EET is strongly induced by fenofibrate treatment</i>	60
3.2 <i>Heterologous expression of CYP enzymes</i>	62
3.2.1 <i>Recombinant baculovirus</i>	62
3.2.2 <i>Expression of selected CYP isoforms in Sf-9 cells</i>	64
3.3. <i>CYP-dependent formation of secondary AA metabolites, HEETs</i>	67
3.3.1 <i>CYP2C23-dependent formation of HEET in renal microsomes</i>	67
3.3.2 <i>Metabolism of EETs and 20-HETE by recombinant CYP isoforms</i>	70
3.4 <i>CYP-dependent metabolism of ω-3 fatty acids</i>	73
3.4.1 <i>Resolution and identification of epoxy- and hydroxy- derivatives of EPA, DPA and DHA</i>	74
3.4.2 <i>Metabolism of ω-3 fatty acids by mouse, rat and human renal microsomes and human liver microsomes</i>	77
3.4.3 <i>Metabolism of ω-3 fatty acids by recombinant epoxygenases</i>	80
3.4.3.1 <i>Comparison of enzymatic activities towards AA, EPA, DPA and DHA</i> 81	
3.4.3.2 <i>CYP2C isoform-specific metabolite patterns</i>	82
3.4.4 <i>Metabolism of ω-3 fatty acids by recombinant hydroxylases</i>	92
3.4.4.1 <i>Comparison of enzymatic activities towards AA, EPA, DPA and DHA</i> 92	
3.4.4.2 <i>CYP4A/4F isoform-specific metabolite patterns</i>	94
4. Discussion	103
4.1 <i>CYP-dependent EET/HEET-formation as a novel target for the treatment of high blood pressure</i>	103
4.1.1. <i>Downregulation of EET/HEET formation in animal models of hypertension</i>	105
4.1.2 <i>Increased EET hydrolysis in animal models of hypertension</i>	107

4.2 Regulation of EET formation by PPAR α agonists	108
4.2.1 Effect of fenofibrate in different animal models	108
4.2.2 Effect of fenofibrate in dTGR.....	110
4.2.2.1 Effect of fenofibrate on inflammation and end-organ damage in dTGR.....	110
4.2.2.2 Mechanisms of fenofibrate-induced prevention of inflammation in dTGR.....	110
4.2.2.3 Effect of fenofibrate on renal EET formation in dTGR.....	112
4.2.3 CYP-dependent AA-metabolites as endogenous PPAR α activators	116
4.2.4 Hypothesis on the mechanism of fenofibrate action on high blood pressure and end-organ damage	119
4.3. ω -3 fatty acids as an alternative source for CYP-dependent eicosanoids.....	121
4.3.1. CYP-dependent metabolism of ω -3 fatty acids	121
4.3.2. Profile of CYP-dependent ω -3 metabolites.....	124
4.3.3 Stereospecificity of individual CYP isoforms in 17,18-double bond epoxidation.....	126
4.3.4 Potential biological significance of CYP-dependent ω -3 metabolites	128
4.4 Perspectives	131
5. Bibliography.....	133
6. List of publications, awards and conferences.....	153
7. Curriculum vitae	155
8. Eidesstattliche Erklärung	156

Summary

Background

Cytochrome P450 (CYP)-dependent arachidonic acid (AA) metabolism is increasingly recognized to play an important role in the regulation of renal vascular and tubular function. The primary metabolites involve 20-hydroxyeicosatetraenoic acid (20-HETE) and a series of regioisomeric epoxyeicosatrienoic acids (EETs). 20-HETE is produced by CYP4A and CYP4F and EETs by CYP2C and CYP2J isoforms. EETS can be further converted by CYP4A-catalyzed hydroxylation to hydroxy-epoxyeicosatrienoic acids (HEETs). Providing a starting point for the present study, it was found that the CYP-dependent renal AA metabolism to EETs and HEETs is strongly downregulated in a rat model of angiotensin II (ANG II)-induced hypertension and inflammatory end-organ damage.

Objectives:

This study is part of a long-term project aimed at elucidating new possibilities for the treatment of hypertension and end-organ damage by directly influencing the renal CYP-dependent AA metabolism. The specific aims were as follows:

- (i) to test the effect of the PPAR α activator fenofibrate on the recovery of renal CYP-dependent EET and HEET production in a rat model of ANG II-induced hypertension and end-organ damage
- (ii) to analyze the CYP-dependent metabolism of fish oil ω -3 polyunsaturated fatty acids (ω -3 PUFAs), such as eicosapentaenoic acid (EPA) and docosahexaenoic acid (DHA), as a source of alternative physiologically active eicosanoids.

Results

A. Regulation of renal CYP-dependent EET/HEET production by fenofibrate

1. Double transgenic rats overexpressing human renin and angiotensinogen (dTGR) and Sprague-Dawley (SD) control rats were treated for three weeks with fenofibrate. Fenofibrate treatment normalized blood pressure and kidney function and resulted in:

- a significant increase in renal microsomal EET production: 2.2 fold for dTGR-Fenofibrate vs. untreated dTGR, and 2.5–fold for SD-Fenofibrate vs. untreated SD.

-
- a significant increase in renal microsomal HEET production: 6-fold in dTGR and 3,5-fold in SD rats.
2. CYP2C23 was identified as the predominant renal AA epoxygenase in dTGR and SD rats. CYP2C23 protein expression was strongly induced by Fenofibrate under both pathological and physiological conditions.
 3. A novel pathway of HEET formation was discovered. Rat renal microsomes produced HEETs predominantly via CYP2C23-catalyzed epoxidation of 20-HETE and only to a minor extent by the formerly known CYP4A-catalyzed EET hydroxylation.

B. Omega-6 and Omega-3 Fatty Acids as Substrates for Cytochrome P450 Enzymes

1. Enzymatically active CYP isoforms were produced in a baculovirus/insect cell system. The CYP isoforms analyzed included the major AA hydroxylases from human (CYP4A11 and CYP4F2), and mouse (Cyp4a12a and Cyp4a12b) as well as the AA epoxygenases from human (CYP2C8 and CYP2C9), and rat (CYP2C11 and CYP2C23).
2. The recombinant CYP enzymes converted EPA, DHA and DPA (docosapentaenoic acid) with catalytic efficiencies almost equal or even higher compared to AA.
3. The CYP4A and CYP4F enzymes, which preferentially function as AA ω -hydroxylases, showed a less strict regioselectivity with the ω -3-PUFAs and additionally epoxidized the ω -3 double bond. For example, CYP4A11 displayed a ratio of ω : (ω -1) hydroxylation of 85: 15 with AA, 31: 69 with EPA and 50: 50 with DHA.
4. The CYP2C enzymes produced isoform-specific patterns of regioisomeric epoxy-derivatives from EPA, DPA and DHA. Moreover the regiospecificity was substrate-dependent. For example, CYP2C23 epoxidized AA preferentially at the 11,12-, EPA at the 17,18-, DPA at the 10,11- and DHA at 10,11- and 19,20-double bonds.
5. All epoxygenases except CYP2C9 preferentially attacked the ω -3 double bonds of EPA and DHA. Chiral-phase HPLC revealed that each CYP isoforms has a distinct stereoselectivity when epoxidizing the 17,18-double bond of EPA.

Conclusions

The present study shows that treatments with PPAR α activators and with ω -3 PUFAs may represent promising approaches to influence the CYP-dependent renal

AA metabolism under physiological and pathological conditions. The PPAR α activator fenofibrate acts as a strong inducer of CYP2C23-catalyzed EET and HEET generation and protects against ANG II-induced hypertension and renal damage. These results suggest that CYP-dependent EET/HEET production may serve as an anti-inflammatory control mechanism. The second part of the studies demonstrates that EPA, DHA and DPA are efficient alternative substrates of major AA metabolizing CYP isoforms. Therefore, diets rich in ω -3 PUFAs can be expected to significantly modulate the production of physiologically active metabolites by CYP enzymes in various tissues and organs. This shift in CYP-dependent eicosanoid formation may play an important role in mediating the beneficial cardiovascular effects of ω -3 PUFAs.

Zusammenfassung

Hintergrund

Der Cytochrom P450 (CYP)-abhängiger Arachidonsäure (AA) Metabolismus wird zunehmend als wichtiger Bestandteil der Regulation renaler Gefäß- und Tubulusfunktionen wahrgenommen. Primärmetabolite sind 20-Hydroxyeikosatetraensäure (20-HETE) und eine Reihe regioisomerer Epoxyeikosatriensäuren (EETs). 20-HETE wird von CYP4A und CYP4F und EETs von CYP2C und CYP2J Isoformen gebildet. EETs können von den CYP4A Isoformen weiter zu Hydroxy-Epoxyeikosatriensäuren (HEETs) hydroxyliert werden. Ausgangspunkt für diese Studie war die Erkenntnis, dass in der Niere eines Rattenmodell mit Angiotensin II (ANG II)-induziertem Bluthochdruck und endzündlichem Endorganschaden der CYP-abhängige AA-Metabolismus zu EETs und HEETs stark herunter reguliert ist.

Zielsetzung

Diese Studie ist Teil eines Langzeitprojektes zur Entwicklung neuer Möglichkeiten der Behandlung von Bluthochdruck und Endorganschäden durch direkte Beeinflussung des CYP-abhängige AA-Metabolismus in der Niere. Die spezifischen Ziele waren folgende:

- (i) Klärung des Effektes des PPAR α Aktivators Fenofibrat auf die Erholung der CYP-abhängigen EET und HEET Bildung im Rattenmodell mit ANG II-induziertem Bluthochdruck und endzündlichem Endorganschaden
- (ii) Analyse des CYP-abhängigen Metabolismus von ω -3 mehrfachungesättigten Fettsäuren (ω -3 PUFAs) aus Fischöl, wie beispielsweise Eikosapentaensäure (EPA) und Docosahexaensäure (DHA), als Quelle alternativer physiologisch aktiver Eikosanoide.

Ergebnisse

A. Regulation der renalen CYP-abhängigen EET und HEET Bildung durch Fenofibrat

1. Doppelt-transgene Ratten mit einer Überexpression des humanen Renin und Angiotensinogen (dTGR) und Sprague-Dawley (SD) Kontrollratten wurden

für drei Wochen mit Fenofibrat behandelt. Die Fenofibrat Behandlung hatte eine Normalisierung von Blutdruck und Nierenfunktion zur Folge und führte zu:

- einen signifikanten Anstieg der renalen mikrosomalen EET Produktion: 2,2 fach für dTGR-Fenofibrat vs. unbehandelte dTGR und 2,5 fach für SD-Fenofibrat vs. untreated SD
 - einen signifikanten Anstieg in renaler mikrosomaler HEET Produktion: 6 fach in dTGR und 3,5 fach in SD Ratten.
2. CYP2C23 wurde als vorherrschende renale AA Epoxygenase in dTGR und SD Ratten identifiziert. Die CYP2C23 Protein Expression wurde durch Fenofibrat Behandlung stark induziert, sowohl unter pathologischen als auch unter physiologischen Bedingungen.
 3. Ein neuer Weg der HEET Bildung wurde entdeckt. Rattennierenmikrosomen bilden HEETs hauptsächlich über CYP2C23 katalysierte Epoxydation von 20-HETE und nur zu einem geringen Teil über die bereits bekannte CYP4A-katalysierte EET Hydroxylierung.

B. Omega-6 und Omega-3 Fettsäuren als Substrate für Cytochrom P450

Enzyme

1. Enzymatisch aktive CYP Isoformen wurden in einem Baculovirus/Insektenzellsystem hergestellt. Die analysierten CYP-Isoformen beinhalteten die wichtigsten AA Hydroxylasen des Menschen (CYP4A11 und CYP4F2) und der Maus (Cyp4a12a und Cyp4a12b), sowie die AA Epoxygenasen des Menschen (CYP2C8 und CYP2C9) und der Ratte (CYP2C11 und CYP2C23).
2. Die rekombinanten CYP Enzyme wandelten EPA, DHA und DPA (Docosapentaensäure) mit vergleichbarer oder sogar höherer katalytischer Effizienz als AA um.
3. Die CYP4A und CYP4F Enzyme, die vorrangig als AA Hydroxylasen fungieren, zeigten eine weniger strikte Regioselektivität mit ω -3 PUFAs und epoxidierten zusätzlich die ω -3 Doppelbindung. Zum Beispiel zeigte CYP4A11 ein ω : (ω -1) Hydroxylierungsverhältnis von 85: 15 bei AA, 31: 69 bei EPA und 50: 50 bei DHA.

-
4. Die CYP2C Enzyme produzierten Isoform-spezifische Muster regioisomerer Epoxyderivate von EPA, DPA und DHA. Zudem war die Regiospezifität substratabhängig. Zum Beispiel epoxydierte CYP2C23 bei AA vorrangig die 11,12-, bei EPA die 17,18-, DPA und die 10,11- und bei DHA die 10,11- und die 19,20-Doppelbindung.
 5. Alle Epoxygenasen außer CYP2C9 griffen vorrangig an der ω -3 Doppelbindung von EPA und DHA an. Chiral-Phasen HPLC zeigte, dass jede CYP Isoform eine deutliche Stereoselektivität bei der Epoxydation der 17,18-Doppelbindung von EPA hatte.

Schlußfolgerung

Die vorliegende Studie zeigt, dass eine Behandlung mit PPAR α Aktivatoren und mit ω -3 PUFAs ein vielversprechenden Ansatz zur Beeinflussung des CYP-abhängigen renalen AA-Metabolismus unter physiologischen und pathologischen Bedingungen sein könnte. Der PPAR α Aktivator Fenofibrat induziert die CYP2C23-katalysierte EET und HEET Bildung stark und schützt vor ANG II-induziertem Bluthochdruck und Endorganschaden. Diese Ergebnisse weisen darauf hin, dass die CYP-abhängige EET/HEET Produktion als antiinflammatorischer Kontrollmechanismus dienen könnte. Der zweite Teil der Studie zeigt, dass EPA, DHA und DPA effiziente Substrate für die hauptsächlich AA metabolisierenden CYP Isoformen sind. Daher kann man erwarten, dass Diäten, die reich an ω -3 PUFAs sind, die Produktion physiologisch aktiver Metabolite durch CYP Enzyme in verschiedensten Geweben und Organen signifikant verändern. Diese Veränderung der CYP-abhängigen Eikosanoïdbildung könnte eine wichtige Rolle in der Vermittlung der heilsamen kardiovaskkulären Effekte von ω -3 PUFAs spielen.

Abbreviations

- 20-HETE → 20-hydroxyeicosatetraenoic acid
ACh → acetylcholine
ANG I → angiotensin I
ANG II → angiotensin II
AOPEN → angiotensinogen
APS → ammoniumperoxydisulfat
BK channel → large conductance Ca^{2+} -activated K^+ channel
COX → Cyclooxygenases
CPR → NADPH-dependent cytochrome P450 reductase
CYP → Cytochrome P450
DAG → diacylglycerol
DART1 → Diet and Reinfarction trial
DHA → docosahexaenoic acid
DPA → docosapentaenoic acid
DR rats → Dahl salt resistant
DS rats → Dahl salt sensitive rats
DHET → dihydroxy-EETs
DOCA → desoxycorticosterone acetate
dTGR → Double transgenic rats overexpressing human renin and angiotensinogen
EETs → epoxyeicosatrienoic acids
EETeTr → epoxyeicosatetraenoic acids
EDHF → Endothelium Derived Hyperpolarizing Factor
EDP → epoxydocosapentaenoic acids
EDTeTr → epoxydocosatetraenoic acids
ENaC → epithelial Na channels
EPA → eicosapentaenoic acid
eSH → epoxide hydrolase
hAOPEN → human angiotensinogen
HDHETs → hydroxy-dihydroxy-eicosatrienoic acid
HEETs → hydroxy-epoxyeicosatrienoic acids
HEPEs → hydroxyeicosapentaenoic acids

HF → High fat
HPLC → High Performance Liquid Chromatography
hREN → human renin
IP₃ → inositol-1,4,5-triphosphate
LOX → lipoxygenases
methyrapone → 2-methyl-1,2-di-3-pyridyl-1-propanon
ω-3 PUFAs → ω-3 polyunsaturated fatty acids
NP-HPLC → Normal Phase High Performance Liquid Chromatography
PIP₂ → phosphatidyl-1d-myo-inositol-(4,5)-diphosphate
PLA₂ → phospholipase A₂
PLC → phospholipase C
PMSF → phenylmethylsulfonyl fluoride
PT → proximal tubules
PPAR → peroxisome proliferator activated receptor
PUFA → polyunsaturated fatty acid
RAS → renin–angiotensin system
RXR → retinoid X receptor
RP-HPLC → reverse phase HPLC
R_t → retention time
SD → Sprague-Dawley rats
SDS-PAGE → SDS-Polyacrylamide-Gel-Electrophoresis
SHR rats → spontaneously hypertensive rats
TALH → Thick Ascending limb of loop of Henle
TEMED → N, N, N', N'-tetra-methylethyldiamine
VSMC → vascular smooth muscle cell
WKY rats → Wistar-Kyoto rats

1. Introduction

1.1 Cytochrome P450 enzymes

1.1.1. Function and mechanism of CYP catalyzed reactions

Cytochromes P450 (CYP) constitute a superfamily of enzymes with unique spectral and catalytic properties (Capdevila et al., 2000). They are:

- heme-thiolate proteins which show a characteristic absorption maximum at 450 nm after binding carbon monoxide to the reduced heme iron (Omura and Sato, 1964)
- components of monooxygenase systems that are involved in the oxidative metabolism of numerous physiological and xenobiotic compounds (Guengerich, 1993; Capdevila et al., 1993, Nelson et al., 1996).

CYP enzymes activate molecular oxygen and deliver an active form of atomic oxygen to the substrate, while the remainder is reduced to water.



The electrons required for this reaction are transferred from NADPH or NADH to CYP heme iron. In most of eukaryota, CYPs are integrated into the endoplasmatic reticulum membrane and they receive electrons from an NADPH-dependent cytochrome P450 reductase (CPR) (Sato and Omura, 1978). CPR contains two prosthetic groups: FAD and FMN (Figure 1.1).

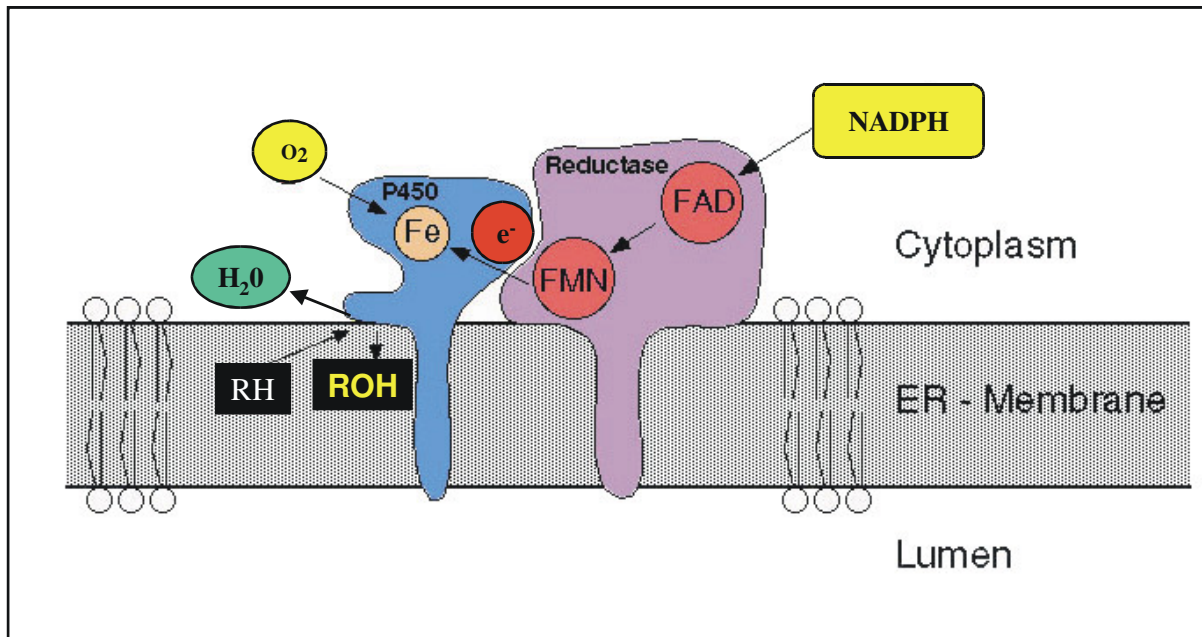


Figure 1.1 Schematic structure of a mammalian microsomal cytochrome P450 system. CYP enzymes and CPR reductase are proteins bound to membrane of endoplasmic reticulum. CYP contains heme and CPR reductase contains FAD and FMN as prosthetic groups. CPR reductase transfers electrons from electron donor to CYP enzyme. Reduced CYP enzyme activates molecular oxygen and transfers one oxygen atom to the substrate. Result of the reaction is oxidized substrate and one molecule of water.

CYP-dependent substrate conversion occurs in 7 steps (Figure 1.2):

1. Binding of the substrate (RH) to CYP which is in oxidized state (Fe^{3+})
2. Transfer of the first electron from the CPR to the heme iron (Fe^{3+}) which reduces it to (Fe^{2+})
3. Binding of molecular oxygen to the reduced heme iron (Fe^{2+}) and production of an superoxide anion (O_2^-)
4. Transfer of the second electron to the CYP and production of a peroxide (O_2^{2-})
5. Peroxide (O_2^{2-}) releases one oxygen atom, which binds protons and yields H_2O
6. The remaining activated oxygen atom is transferred to the substrate, which yields oxidized substrate (ROH)
7. Oxidized substrate is released from the CYP active center. Enzyme returns to the oxidized state, ready to react again (Fe^{3+}).

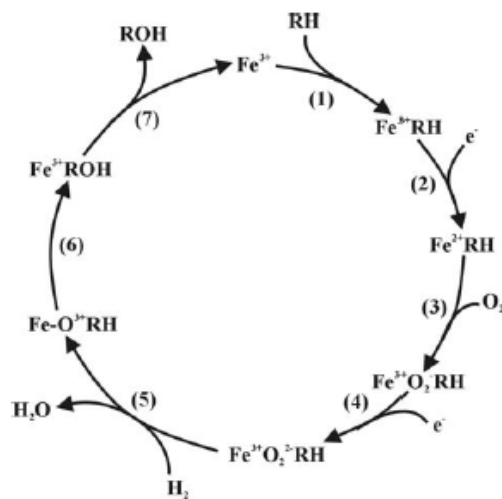


Figure 1.2 Mechanism of CYP-dependent monooxygenase reaction (Lewis, 1996).

1.1.2 Distribution of CYPs and their substrate specificity

CYPs are ubiquitous proteins widely distributed in plants and animals. They are expressed in all mammalian cell types so far investigated. In mammals, nature and distribution of CYP isoforms is species-specific and age-, sex- and organ-dependent. For example in rodents, CYP1A1 is expressed very early in development, whereas most other enzymes either appear near birth (CYP2B, CYP2C23, and CYP3A) or between 2 and 4 weeks following birth (CYP2A, CYP2C6, CYP2C7, CYP2C11, CYP2C12, and CYP4A10). There are also examples of an expression in sex-dependent manner (CYP2A, CYP2C11, CYP2C12, CYP3A, and CYP4A10); Rich and Boobis, 1997.

There are more than 2500 described CYP enzymes grouped into families and subfamilies considering sequences homology. CYPs belong to the same family if they have more than 40 % sequence homologies. In order to classify CYP isoforms in the same subfamily, they have to have more than 55 % sequence homologies (Nelson, 2003).

Although firstly described as “hepatic drug detoxification system“, it is now known that, in addition to drugs and xenobiotics, CYP can also metabolize endogenous substrates (Mitani, 1979; Kadis, 1978). CYPs are involved in the metabolism of various xenobiotic and endogenous substances:

-
- Arachidonic acid metabolism and eicosanoid biosynthesis
 - Cholesterol, sterol and bile acid biosynthesis
 - Steroid synthesis and catabolism
 - Vitamin D3 synthesis and catabolism
 - Retinoic acid hydroxylation
 - Biogenic amine and neuroamine metabolism
 - Metabolism of procarcinogenic substances
 - Metabolism of pharmaceuticals
 - Metabolism of foreign chemicals and pollutants.

These enzymes have a variety of gene regulatory mechanisms. Many of them can be induced by hormonal signals. One example is the induction by steroid hormones, which are under strict endocrine control (ACTH). Another possible way of regulation is via peroxisome proliferators like clofibrate. These drugs bind to PPAR (peroxisome proliferator activated receptor), and then migrate further to the nucleus, heterodimerizes with RXR (retinoid X receptor) and bind to gene promoter and activate transcription of the CYP4A family (Johnson et al., 1996). Aromatic hydrocarbons can also induce CYPs (for example CYP1 family). Aromatic hydrocarbons bind to the Ah receptor (Ah-aryl hydrocarbon). In order to reach the nucleus and activate gene transcription, the Ah receptor nuclear translocator is necessary. These two proteins together bind to the DNA and activate transcription (Rushmore and Kong, 2002). Chemicals like ethanol (CYP2E) or barbiturates (CYP2B) can also induce CYPs. Phenobarbital induces rat CYP2B enzymes through phenobarbital receptor called CAR, which dimerizes with RXR and bind to gene promoter. The inducibility of many CYPs is probably related to their role in detoxification (Nelson, 2003).

1.1.3 CYP-dependent AA metabolism

Arachidonic acid is a polyunsaturated fatty acid (PUFA) containing 20-carbon atoms and 4 cis-double bonds. The last double bond starts at the 6th C-atom counted from the methyl end of the chain (termed the *ω-end*). Mammals are not able to synthesize the *ω*-6 fatty acids and therefore AA and its precursor, linoleic acid (18:

2), are essential fatty acids. In vivo, AA is esterified at the sn2-position of cell membrane glycerophospholipids. Release of AA into intracellular medium is under control of extracellular signals such as bradykinin, angiotensin II, noradrenalin or endothelin. These agonists activate phospholipase C (PLC), which hydrolyses 1-phosphatidyl-1d-myo-inositol-(4,5)-diphosphate (PIP₂) to inositol-1,4,5-triphosphate (IP3) and diacylglycerol (DAG). IP3 releases intracellular Ca⁺⁺ which activates cytosolic phospholipase A2 (PLA₂), a lipase that is responsible for AA release from phospholipids in many cell types. AA can also be released from DAG by action of DAG-lipase.

Free AA released from phospholipid pools is available for oxidative metabolism by 3 different enzyme systems (Figure 1.3):

- **Cyclooxygenases (COX)** metabolize AA to prostaglandine endoperoxide PGH₂, which is further converted to prostaglandins, thromboxanes and prostacyclin
- **Lipoxygenases (LOX)** convert AA to hydroperoxy intermediates, which are precursors for leukotriens, HETEs and lipoxins
- **Cytochrome P450** metabolizes AA by 3 different types of reactions:
 - *Olefin epoxidation* results in the production of four cis-epoxyeicosatrienoic acids (14,15-, 11,12-, 8,9-, and 5,6-EET) which can be formed as R, S or S, R enantiomer (Figure 1.4)
 - *ω-terminal hydroxylation* forms C16-C20 alcohols of AA (16-, 17-, 18, 19-, 20-hydroxyeicosatetraenoic acids-HETEs) Figure 1.4.
 - *Allylic oxidation* forms several midchain conjugated dienols (5-, 8-, 9-, 11-, 12-, and 15-HETE).

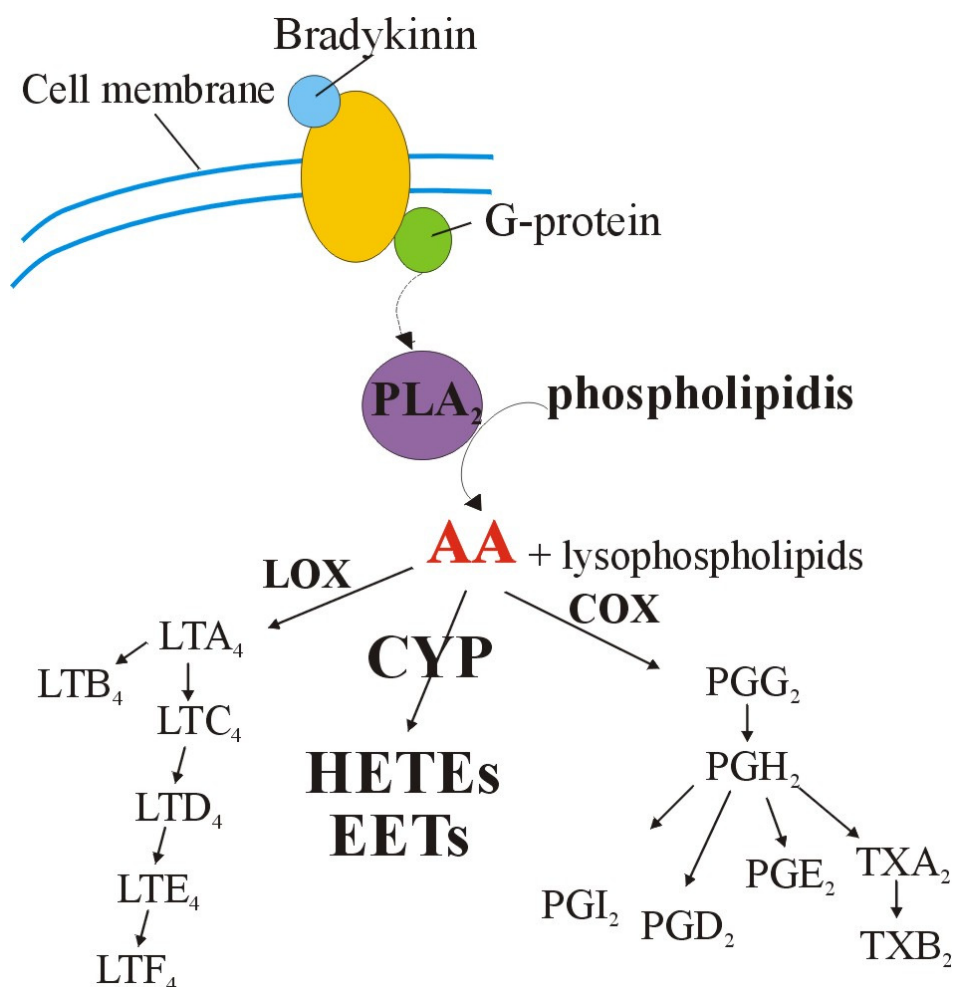


Figure 1.3 Metabolism of AA. Free AA can be metabolized by COX, LOX and CYP enzymes after extracellular signal-induced release from membrane phospholipid pools. Bradykinin is used as an example for extracellular stimuli activating phospholipases after binding to their G-protein coupled receptors.

Members of CYP2C and 2J subfamilies are the major AA epoxygenases, which convert AA to EETs, metabolites with one epoxidized double bond. EETs can be further converted to dihydroxy-EETs (DHET) by soluble epoxyde hydrolase. CYP4A and CYP4F subfamily members represent major AA hydroxylases and produce 19/20-HETE as main products (Figure 1.4).

In the 1970s, scientific attention was focused on role of CYP enzymes in drug and xenobiotic metabolism. First, however, still indirect evidence for role of CYPs in AA metabolism was provided in 1976 by a report showing that CYP inhibitors block AA-induced human platelet aggregation (Cinti and Feinstein, 1976). Five years later, Capdevila and coworkers reported that microsomal fractions and

reconstituted CYP systems catalyze AA oxidation to products chromatographically distinct from prostanoids (Capdevila et al., 1981).

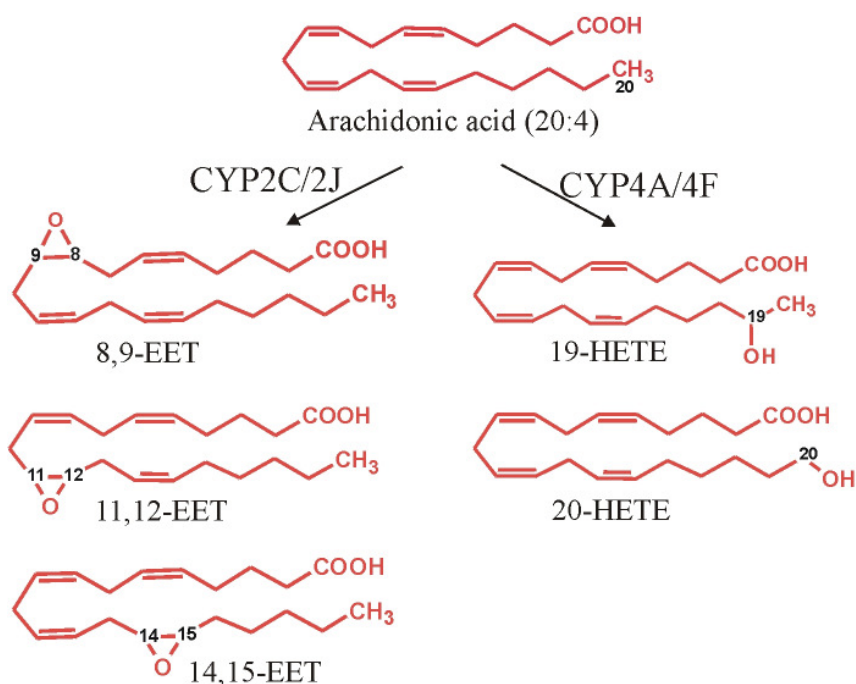


Figure 1.4 Structural formulas of AA and its most important CYP-dependent metabolites. AA can be epoxidized by CYP2C and CYP2J subfamily members to 4 possible regioisomeric EETs, 5,6-; 8,9-; 11,12- and 14,15-EET. Isoforms of the CYP4A and CYP4F subfamilies can hydroxylate AA to 19- and 20-HETE.

After establishing EETs as endogenous constituents of organs such as liver, kidney, lung, human and rat plasma and urine as well as demonstration of their potent biological activities (Capdevila et al., 1983, Capdevila et al., 2000), CYP-dependent AA metabolism attracted considerable interest, in particular, in the cardiovascular field.

1.1.4 CYP2C-dependent biosynthesis of EETs

Members of CYP2C and CYP2J subfamilies are described as AA-epoxygenases. Identified isoforms of these two subfamilies include rat 2C11, 2C13, 2C23 and 2C24; rabbit 2C1 and 2C2; mouse 2c29, 2c37, 2c38, 2c39, 2c40 and 2c44; human 2C8, 2C9, 2C19 and 2J2. Low amounts of EETs are also produced by 1A1, 1A2 and 2E1, which however preferentially act as AA-hydroxylases (Roman, 2002).

Each CYP isoform shows a specific regio- and stereospecificity. EET distribution is organ specific and depends on the set of CYP isoforms expressed in the given organ. For example, rat hypothalamic microsomes form 5,6-EET as the major product (Capdevila et al., 1983), but rat liver and kidney microsomes form 11,12-EET as the predominant regioisomer (Imaoka et al., 1993).

1.1.4.1 Human CYP2C isoforms

There are four human CYP2C isoforms: CYP2C8, CYP2C9, CYP2C18, and CYP2C19 (Goldstein, 2001). They were firstly described as very efficient drug and xenobiotics metabolizing enzymes. For example, CYP2C9 is responsible for the metabolism of about 100 drugs, representing about 20 % of all drugs in clinical use (Kirchheiner et al., 2005). More than 15 years ago it was reported that human CYP2Cs are very important metabolizers of endogenous substances such as AA and steroids (Daikh et al., 1994). Human CYP2C isoforms share 85-95 % nucleotide identity (Table 1.1).

Table 1.1 Homology of nucleotide sequences of human CYP2C.

	CYP2C8	CYP2C9	CYP2C18	CYP2C19
CYP2C8	100 %	84,8 %	84,8 %	84,9 %
CYP2C9	84,8 %	100 %	87,5 %	94,8 %
CYP2C18	84,8 %	87,5 %	100 %	87,4 %
CYP2C19	84,9 %	94,8 %	87,4 %	100 %

CYP2C8 is together with CYP2C9 the predominant CYP2C isoform in kidney and liver (Dai et al., 2001). In liver, CYP2C8 is involved in drug metabolism. CYP2C8 metabolizes benzo(α)pyrene (Yun et al., 1994), (R)-warfarin (Kaminsky, 1993), retinol (Leo et al., 1988), and the anticancer drug paclitaxel. CYP2C8 mRNA was also detected in adrenal gland, brain, uterus, mammary gland, and ovary (Klose et al., 1999). As an AA-epoxygenase it is highly specific, 94 % of total product are EETs. The regioisomers 11,12-EET and 14,15-EET are formed in an almost 1: 1

ratio (Dai et al., 2001). It is enantioselective for 11(R),12(S)-EET and 14(R),15(S)-EET, both with optical purities of 82 %. CYP2C8 is a highly polymorphic gene. In European and African American population there are two dominant variants of 2C8. CYP2C8*2 has an allelic frequency of 18 % in African-American population. CYP2C8*3 occurs in African-American population with 3 % but in Caucasians the frequency is much higher, 13 %. CYP2C8*2 metabolizes AA with conversion rate similar to that of wild type. CYP2C8*3 reaches only one third of the wild type activity (Dai et al., 2001).

CYP2C9 is the major AA-epoxygenase in human liver, where it is responsible for ~50 % of total EET production (Rifkind et al., 1995). CYP2C9 metabolizes AA to 8,9-EET, 11,12-EET and 14,15-EET, and EETs represent ~90 % of total AA metabolites. 14,15-EET is the main product with approximately 50 % of total epoxy product. 8,9-EET and 11,12-EET are generated in ratio close to 1: 2. CYP2C9 is moderately selective for 14(R),15(S)-EET (optical purity: 62 %). When epoxidizing 11,12-double bond, CYP2C9 forms 11(S),12(R)-EET with optical purity of 70 % (Daikh et al., 1994). CYP2C9 is found in almost all tissues and organs like liver, kidney, pancreas, prostate, spleen, skin, myocardium etc. (Enayetallah et al., 2004). Various polymorphisms have been described for CYP2C9 but two of them, CYP2C9*2 and CYP2C9*3, are significant with allele frequencies of 15 % and 8 %, respectively, in Caucasian population (Schwarz et al., 2003). These polymorphisms are very important in drug metabolism, since carriers of certain alleles are poor metabolizers for several drugs like the anticoagulant warfarin (Rettie et al., 1994), the antidiabetics such as tolbutamide, the anticonvulsant like phenytoin (Veronese et al., 1991), tetrahydrocannabinol (Bornheim et al, 1992) and NSAIDs. These polymorphisms also strongly influence AA metabolism. CYP2C9*1 and CYP2C9*2 epoxidize AA with similar efficiencies but CYP2C9*3 reaches less than 20% of the wild type activity (M. Öchsner and W.-H. Schunck, unpublished data).

CYP2C18 is an isoform whose function is still unclear. Its mRNA was found in the brain, uterus, mammary gland, kidney, and duodenum (Klose et al., 1999). Goldstein (2001) reported that CYP2C18 protein has not been detected in any tissue. In contrast, Ohhira and coworkers (2006) reported that CYP2C18 is expressed in human liver where it has role in metabolism of xenobiotica. In addition, Imaoka et al., 2005 reported a weak activity of CYP2C18 towards AA.

Table 1.2 Regioselectivity of CYP2C isoforms in AA epoxidation. Data are summarized from following reports 1) Dai et al., 2001 2) Daikh et al., 1994 3) Holla et al., 1999, 4) Karara et al., 1993.

	8,9-EET	11,12-EET	14,15-EET
CYP2C8 ¹⁾	0 %	52 %	48 %
CYP2C9 ²⁾	18 %	30 %	52 %
CYP2C11 ³⁾	19 %	42 %	39 %
CYP2C23 ⁴⁾	27 %	54 %	14 %

CYP2C19 is expressed only in the liver where it is involved in drug metabolism. It can metabolize *S*-mephenytoin, the antiulcer drug omeprazole and other important proton pump inhibitors (Flockhart et al., 1995). Biotransformation of the antimalarial drug proguanil to its active metabolite cycloguanil is partially dependent on CYP2C19. CYP2C19 metabolizes arachidonic acid to all four EETs regioisomers and 20-HETE, where EETs and HETE are formed in similar quantities (Imaoka et al., 2005). There are at least 7 different inactivating mutations in CYP2C19, which can include null mutations (prevent expression of the protein) or amino acid changes (affect catalytic activity of the protein). CYP2C19 mutations occur with high frequency in Asian populations.

1.1.4.2 Rat CYP2C isoforms

The rat CYP2C subfamily consists of 8 members (2C6, 2C7, 2C11, 2C12, 2C13, 2C22, 2C23 and 2C24). In contrast to human CYP2Cs, rat CYP2C isoforms are expressed in a sex-specific manner. For example, CYP2C7 and CYP2C12 are female-specific whereas CYP2C11 and CYP2C13 are expressed in male rats. Almost all isoforms are expressed in the liver (2C6, 2C7, 2C11, 2C12, 2C13 and 2C23). CYP2C11 represents 25-40 % of liver microsomal CYP protein. CYP2C11, CYP2C23 and CYP2C24 are expressed in the kidney. Among them, CYP2C23 is the most abundant (Holla et al., 1999).

CYP2C11 is the major AA-epoxygenase in the rat liver. About 70 % of CYP2C11-dependent AA metabolites are EETs. CYP2C11 epoxidizes AA to 8,9 EET, 11,12-EET and 14,15-EET. 11,12- and 14,15-EET were formed in similar quantities (~40 %). This isoform does not show significant stereospecificity. 8,9- and 14,15-EETs are nearly racemic whereas 11(R),12(S)-EET was the predominant product of 11,12-epoxidation (Holla et al., 1999).

CYP2C23 is the major AA epoxygenase in the kidney and it is also highly expressed in the liver. In addition, CYP2C23 is expressed in other organs like lung, spleen, heart, brain and testis (Imaoka et al., 2005). This isoform metabolizes AA mainly to epoxides (8,9-EET, 11,12-EET and 14,15-EET) and to a lesser extent to HETEs. 11,12-EET is the major product with 54 % of total product whereas 8,9-EET and 14,15-EET represent 27 and 14 % of total product, respectively (Karara et al., 1993).

1.1.5 CYP4A/4F dependent biosynthesis of HETEs

CYP4A and CYP4F subfamilies are major AA-hydroxylases. 20-HETE represents the principal product of CYP-dependent AA hydroxylation. The CYP4A subfamily consists of 20 isoforms, which are found in human, rat, mouse, rabbit, hamster, guinea pig, koala, cat and pig (Okita and Okita, 2001). Expression of CYP4A/4F is the highest in the kidney.

1.1.5.1 Human CYP4A/4F isoforms

CYP4A11 is the only active human CYP4A isoform (Bellamine et al., 2003). It is expressed in the liver and kidney (Nishimura et al., 2003). It was detected in the liver as a predominant lauric acid hydroxylase but hydroxylation of AA in the liver was mainly dependent on CYP4F2 (Lasker et al., 2000; Powell et al., 1998). The contribution of CYP4A11 to AA metabolism is significantly higher in the kidney than in the liver.

CYP4F2 is expressed in the kidney and liver and in both organs it represents the major AA hydroxylase (Powell et al., 1998). In addition to CYP4F2, there are four

more human 4F subfamily members: 4F3, 4F8, 4F11 and 4F12. The 4F subfamily is also detected in rats (4 isoforms), mouse (5 isoforms), sheep (1 isoform) and fish (1 isoform); Roman, 2002.

1.1.5.2 Rat CYP4A isoforms

There are four rat CYP4A isoforms (CYP4A1, CYP4A2, CYP4A3 and CYP4A8). All isoforms are good metabolizers of lauric acid. CYP4A1 converts lauric acid several times faster compared to other isoforms (Nguyen et al., 1999). All isoforms metabolize AA primarily to 20-HETE. Interestingly, CYP4A2 and CYP4A3 can also epoxidize AA at the 11,12 position (Wang et al., 1996; Nguyen et al., 1999). CYP4A isoforms are gender- and age- specific. The level of CYP4A2 and CYP4A3 protein is very low in female. CYP4A2 is not expressed till the age of 5 weeks when it becomes the kidney CYP4A isoform with the highest expression. CYP4A1 reaches its maximum of expression at the age of 3 weeks and then decreases to the 20 % of maximal expression. Although it is not highly expressed, CYP4A1 represents the major AA-hydroxylase in adult rat (Okita and Okita, 2001).

1.1.5.3 Mouse Cyp4a isoforms

The Cyp4a subfamily members expressed in mouse include Cyp4a10, Cyp4a12 and Cyp4a14. (Henderson et al., 1994; Heng et al., 1997; Holla et al., 2001; Honeck et al., 2000; Stec et al., 2003). There are two Cyp4a12 genes, Cyp4a12a and Cyp4a12b, that result from a tandem 100 kb duplication within the Cyp4abx cluster on chromosome 4 (Nelson et al., 2004). All isoforms hydroxylate lauric acid in high rates but only Cyp4a12a and Cyp4a12b can metabolize AA efficiently. Cyp4a10 and Cyp4a14 metabolize AA only at nonphysiological high AA concentrations. Cyp4a10 hydroxylates AA to 19/20-HETE whereas Cyp4a14 epoxidizes AA to 11,12-EET. In mouse, Cyp4a isoforms are expressed in a sex-specific manner. Females express Cyp4a10 and Cyp4a14 and males Cyp4a10 and Cyp4a12a isoforms (Muller et al., 2006).

1.1.6 Biological activities of EETs and HETEs

CYP-dependent AA metabolites, and their biological effects have been intensively studied over last 20 years. They function as mediators in variety of different signal transductions regulating processes in kidney, vasculature, heart, lungs, brain, gastrointestinal tract, pancreas etc. They also play important roles in inflammation and angiogenesis. The following chapter is to briefly summarize their effects on renal function and vascular tone (for extensive reviews see: McGiff and Quilley, 2001; Roman, 2000, Spector and Norris, 2007); Figure 1.5.

EETs have antihypertensive properties. In *the kidney*, EETs inhibit sodium transport what leads to reduced blood pressure. EETs can regulate sodium transport affecting several different transport mechanisms. They inhibit translocation of Na⁺H exchanger in apical membrane of proximal tubules (PT) (Dos Santos et al., 2004). EETs can also inhibit Na⁺K⁺-ATPase in PT (Romero et al., 1991). In cortical collecting duct and connecting tubule, epithelial Na channels (ENaC) are involved in sodium reabsorption. EETs inhibit ENaC channels and therefore reduce sodium retention (Wei et al., 2004)

In *the vasculature*, EETs are produced in the endothelial cells and their main action appears to be on the VSMC where they activate BK channels, hyperpolarize VSMC and thus induce vasodilatation (Campbell et al., 1996).

EETs are:

- synthesized in endothelium,
- potent vasodilators and
- activate BK channels.

Based on these findings the hypothesis was developed that EETs serve as EDHF (Endothelium Derived Hyperpolarizing Factor). EDHF is defined as a component of the vasodilator response, which remains after inhibition of NO synthase and COX. The relative contribution of EDHF can reach 50 % of the total response to acetylcholine (ACh) as described in some vessels such as renal afferent arterioles. (Quilley et al., 1997). Extensive studies showed that inhibition of CYP attenuate EDHF vasodilator responses to ACh, bradykinin and AA (Campbell et al., 1996, Hecker et al., 1994, Fulton et al., 1992). EDHF responses are enhanced by beta-

naphtoflavone an inducer of CYP1A and CYP2C isoforms (Popp et al., 1996). Many anesthetics, which are known to inhibit CYP2C enzymes, attenuate the EDHF response (Lischke et al., 1995a, Lischke et al., 1995b). EDHF-mediated response is also reduced by NO, which decreases the expression of CYP enzymes and blocks EET synthesis (Kessler et al., 1999). In contrast, there are studies, which show that epoxygenase inhibitors do not block EDHF response in certain arteries. These controversial findings led to the conclusion that EETs serve as EDHF in renal and coronary arteries but not in other vascular beds such as mesenteric and hepatic arteries where the EDHF response is obviously mediated by other substances (Roman, 2002).

20-HETE exhibits antihypertensive actions in the kidney. Similar as described above for EETs, 20-HETE regulates blood pressure by inhibiting sodium transport (Figure 1.5). 20-HETE is synthesized mainly in PT and in the thick ascending limb of loop of Henle (TALH) and at both sites inhibits salt reabsorption. In PT, 20-HETE inhibits Na^+K^+ -ATPase activity by inhibiting protein-kinase C dependent phosphorylation of the alpha-subunit of Na^+K^+ -ATPase (Schwartzman et al., 1985). 20-HETE also inhibits the translocation of Na^+H exchanger in the apical membrane of PT (Dos Santos et al., 2004). In TALH, 20-HETE inhibits the $\text{Na}^+\text{K}^+, 2\text{Cl}^-$ cotransporter that means the major pathway for salt reabsorption in this part of the nephron (Escalante et al., 1991). In the apical membrane of the TALH cells, 20-HETE blocks K^+ efflux through K^+ channel (Lu et al., 1998). Blockade of K^+ efflux limits the amount of K^+ available for transport through the $\text{Na}^+\text{K}^+, 2\text{Cl}^-$ cotransporter and reduces the lumen positive potential, which is the main driving force for passive reabsorption of cations in this portion of the nephron.

20-HETE has prohypertensive properties in the vasculature. 20-HETE is synthesized in vascular smooth muscle cells where it inhibits the large conductance Ca^{2+} -activated K^+ channel (BK channel), resulting in depolarization of the vascular smooth muscle cell (VSMC), Ca^{2+} entry, and potent vasoconstriction (Imig, 2000). Cat cerebral VSMCs produce 20-HETE, which activates L-type Ca^{2+} channel current and promotes cerebral vasoconstriction (Gebremedhin et al., 1998). Randriamboavonjy et al. (2003) reported vasoconstrictory action of 20-HETE in porcine small coronary arteries where 20-HETE acts through activation of the Rho-kinase which results in higher Ca^{2+} sensitivity. Furthermore, 20-HETE-dependent

activation of PKC leads to inhibition of whole-cell K⁺ current in cat cerebral VSMC and elicits vasoconstriction of cerebral arteries (Lange et al., 1997). 20-HETE also activates Ras/MAPK pathway in VSMC and promotes VSMC contraction and proliferation (Muthalif et al., 1998; Muthalif et al., 2000).

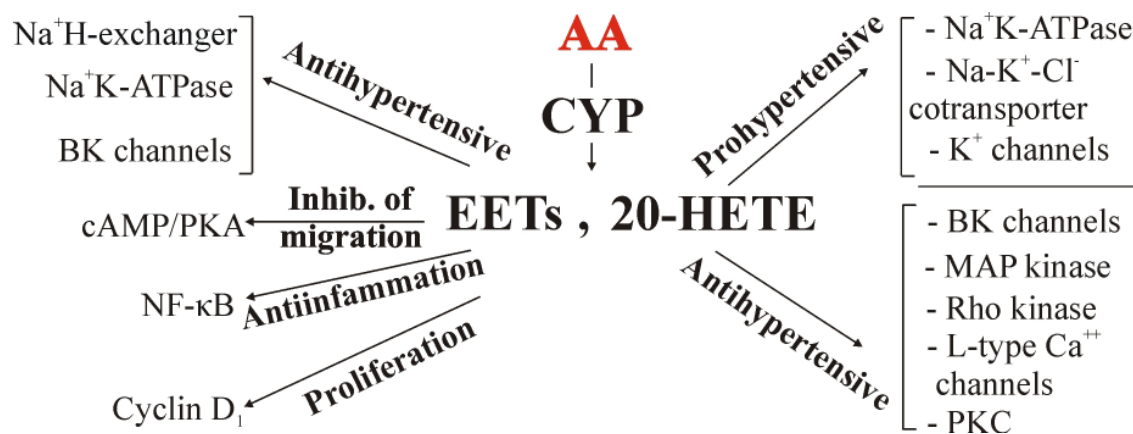


Figure 1.5 Biological effects of 20-HETE and EETs in the cardiovascular system.

1.1.7 Alterations in CYP-dependent AA metabolism in animal models of hypertension

A number of reports suggest an association between altered production of 20-HETE and EETs and high blood pressure. In this chapter, several animal models of hypertension, which have altered CYP-dependent metabolism, will be introduced (reviewed in Roman, 2002).

DOCA-salt hypertension

DOCA (desoxycorticosterone acetate) is a synthetic mineralocorticoid and it induces salt retention. Rats under DOCA-salt treatment develop hypertension. This model is characterized by elevations in plasma endothelin levels, which is known to stimulate release of 20-HETE in renal vasculature (Oyekan et al., 1997). In DOCA-salt-treated rats, the level of 20-HETE is increased by four-fold. Inhibition of CYP activity with ABT (1-aminobenzotriazole) in DOCA-salt treated rats prevents the development of hypertension (Oyekan et al., 1999) and reduces renal and cardiac end-organ damage (Muthalif et al., 2000).

Interestingly, Honeck et al. (2000) described that in DOCA-salt induced hypertension in mice, 20-HETE formation is reduced rather than increased. Bezafibrate treatment induced Cyp4a expression and formation of 20-HETE and ameliorated development of hypertension.

These findings demonstrate that hypertension can be associated with both enhanced and diminished renal 20-HETE production. To explain this fact it is important to note that 20-HETE has opposite properties in the vascular and tubular system of the kidney. In the vasculature, 20-HETE plays a prohypertensive role and an increase in vascular 20-HETE contributes to hypertension (DOCA-salt treated rats). In contrast, 20-HETE in tubules has anti-hypertensive properties and reduction in tubular 20-HETE level can lead to hypertension (DOCA-salt treated mouse).

Angiotensin II-induced hypertension

The renin-angiotensin system (RAS) is the most important regulator of the blood pressure. RAS regulates several molecular mechanisms, which control blood pressure, like vasoconstriction or sodium retention in the kidney. Renin is responsible for the cleavage of angiotensinogen (AOPEN), yielding the inactive decapeptide angiotensin I (ANG I), which is further enzymatically processed to the biologically active octapeptide ANG II.

Two models for ANG II-induced hypertension have been described (experimental and genetic). ANG II-infused rats develop hypertension and organ damage. ANG II stimulates the formation of 20-HETE in the renal circulation (Croft et al., 2000) and in the isolated perfused rabbit kidney (Carroll et al., 1996). Muthalif et al. (2000) addressed the question if ANG II treated rats have hypertension due to elevated level of 20-HETE. The study showed that chronic ABT blockade of the renal formation of 20-HETE in rats treated with ANG II, reduced blood pressure to normal.

On the other hand there is a genetic model of ANG II-induced hypertension. These so-called double-transgenic rats overexpress the human genes for renin and angiotensinogen. DTGR is the model, which allows detailed studying of human renin and angiotensin interaction. Two rat transgenic lines were generated, one expressing human renin (hREN) and the other expressing human angiotensinogen (hAOPEN). Cross-breeding of these two lines (hREN X hAOPEN) generates

double-transgenic animals, which produce high amount of ANG II, and develop severe hypertension. DTGR animals die of cardiac and renal damage at an age of 8 weeks. The heart shows necrosis and fibrosis, whereas the kidney resembles the hemolytic-uremic syndrome vasculopathy (reviewed by Luft et al., 1999).

DTGR animals have altered renal AA metabolism. AA-epoxygenase activity is significantly decreased and expression of the predominant renal EET-generating CYP isoform, CYP2C23, is progressively lost in renal cortical tubules (Kaergel et al., 2002). Decreased EET production might be involved in mediating hypertension and inflammatory end-organ damage.

High fat (HF) diet-induced hypertension

Rats fed with high fat diet develop significantly higher systolic blood pressure, body weight, and fat: body weight ratio compared to control group. The renal ω -hydroxylase and epoxygenase activities of HF rats are decreased by approx. 45 %. Changes in the rate of 20-HETE and EET formation in different renal zones were consistent with the levels of expression of CYP4A and CYP2C23 proteins, respectively. The reduction in the synthesis of these eicosanoids may play an important role in the regulation of renal function and blood pressure in obesity-induced hypertension (Wang et al., 2003).

SHR - Spontaneously hypertensive rat

In spontaneously hypertensive rats (SHR rats), blood pressures increases constantly between 5 to 10 weeks of age while, under similar conditions, comparable (but not isogenic) Wistar-Kyoto (WKY) rats remain normotensive. The developmental phase of SHR hypertension is accompanied by parallel increases in CYP4A2 expression and AA ω / ω -1 hydroxylase activity. Chemical or antisense nucleotide inhibition of CYP4A activity or expression lowers the blood pressure of hypertensive SHR rats (McGiff and Quilley, 1999; Carroll, 2000).

Dahl salt sensitive rat

After 10–18 days on a high salt diet, Dahl salt sensitive (DS) animals develop hypertension while comparable Dahl salt resistant (DR) rats remain normotensive. A role for CYP4A2 in the salt sensitivity of DS rat was proposed based on: (a) inhibitor studies, (b) differences between DS and DR rats in the expression and activity of the kidney AA ω / ω -1 hydroxylases, and (c) normalization of Cl

transport in DS rats by 20-HETE (Maier, 2001). Moreover, Capdevila et al. demonstrated that DS rat exhibit an additional problem in the regulation of EET biosynthesis. In DR rats CYP2C23-mediated EET production is strongly upregulated upon salt loading. This mechanism fails in DS rats (Makita et al., 1994, Holla et al., 1993).

1.2 ω -3 polyunsaturated fatty acids

1.2.1 ω -3 and ω -6 fatty acids as essential nutrients

Polyunsaturated fatty acids are fatty acids with two or more double bonds in the carbon chain. Considering the position of the double bond, which is most distant from the -COOH group, they are divided in 3 groups: ω -3, ω -6 and ω -9 fatty acids (most distant double bond from COOH group is located at the 3rd-, 6th-, or 9th- C atom counting from the methyl end of the acyl chain).

ω -3 and ω -6 fatty acids are necessary for normal development and health but mammals cannot synthesize them completely (Figure 1.6).

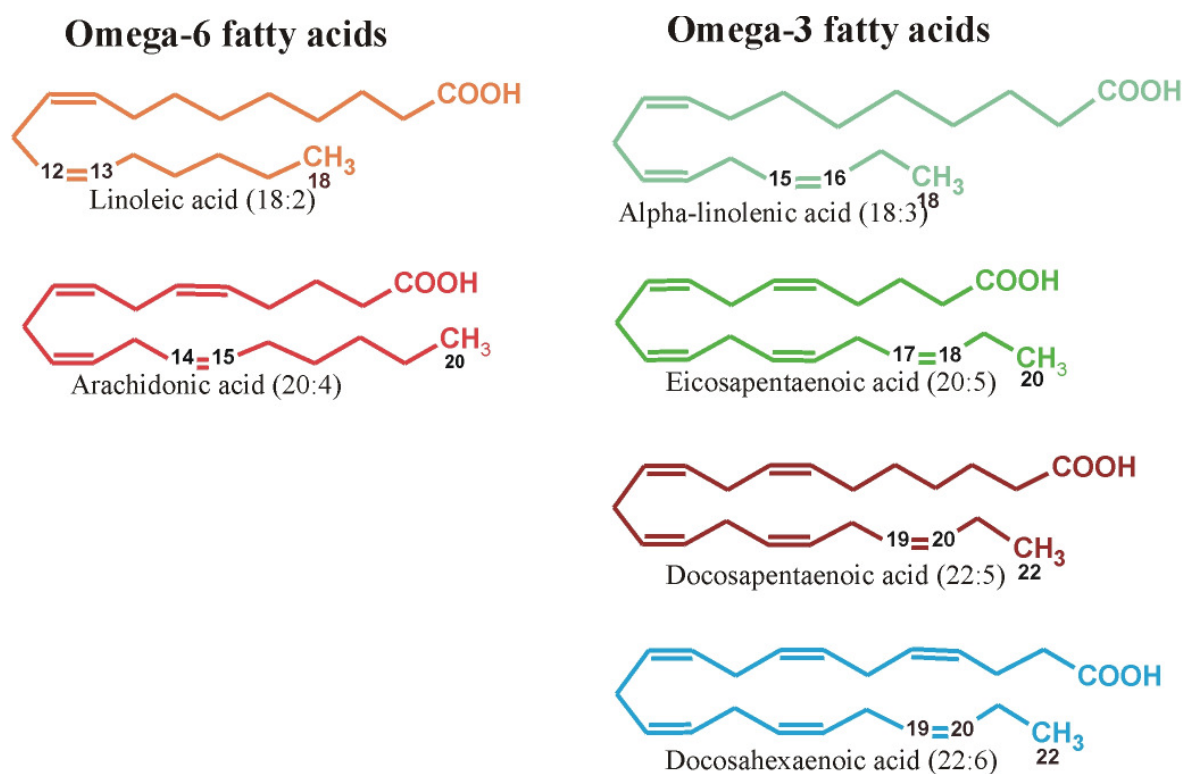


Figure 1.6 Structural formulas of ω -6 and ω -3 fatty acids. Last carbon atoms of the fatty acid chains and ω -3 and ω -6 double bonds are numbered.

PUFAs have to be taken up through the diet. The first members of the ω -3 and ω -6 series are alpha-linolenic (18: 3) and linoleic acid (18: 2), respectively, which are precursors for longchain ω -3 and ω -6 polyunsaturated fatty acids (fatty acid chain length equal or higher than 20 carbon atoms); Figure 1.7.

Physiologically the most important representative of the ω -6 PUFAs is AA (20: 4) whereas the main ω -3 fatty acids are EPA (20: 5) and DHA (22: 6).

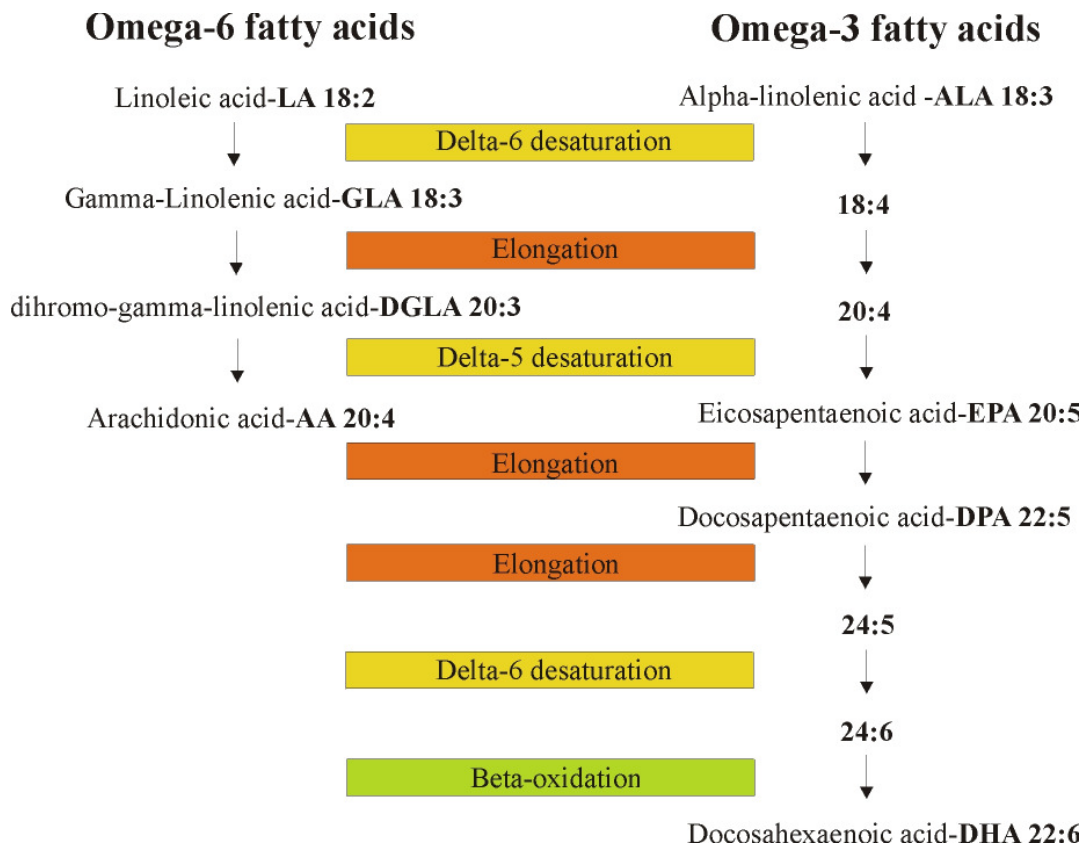


Figure 1.7 Pathway of synthesis of ω -3 and ω -6 fatty acids from their precursors alpha-linolenic acid and linoleic acid, respectively.

A very important feature of ω -3 and ω -6 PUFAs is that they are not interconvertible since desaturases required for this process are not expressed in mammals (Figure 1.8).

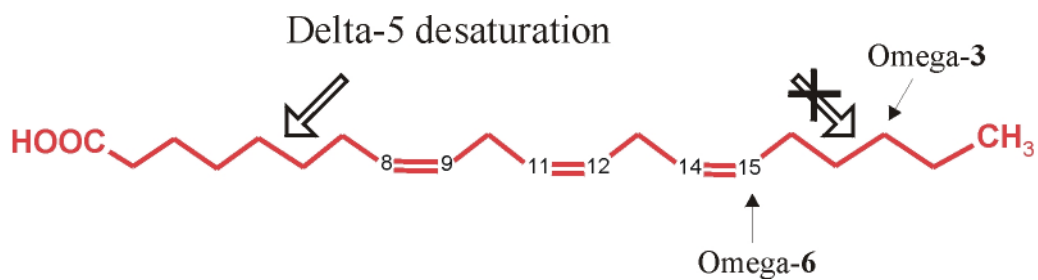


Figure 1.8 Desaturation of dihydro gamma linolenic acid to arachidonic acid. Desaturase, which converts ω -6 to ω -3 fatty acids, is not expressed in mammals.

AA is found in egg yolk, meats in general, and other animal-based foods. Further important sources are corn oil, sunflower oil, and safflower oil. Food that contains high amounts of ω -3 fatty acids include cold water fish, some vegetables, nuts, seeds and oils (Table 1.3).

	Omega-3	Omega-6	O6/O3 ratio
flax seed oil	59.14	14.00	0.24
salmon oil	35.98	4.34	0.12
sardine oil	25.85	5.04	0.19
borage oil	25.00	37.50	1.50
oil, cod liver	20.67	1.87	0.09
flax seed	18.12	4.32	0.24
oil, canola	9.30	20.30	2.18
Nuts, walnuts	9.08	38.10	4.20
wheat germ oil	6.90	54.80	7.94
soybean oil	6.80	51.00	7.50
italian salad dressing	3.30	24.60	7.45
Salmon, farmed	3.16	0.74	0.24
Salmon	2.29	0.26	0.11
herring	1.98	0.44	0.22
chinook	1.83	0.25	0.14
soybean margarine	1.50	19.40	12.93
anchovy	1.49	0.15	0.10
Butter	1.18	1.83	1.55
lard	1.00	10.20	10.20
halibut	0.85	0.09	0.10
bluefish	0.83	0.23	0.27
shrimp	0.63	0.03	0.05
olive oil	0.60	7.90	13.17

Table 1.3 List of foods, which contain high amount of ω -3 fatty acids. Content is presented in grams of fatty acids per 100 grams of edible portion. Table also includes values of ω -6 fatty acids and ratio of ω -6/ ω -3 (Devroey E., www.longevinst.org).

As a dietary source of ω -3 fatty acids, cold-water fish have a great advantage over flax seed and flax seed oil. Cold water fish contain multiple ω -3 fatty acids, among them EPA and DHA, whereas flax seed contains only alpha-linolenic acid which is precursor of EPA and DHA. Alpha-linolenic acid itself does not have important functions in mammals and the capacity of conversion to EPA and DHA is reduced by high ω -6 fatty acid content.

The ratio of ω -6 and ω -3 intake in modern western diet is estimated to 20: 1. This represents a strong shift in direction towards ω -6 in comparison to our ancestors, who ate diet with a ω -6: ω -3 = 1: 1 (Simopoulos, 1999). Numerous studies suggest

that dietary shift towards much less ω -3 and much more ω -6 significantly influences health. This is probably due to the different effects of metabolites of these fatty acids. Most of the ω -6 PUFA metabolites have proinflammatory and proaggregatory effects whereas the similar metabolites of ω -3 PUFA are predominantly beneficial. They are anti-inflammatory, anti-arrhythmic and hypotensive. They can also decrease level of serum triglycerides and inhibit platelet aggregation (for recent reviews see: Simopoulos, 2002; Calder, 2004; Kris-Etherton, 2002).

1.2.2 ω -3 fatty acids as bioactive mediators

1.2.2.1 Beneficial effects of fish oil fatty acids

Over last 30 years many studies and clinical investigations have been carried out on ω -3 fatty acids. They are essential for normal growth and development and may play an important role in the prevention and treatment of cardiovascular diseases, diabetes, arthritis and other inflammatory and autoimmune diseases.

The first studies, which indicated beneficial effects of ω -3 fatty acids on the cardiovascular system, were conducted more than 30 years ago. Low incidence of coronary heart disease in Greenland Inuit's was linked to high consumption of fish and other seafood rich in EPA and DHA (Bang et al., 1980). This study was followed by various epidemiological and observational studies that led to the same conclusion that consumption of fish oil fatty acids reduces risk of cardiovascular diseases (Kris-Etherton et al., 2002). Different clinical studies reported similar results. For example, the Diet and Reinfarction trial (DART1) study reported a 29 % reduction in all-cause mortality over a two-year period in male myocardial infarction survivors advised to increase their intake of oily fish (Burr et al., 1989). The GISSI-Prevention Study showed that ω -3 fatty acid treatment of patients with preexisting coronary heart disease resulted in 15 % reduction in the primary end point of death, nonfatal MI, and nonfatal stroke. There was a 20 % reduction in all-cause mortality ($P=0.01$) and a 45 % reduction in sudden death (Salen and de Lorgeril 1999; Leaf, 2002).

The mechanisms of how fish oil fatty acids exert their beneficial action in the cardiovascular system are only partially understood. It was reported that fish oil has anti-arrhythmic properties what is very important in prevention of sudden cardiac death (Kang and Leaf, 1994). DHA and EPA can inhibit phenylephrine- and endothelin-1- induced cardiac hypertrophy in vitro (Siddiqui et al., 2004; Shimojo et al., 2006). Moreover, ω -3 fatty acids are hypotensive (Morris et al., 1993) and have anti-inflammatory and anti-atherogenic properties by inhibiting a variety of steps leading to endothelial activation and plaque formation (Calder, 2004; De Caterina and Massaro, 2005). They also moderate platelet aggregation (Hashimoto et al., 1984) and lower serum triglycerides (Weber and Raederstorff, 2000).

1.2.2.2 Possible ways of actions of fish oil fatty acids

There are 3 possible ways of ω -3 PUFA actions:

- they are incorporated into phospholipids and thus change the structure and fluidity of biological membranes.
- ω -3 PUFA can directly activate transcription factors (PPAR, liver X receptor) and thus alter gene expression or regulate ion channel activity.
- ω -3 PUFA are, as well as ω -6 PUFA, precursors for a large group of bioactive molecules, termed eicosanoids, which are synthesized by cyclooxygenases, lipoxygenases and CYP enzymes. Competition between AA and EPA and DHA for binding to the COX, LOX and CYP enzymes alters eicosanoid biosynthesis by reducing the production of AA-eicosanoids or / and by synthesizing the new EPA-, and DHA-derived eicosanoids. Both these actions may contribute to the beneficial effects of ω -3 fatty acids.

20 years ago, it was shown for the first time that hepatic and renal microsomes are able to metabolize EPA and DHA to ω -, and ω -1 hydroxy metabolites as well as to epoxides, analogue to CYP-dependent AA metabolism (Van Rollins et al., 1984; Van Rollins et al., 1989). There were a number of following studies, which confirmed that ω -3 PUFA are metabolized by CYPs in animals and human (Van Rollins et al., 1988; Theuer et al., 2005; Oliw and Sprecher, 1991; Knapp et al., 1991).

The principal CYP-dependent metabolites of EPA, DPA and DHA are analogous to that of AA (Figure 1.9). The main hydroxylation products involve 19-and 20-hydroxy-EPA (19-and 20-HEPE), 21- and 22-OH-DPA and 21- and 22-OH-DHA. Epoxidation of EPA yields 5 regioisomeric epoxyeicosatetraenoic acids (EETeTr). Epoxidation of DPA yields 5 regioisomeric epoxydocosatetraenoic acids (EDTeTr) whereas DHA can be epoxidized to six regioisomeric epoxydocosapentaenoic acids (EDP); Figure 1.9.

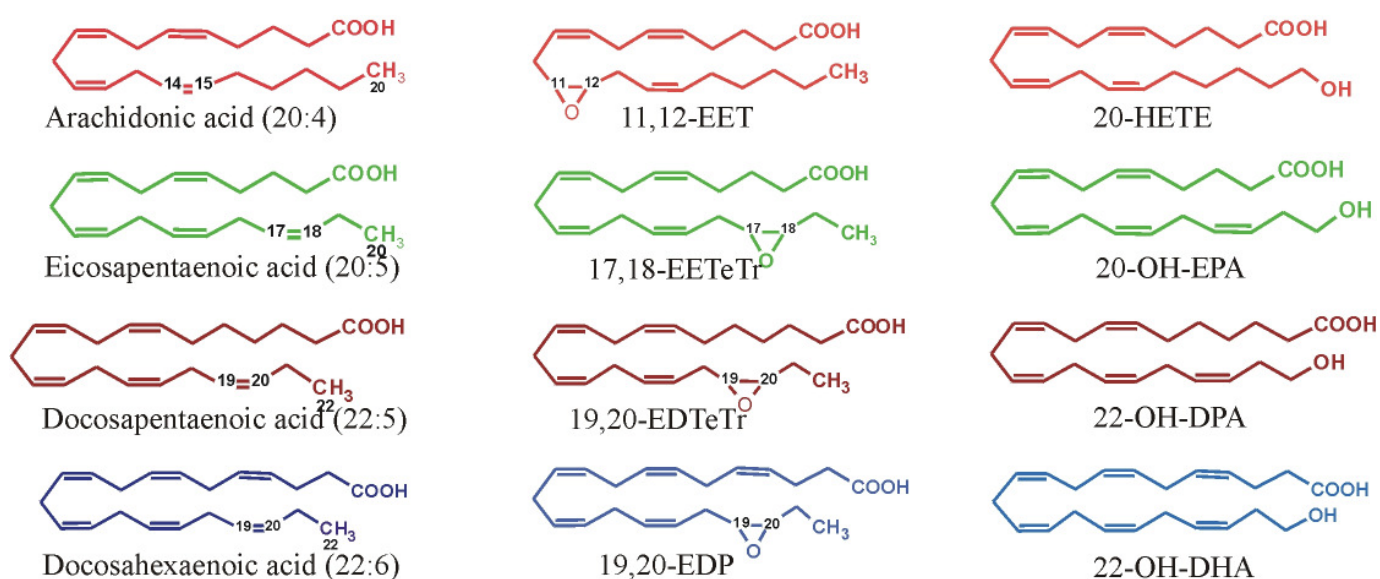


Figure 1.9 Structural formulas of AA, EPA, DPA and DHA and examples of their CYP-dependent epoxy and hydroxy metabolites.

CYP-dependent ω -3 PUFA metabolism was reported only a few years after the report of Capdevila et al. (1981), which demonstrated that P450 systems catalyze AA oxidation. The work of Capdevila was the starting point for a very intensive research on EETs and 19/20-HETE effects whereas till now there are only a few studies on the physiological effects of CYP-dependent EPA/DHA metabolites (see discussion chapter 4.3).

1.3. Objectives and specific aims

During the last decade, experimental evidence has been accumulated suggesting an important role of CYP-dependent AA metabolism in the regulation of renal and vascular function. Various animal models show that alterations in the formation of

primary and secondary CYP-dependent eicosanoids contribute to or even directly cause hypertension and end-organ damage. Providing a second starting point for the present study, diets rich in fish oil ω -3 PUFAs, which are chemically similar to AA, were described to protect against cardiovascular diseases.

The main focus of this study was to elucidate new possibilities for treatment of hypertension and end-organ damage by directly influencing the renal CYP-dependent AA metabolism. The specific aims were as follows:

- to test the effect of the PPAR α activator fenofibrate on the recovery of renal CYP-dependent EET and HEET production in a rat model of ANG II-induced hypertension and end-organ damage
- to analyze the CYP-dependent metabolism of fish oil ω -3 polyunsaturated fatty acids (ω -3 PUFAs, such as EPA and DHA, as a source of alternative physiologically active eicosanoids.

In order to test induction of CYP metabolim, animal studies were conducted in collaboration with Prof. Luft, Dr. Muller and coworkers from the Franz-Volhard Clinic, Berlin-Buch. We used a rat model of ANG II-induced hypertension and end-organ damage and studied the effect of this treatment on the pathology and CYP-dependent AA metabolism.

In order to determine whether ω -3 PUFAs represent alternative substrates for CYP enzymes, we analyzed the metabolism of AA, EPA, DPA and DHA by renal and liver microsomes as well as different recombinant CYP isoforms. This analysis involved a comparison of enzymatic activities as well as of regio- and stereoselectivities.

2. Material and methods

2.1. Cloning of CYPs and preparation of recombinant baculovirus

As described in detail below, recombinant baculoviruses were constructed in two steps (Figure 2.1). The CYP cDNA to be expressed was first cloned into donor plasmid (pFastBac I; Figure 2.2) and then transfected in E. coli (DH10Bac) where the site-specific transposition of an expression cassette from pFastBac I into baculovirus shuttle vector (bacmid) occurred. Transposition occurs between mini-Tn7 element from pFastBac donor plasmid and mini attTn7 attachment site on the bacmid. Transposase, enzyme that is necessary in this process is encoded on helper plasmid. Mini attTn7, place of insertion of expression cassette is in LacZ gene so transposition can be detected by blue/white screening. (Colonies containing bacmid with LacZ disrupted gene are white in presence of X-gal substrate together with inducer IPTG). In order to get recombinant baculovirus, insect cells are transfected with generated bacmid and baculovirus is harvested with supernatant.

2.1.1 Cloning of CYP cDNAs into the donor plasmid pFASTBac I

All CYPs used in this work were cloned in the same manner. cDNAs were generated by RT-PCR (Ready-To-Go kit, Amersham Pharmacia Biotech) using as template 0.5 µg total RNA from human liver (Clontech Laboratories), rat liver, rat kidney (prepared from Sprague–Dawley rats using the RNeasy Mini-Kit from Qiagen), mouse kidney (prepared from male NMRi mouse using the RNeasy Mini-Kit from Qiagen) and mouse liver (prepared from male C57BL/6 mouse using the RNeasy Mini-Kit from Qiagen). Reverse transcription was primed with Oligo(dT) and PCR amplification was performed using the primer pairs shown in Table 2.1. PCR fragments were cloned into pCR2.1 (TOPO-TA-Cloning kit, Invitrogen). Inserts were recloned into pFastBac I using the restriction sites which were introduced with PCR primers (Table 2.2).

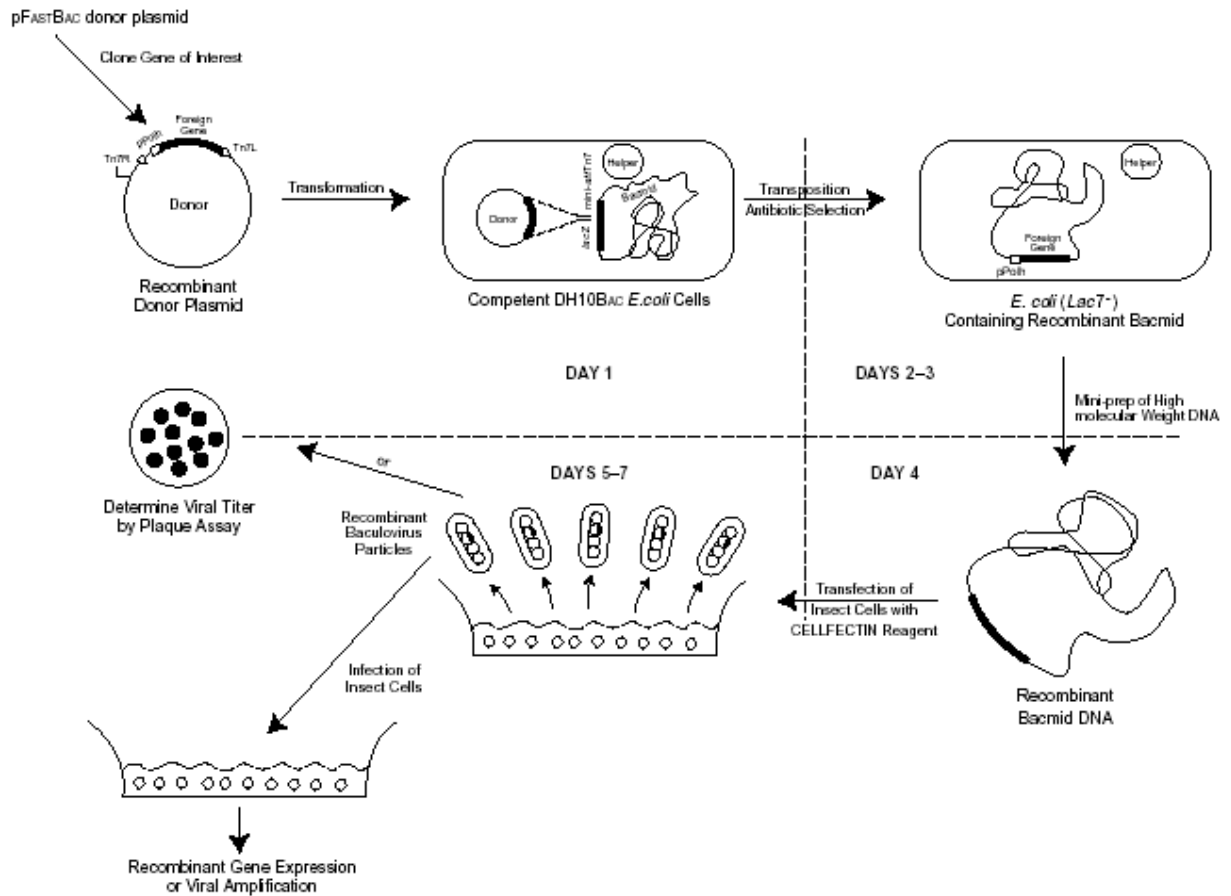


Figure 2.1 The procedure of baculovirus preparation. Recombinant baculovirus was constructed in two steps. The gene to be expressed is first cloned into donor plasmid (pFastBac I) and transfected in *E. coli* (DH10Bac) where the site-specific transposition of an expression cassette from pFastBac I into baculovirus shuttle vector (bacmid) occurs. In order to get baculovirus, insect cells were transfected with generated recombinant bacmid and the baculovirus was harvested with supernatant.

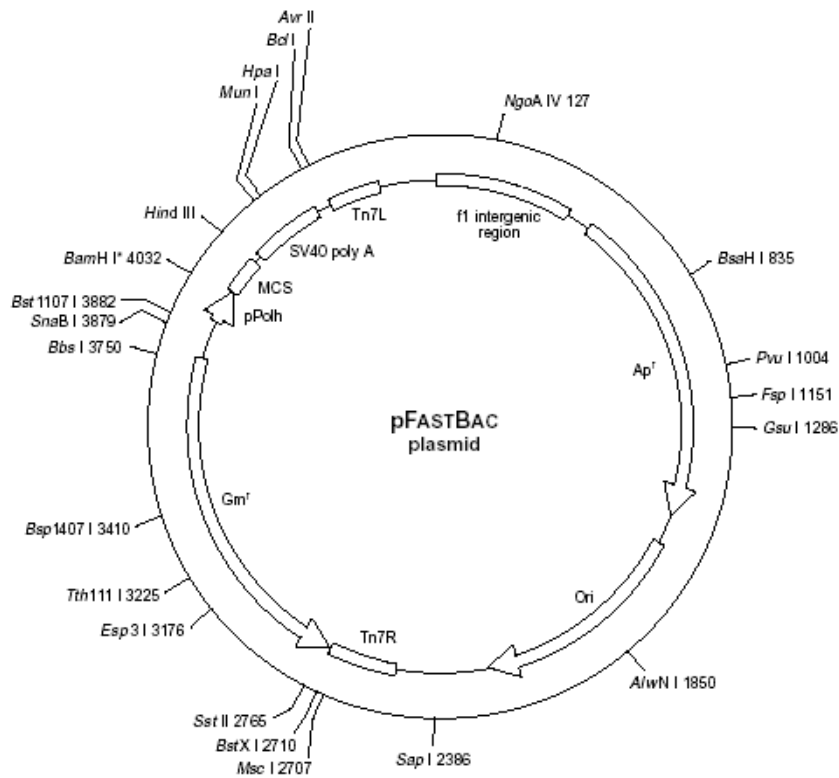


Figure 2.2 Map of the *pFastBac* donor plasmid. The cDNA to be expressed is cloned into the multiple cloning site (MCS). Expression occurs in insect cells under control of strong polyhydridin promoter (*pPolh*). Other important elements are *Tn7R* and *Tn7L* for transposition into the viral DNA.

CYP2C9 was cloned in 2 steps. After reverse transcription, the cDNA was amplified with 2 sets of primers (Table 2.1) and both fragments were cloned into pCR2.1 (Invitrogen). The fragments were excised with EcoRI/HindIII- and HindIII/XhoI, respectively (Table 2.2), and combined by ligation into the EcoRI/XhoI-cleaved pFastBacI. DNA sequencing was performed by Invitex GmbH, Berlin, Germany. cDNAs of Cyp4a12a and Cyp4a12b were amplified by the same primer pairs. To enrich the Cyp4a12b cDNA, the RT-PCR product was digested with Avr II, which cleaves the Cyp4a12a but not the Cyp4a12b. The cDNAs for CYP2C11 and CYP2C23 contained six additional CAC triplets in front of the stop codon to encode proteins with a C-terminal histidine-tag.

Table 2.1 List of specific primer pairs used for amplification of CYP cDNA. All CYP isoforms used in this study are reverse transcribed, amplified and cloned into pCR2.1 and then recloned into pFastBac I. PCR primers contained restriction sites which were further used for cloning into pFastBac I.

CYP	Source of RNA	Sequence of primer pairs used:
CYP2C8	<i>Human liver</i>	<u>Forward</u> CCG CTC GAG CGG GAG AAG GCT TCA ATG G <u>Reverse</u> GAG GTA CCA CAG ATT CTT CAG ACA GG
CYP2C9	<i>Human liver</i>	<u>Forward 1</u> AGG CTT CAA TGG ATT CTC TT <u>Reverse 1</u> ATG GTT GTG CCC TTG GGA ATG AGA <u>Forward 2</u> GGA AAA GTT GAA TGA AAA CAT CAA <u>Reverse 2</u> CCG CTC GAG CGG TCAGAC AGG AAT GAA GCA CAG.
CYP2C11	<i>Rat liver</i>	<u>Forward</u> TCG GAA TTC GCA TGC CAT GGA TCC AGT CCT <u>Reverse</u> CCG CTC GAG CGG TCA GTG GTG GTG GTG GTG GTG GAG ATG AGA GCT TAG AGA
CYP2C23	<i>Rat kidney</i>	<u>Forward</u> TCG GAA TTC GCA ATG GAG CTG CTG GGA TTC AC <u>Reverse</u> CCG CTC GAG CGG TCA GTG GTG GTG GTG GTG GTG TCT AGG AAC AAG GCA
Cyp4a12a	<i>Mouse kidney</i>	<u>Forward</u> ACG CGT AAG CTG TTG TAT CAT GAG TGC <u>Reverse</u> GCT AGC CAT TTG AGC TGT CTT GTT CTG
Cyp4a12b	<i>Mouse liver</i>	<u>Forward</u> ACG CGT AAG CTG TTG TAT CAT GAG TGC <u>Reverse</u> GCT AGC CAT TTG AGC TGT CTT GTT CTG

Table 2.2 List of restriction sites used for cloning of CYP cDNA into pFastBac I. All CYP isoforms used in this study are reverse transcribed, amplified and cloned into pCR2.1 and then recloned into pFastBac I. PCR primers contained restriction sites which were further used for cloning into pFastBac I.

CYP	Restriction sites used for cloning:
CYP2C8	<i>XhoI / KpnI</i>
CYP2C9	<i>EcoRI / Hind III and Hind III / Xho I</i>
CYP2C11	<i>EcoRI / XhoI</i>
CYP2C23	<i>EcoRI / XhoI</i>
CYP4a12a	<i>Mlu I/ Nhe I-site</i>
CYP4a12b	<i>Mlu I/ Nhe I-site</i>

2.1.2 Preparation of recombinant bacmids

2.1.2.1 Generation of recombinant bacmids in *E. coli* DH10Bac

Aliquot of competent DH10Bac cells were thawed on ice and approximately 1 ng recombinant donor plasmid with inserted CYP gene (pFastBac I) was added, following by gently mixing by tapping the side of the tube. The mixture was incubated for 30 min on ice; heat shocked by transferring to 42°C water bath for 45 seconds and then cooled down on ice for 2 min. 900 µl of SOC medium, warmed at room temperature, was added and the mixture was shaken for 4 h at 37°C and 225 rpm. Cells were serially diluted using SOC medium to 10⁻¹, 10⁻² and 10⁻³ and 100 µl of each dilution was plated on LB agar containing 50 µg/ml kanamycin, 7 µg/ml gentamicin, 10 µg/ml tetracycline, 100 µg/ml Bluo-gal and 40 µg/ml IPTG (isopropyl-beta-D-thiogalactopyranoside). After 24-48 h of incubation, 10 white colonies were picked and restreaked to fresh plates to confirm the phenotype.

S.O.C. medium

Bacto-tryptone 20 g
Bacto-yeast extract 5 g
NaCl 0.5 g
1M KCl 2.5 ml
ddH₂O to 1000 ml
adjust pH to 7.0 with 10 N NaOH,
autoclave to sterilize,
add 20 ml of sterile 1 M glucose immediately before use

LB agar

Bacto-tryptone 10 g
Bacto-yeast extract 5 g
NaCl 10 g
ddH₂O 800 ml
Adjust pH to 7.5 with NaOH
Add 15 g agar
Melt agar into solution in the microwave
Adjust volume to 1L with ddH₂O
Sterilize by autoclaving

2.1.2.2 Isolation and preparation of recombinant bacmids

A single colony with verified phenotype was inoculated and cultured in 2 ml LB medium with 50 µg/ml kanamycin, 7 µg/ml gentamycin, and 10 µg/ml tetracycline. The culture was kept at 37°C for 16 h with constant shaking at 250 rpm. After 16 h, 1.5 ml of culture was centrifuged for 1 min at 14000 g and room temperature. The supernatant was removed and pellet was resuspended in 0.3 ml of Solution 1. 0.3 ml of Solution 2 was added and the mixture was incubated for 5 min at room temperature. 0.25 ml of ice-cold Solution 3 was added and mixture was inverted upside down a few times, followed by 10 min incubation on ice. The mixture was centrifuged for 10 min at 14000 g. The supernatant was transferred to a new tube containing 600 µl isopropanol and briefly vortexed followed by 15 min

centrifugation at 14000 g. Supernatant was removed and 600 μ l 70 % EtOH was added. Tube was inverted several times to wash the pellet followed by 5 min centrifugation at 14000 g. Supernatant was removed as much as possible and pellet was left to air dry at room temperature for 5-10 min. DNA was dissolved in 40 μ l TE buffer.

Solution 1 (store in fridge)

50 mM Glucose
25 mM TRIS/HCl (pH 8)
10 mM EDTA,
100 μ g RNase / ml

Solution 2

0.2N NaOH
1 % SDS

Solution 3 (Before use cool on ice)

3M Potassium Acetate,
TE buffer
10 mM TRIS /HCl
1 mM EDTA,
pH 8.0

2.1.2.3 Analysis of recombinant bacmid

PCR was used to verify if recombinant bacmid contains gene of interest since the size of prepared bacmid was >135kbp and classical way to confirm insertion of gene of interest using endonuclease restriction analysis was difficult. pUC/M13 primer pairs were used for amplification and they were directed at sequences on either side of the mini att Tn7 site within the lacZa complementation region of the bacmid.

PCR mixture

1 μ l bacmid DNA
1 μ l of each primer (end concentration of 500 nM)
23 μ l water
25 μ l 2X PCR mix

PCR was performed for 35 cycles under following conditions:

94°C- 3 min

94°C– 45 sec

55°C– 45 sec

72°C- 3 min

72°C –8 min

10°C - overnight

To check the size of the PCR product, 1 % agarose gel in 1X TAE buffer was prepared. 2 µl of the PCR product were diluted in 4 µl of distilled water and 1 µl of Blue /Orange 6X Loading Dye (Promega). The 1 kb DNA ladder (Invitrogen) was used as a marker. The samples were running for 30 min at 100 V. Agarose gel was stained in etidiumbromide and visualized under UV light.

TAE Buffer 10X

0.4 M Tris

0.01 M EDTA-Na₂-salt

0.2 M Acetic acid

2.1.2.4 Transfection of insect cells

Insect Sf9 cells were cultured as described in 2.2.1 up to a cell density of 2×10^6 cells/ml and aliquots corresponding to 0.9×10^6 cells/well were plated in 6-well plate. 2 ml ExCell 401 medium (JRH Biosciences, Lenexa, USA) with 10 % heat-inactivated fetal calf serum, 50 U penicillin, and 50 µg streptomycin/ml was added to each well. Cells were allowed to attach for more than 1h. The transfection mixture was prepared in ExCell 401 medium with 10 % FCS without antibiotics.

Mix A: 5 µl bacmid in 100 µl of the medium

Mix B: 6 µl Cellfectin in 100 µl of the medium.

Mix A&B were mixed and incubated at room temperature 15-45 min and 800 µl medium was added to give the final volume of the transfection mixture (1 ml). Cells were washed with medium without antibiotics and per well was added 1 ml of the transfection mixture. Cells were incubated at 27° C for 5 h and medium was

changed to ExCell 401 medium with 10 % FCS and 100 U penicillin, and 100 µg streptomycin/ml. Cells were incubated for 72 h at 27°C.

2.1.2.5 Harvesting and amplification of recombinant baculovirus

The medium from each well of the 6-well plate was harvested and clarified by centrifugation for 5 min at 500 g. The virus-containing supernatant was collected (“primary virus”). The primary virus was amplified using Sf9 cells, which were cultured as described in 2.2.1. 50 ml of the culture with a density of 2×10^6 cells/ml was infected with 0.5 ml of the primary virus. The amplified virus was harvested 48 h post-infection. This resulted in approximately 100-fold amplification of the virus. Virus was stored at 4°C, protected from light. In general, a virus titer of $\sim 2 \times 10^9$ /ml was reached. The virus titer was determined as follows:

- 5×10^5 Sf9 cells were plated per well in 12-well plate. They were diluted in total volume of 2 ml ExCell 401 medium (JRH Biosciences, Lenexa, USA) with 10 % heat-inactivated fetal calf serum, 50 U penicillin, and 50 µg streptomycin/ml. Cells were incubated at 27°C for 1 h to allow them to settle on the plate.
- Medium was changed and virus was added to the cells. Each well was infected with higher virus dilution. One well was not treated with the virus (negative control).
- 72 h post-infection, cells were observed using a light microscope. Control cells were growing together on the plate. Infected cells, depending on the virus concentration used, showed smaller or bigger gaps between the groups of cells that were growing together. Infected cells were also bigger compared to control cells.
- The amount of virus used in the well where all cells appeared infected was used for determination of viral titer

$$\text{Viral titer (pfu/ml)} = \frac{\text{Total no. of cells (5 x 10}^5\text{)}}{\text{Viral inoculum (ml)}} \times \text{Viral dilution}$$

2.2 Heterologous expression of CYP enzymes in the baculovirus / Sf9 insect cell system

2.2.1 Culturing of insect Sf9 cells

Spodoptera frugiperda (Sf9) insect cells were grown in suspension culture at 27° C with constant shaking at 120 rpm. Cell growth medium was ExCell 401 medium (JRH Biosciences, Lenexa, USA) with 10 % heat inactivated fetal calf serum (FCS, Invitrogen), 100 U/ml penicillin and 100 µg/ml streptomycin (Invitrogen).

Generation time of the cells was 24 h and after 3 days cells reached a density of 2×10^6 cells/ml. To keep them in the logarithmic phase, cells were diluted every third day to a density of 0.5×10^6 cell/ml. Cells were stained with Trypan Blue (0.4 %) to differentiate dead and alive cells and to count them. Trypan blue stains dead cells in deep blue. Number of alive and dead cells was counted using Neubau chamber. Less than 5 % dead cells were expected in healthy cultures during logarithmic growth.

2.2.2 Expression of CYP Sf9-insect cells

100 ml Sf9 insect cell cultures in concentration of 2×10^6 cell/ml, grown in 500 ml Erlenmeyer flask were infected with baculovirus using a multiplicity of infection (MOI) of about 1 (optimal virus titer requires careful testing for each individual virus preparation). Infected cells were held at 27° C and at 120 rpm. 24 h post-infection, medium was supplemented with 5 µM haemin chloride. Haemin supplementation is crucial for CYP synthesis since heme represents catalytic center of the enzyme. 48 h post-infection cells were either harvested and microsomes were prepared (2.2.6) or cell lysate was used for CO difference spectra measuring (2.2.4).

2.2.3 Co-expression of CYP and hCPR enzymes in Sf9-insect cells

Sf9 cell culture conditions for co-expression of CYP and hCPR enzymes were the same as in the case of single CYP expression (2.2.2). Cells were infected with hCPR and CYP baculoviruses simultaneously (Table 2.3). 24h post-infection, 5µM heminchlorid together with 30 µM methyrapone (2-methyl-1,2-di-3-pyridyl-1-propanon) and 100 µM riboflavin were added. 48 h post-infection, cells were harvested and microsomes were prepared (2.2.6).

Table 2.3 Amounts of CYP and hCPR viruses used for infection of insect cells. 100 ml of the insect cell cultures were infected with following virus ratios. The CYP:hCPR ratio in microsomes used in this study was between 0.65 and 2 (Table 3.6).

<i>CYP</i>	<i>CYP virus (ml)</i>	<i>hCPR virus (ml)</i>
<i>CYP2C8</i>	1	1
<i>CYP2C9</i>	1.5	3
<i>CYP2C11</i>	0.6	0.3
<i>CYP2C23</i>	0.6	0.3
<i>Cyp4a12a</i>	0.7	1
<i>Cyp4a12b</i>	0.7	1

2.2.4 Determination of CYP concentration

Reduced CYP enzymes after exposing to carbon monoxide strongly absorb light at a wavelength of 450 nm (CO difference spectra). This phenomenon is used to determine concentration of P450 (P-pigment, 450 stands for 450 nm). Measuring absorbance of reduced CYP exposed to CO at 450 nm and using Lambert Beer law that describes relation between absorbance and concentration, it is easy to recalculate CYP concentration.

$$E = \epsilon * c * d$$

E - absorbance

ϵ - the molar extinction coefficient with units of $L \text{ mol}^{-1} \text{ cm}^{-1}$

d - the path length of the sample (the path length of the cuvette in which the sample is contained)

c - the concentration of the compound in solution, expressed in mol L^{-1}

40 μl of microsomes were diluted in 800 μl of COD measuring buffer and CYP was reduced by adding few grains (on spatula tip) of sodium dithionite. Sample was transferred to cuvette and baseline was measured in the wavelength range from 400 to 500 nm. CO was bubbled through the sample for 1 min. The spectrum was measured again in the same wavelength range and presented as a difference between baseline (“reduced” value) and “reduced + CO” value.

The difference between absorbance at 450 nm and 490 nm was used to calculate the concentration using Lambert Beer law with an extinction coefficient of $\epsilon = 91 \text{ mM}^{-1} \text{ cm}^{-1}$ (Omura and Sato, 1964).

COD measuring buffer:

0.1 M $\text{K}_2\text{HPO}_4/\text{KH}_2\text{PO}_4$ -Puffer

20 % Glycerin

0.3 % Emulgen 911

0.1 % Natriumcholat,

pH 7.4

2.2.5 NADPH-CYP reductase activity determination

Enzymatic activity of the NADPH-cytochrome P450 reductase (CPR) was determined using cytochrome c as electron acceptor. To prevent a possible interference with cytochrome oxidase, this enzyme was inhibited by KCN. Reduction of cytochrome c was followed spectrophotometrically at 550 nm for 1 min. CPR activity was calculated using Lambert Beer law (molar extinction coefficient, $\epsilon = 21 \text{ mM}^{-1} \text{ cm}^{-1}$).

$$\text{Activity (U/ml)} = \frac{(\Delta E * \text{total volume (1.5 ml)} * \text{sample dilution})}{\epsilon * \text{sample volume (0.05 ml)}}$$

Microsomes were twenty-fold diluted in reductase buffer; 50 μ l of this dilution was mixed with 1 ml reductase buffer, 1 μ l FAD/FMN to stabilize reductase, 250 μ l cytochrome c, and 100 μ l KCN was added. Control absorbance was measured in plastic cuvette (d=1cm), at 550 nm for 1 min. No absorbance change is expected without NADPH, the donor of electrons that are transferred to cytochrome c by CPR. 100 μ l NADPH solution was added and absorbance was measured again. Calculated activity is expressed in Units per ml (U/ml, 1 U=1 μ mol cyt c/min).

Reductase buffer:

50 mM Tris/HCl,
1 mM EDTA, pH 7.5

Concentrations of stock solutions used:

FAD/FMN –1 mM in H₂O
Cytochrome c – 0.3 mM in reductase buffer
KCN –50 mM in reductase buffer
NADPH –1.5 mM in reductase buffer

2.2.6 Sf9 microsomes preparation

Microsomes are small vesicles derived from endoplasmic reticulum during cell disruption. Preparation of microsomes includes cell washing, cell disruption and differential centrifugation.

48 h after infection, Sf9 cells were spun down at 500 g and 4° C for 5 min, washed with 1x PBS, (volume used is equal to 1/2 of starting cell culture volume) and spun down again using same conditions. Pellet was resuspended in microsome buffer (volume used was 1/10th of starting cell culture) and phenylmethylsulfonyl fluoride (PMSF) (100 mM in isopropanol) was added to inhibit protease activity after disruption of cells (1/1000th dilution). Cells were lysed by brief sonification (4 times for 10 sec at about 100 W, 30 % of maximal capacity, Braunsonic 300S, B. Braun Melsungen, Werk Apparatebau) with 30 sec intervals for cooling. Cells were constantly kept on ice. Cell debris and mitochondria were pelleted from cytoplasm by centrifugation at 10.000 g and 4°C for 10 min. Supernatant was further

ultracentrifuged at 100.000 g and 4°C for 65 min. The pellet was homogenized and dissolved in microsome buffer. Microsomes were aliquoted, frozen in liquid nitrogen and stored at -80°C.

Microsome Buffer:

0.1 M K₂HPO₄/KH₂PO₄-Buffer,
20 % Glycerin,
1mM EDTA,
pH 7.4

2.2.7 Determination of protein concentration

Protein concentration was determined using the Lowry method (Lowry et al., 1951). This method is based on quantitation of the color obtained from reaction of protein tyrosyl residues and Folin-Ciocalteu phenol reagent (Merck). Absorbance was measured at 750 nm. Bovine serum albumin was used as standard protein.

2.2.8 Western blot analysis

Protein separation was performed using vertical discontinuous SDS-Polyacrylamide-Gel-Electrophoresis (SDS-PAGE) method described by Laemmli (Laemmli, 1970). Separating and stacking gels were prepared as described below.

Acrylamide concentration of separating gel was 10 %. After mixing acrylamide with water and separating gel buffer, APS and TEMED were added. After complete polymerization, 4 % stacking gel was layered over separating gel.

Samples for protein separation were prepared using ROTILOAD sample buffer (Roth). Samples were solubilized by heating at 95°C for 5 min and cooled down on ice. SeeBlue®Plus2 (Invitrogen) was used as the molecular weight marker. This marker contains proteins in size from 4 to 250 kDa. After loading samples on the gel, electrophoresis was performed in SDS running buffer at 90 V for 30 min increasing to 120 V until the blue dye of ROTILOAD runs through the gel into the running buffer. Samples separated via SDS-PAGE were transferred onto a nitrocellulose membrane (Hybond C, 0.45 µm pore radius, Amersham/Pharmacia) by electroblotting using the semi-dry technique. Blotting was performed at 0.8

mA/cm² of membrane for 60 min. Membranes were incubated for 45 min in blocking solution. The primary antibody (Table 2.4) was added at a standard dilution of 1: 10000 and incubated overnight at 4°C. Following four times five-min washing steps with washing buffer, the membranes were incubated with the horseradish peroxidase-coupled secondary antibody at a dilution 1: 10000 in blocking solution for 45 min at room temperature. Following four times five-min washes with washing buffer blot was developed using Lumi-Light Western Blotting Substrate (Roche) according to the manufacturer's instructions. Membrane was exposed to ECL-Film („enhanced chemiluminescence“, Amersham/Pharmacia).

Separating gel (10 %)

2 ml 30 % acrylamide / bisacrylamide mixture
(29.2 % acrylamide, 0.8 % N, N'-methylen-bis-acrylamide)
1.5 ml Separating buffer
2.5 ml Aqua dest.
24 µl APS (ammoniumperoxydisulfat) (200 mg/ml)
2.4 µl TEMED (N, N, N', N'-tetra-methylaethylendiamine)

Stacking gel (4 %)

0.5 ml 30 % acrylamide / bisacrylamide mixture
(29.2 % acrylamide, 0.8 % N, N'-methylen-bis-acrylamide)
0.937 ml Stacking buffer
2.313 ml Aqua dest.
25 µl APS (200 mg/ml)
1.5 µl TEMED

Separating gel buffer:

375 mM Tris
0.1 % SDS,
pH 8.8

Stacking gel buffer:

125 mM Tris
0.1 % SDS,
pH 6.8

SDS running Buffer

25 mM Tris
192 mM Glycin
0.1 % SDS

Transfer Buffer

25 mM Tris
192 mM Glycin
5 % Methanol,
pH 8

Blocking Buffer

0.1 M Tris/HCl,
0.5 M NaCl
1 % Pepton
0.1 % Tween 20
pH 7.5

Washing Buffer

0.1 M Tris/HCl,
0.5 M NaCl
0.1 % Tween 20
pH 7.5

Table 2.4 *The list of the antibodies used for Western blotting.*

<i>Antibody</i>	<i>Source</i>
<i>Rabbit-anti-CYP2C11</i>	<i>Daiichi Pure Chemicals Co.</i>
<i>Goat-anti-CYP4A1</i>	<i>Daiichi Pure Chemicals Co.</i>
<i>Goat-anti-Rat-CPR</i>	<i>Daiichi Pure Chemicals Co.</i>
<i>Rabbit-anti-CYP2C23</i>	<i>Dr. J. Capdevilia, Vanderbilt University, TN, USA</i>
<i>Goat-anti-Rabbit-IgG-POD^a</i>	<i>Sigma</i>
<i>Rabbit-anti-Goat-IgG-POD^a</i>	<i>Sigma</i>

^a *Secondary antibodies are conjugated with Horseradish peroxidase (POD)*

2.3 Metabolism of fatty acids by recombinant CYP enzymes

2.3.1 CYP-dependent metabolism of fatty acids

¹⁴C radiolabelled fatty acids; AA, EPA, DPA and DHA (Table 2.5) were metabolized using microsomes from insect cell co-expressing recombinant CYP and human NADPH-dependent hCPR.

Standard conditions of fatty acid metabolism were 10 pmol of recombinant microsomal CYP converting 1 nmol of substrate in final volume of 100 µl.

The sodium salt of substrate was prepared as follows: 1 nmol of substrate stock solution was diluted in 10 µl ethanol. 0.5 µl of 10mM Na₂CO₃ was added. The mixture was evaporated under nitrogen. Microsomes were diluted in reaction buffer and added to dried substrate. The mixture was preincubated at 37° C with shaking for 5 min. 5 µl of 10 mM NADPH (in 0.15 M KCl) that serves as an electron donor was added to start reaction.

Table 2.5: Characteristics of substrates used for conversion.

<i>Substrate</i>	<i>Specific activity</i>	<i>Volume activity</i>	<i>Source</i>
<i>AA</i>	<i>56.0mCi/mmol, 2.07 GBq/mmol</i>	<i>0.05 mCi/ml 1.85 Bq/ml</i>	<i>Hartmann</i>
<i>EPA</i>	<i>55.6 mCi/mmol, 2.1 GBq/mmol</i>	<i>0.1 mCi/ml 3.7 Bq/ml</i>	<i>Hartmann</i>
<i>DPA</i>	<i>55.6 mCi/mmol, 2.1 GBq/mmol</i>	<i>0.1 mCi/ml 3.7 Bq/ml</i>	<i>Hartmann</i>
<i>DHA</i>	<i>55.6 mCi/mmol, 2.1 GBq/mmol</i>	<i>0.1 mCi/ml 3.7 Bq/ml</i>	<i>Hartmann</i>

Incubation was performed 3-60 min, depending on the CYP activity. Addition of 5 µl of 0.4 M citric acid stopped reaction and reaction mixture was immediately cooled down on ice. Extraction of fatty acid metabolites was performed using 500 µl ethylacetate which was mixed with reaction mixture and vortexed for 30 sec. Samples were centrifuged at 11000 g for 2 min and the supernatant, containing metabolites and remaining substrate dissolved in ethylacetate, was collected. The same procedure was repeated one more time. Total collected supernatant was

evaporated under nitrogen. Fatty acid metabolites and remaining substrate were dissolved in 50 µl ethanol. The total amount of extracted radioactivity was determined measuring 2 µl aliquots by scintillation counting (scintillation counter, 1900TR, Packard, USA). 45 µl of sample was used for separation of the metabolites on RP- HPLC.

Reaction buffer

100 mM potassium phosphate buffer,
pH 7.2

2.3.2 RP-HPLC separation of CYP-dependent AA, EPA, DPA and DHA metabolites

Products of CYP-dependent fatty acid metabolism (2.3.1) were resolved and quantified using High Performance Liquid Chromatography (HPLC). The components of the reverse phase HPLC (RP-HPLC) (Shimadzu) are listed in Table 2.6.

Table 2.6: Components of HPLC system.

<i>System components</i>	<i>Description (Company)</i>
<i>System controller</i>	<i>SCL-10A (Shimadzu)</i>
<i>Pumps</i>	<i>LC-10AD (Shimadzu)</i>
<i>Autosampler</i>	<i>SIL-10AD (Shimadzu)</i>
<i>Column oven</i>	<i>CTO-10AS (Shimadzu)</i>
<i>Degasser</i>	<i>DGU-14A (Shimadzu)</i>
<i>Radioactivity detector</i>	<i>„Radioflow Detector LB509“ (EG&G Berthold)</i>
<i>UV-Detector</i>	<i>SPD-M10A (Shimadzu)</i>
<i>Column</i>	<i>Nucleosil 100-5C18HD (250x4mm) (Macherey & Nagel)</i>
<i>PC-Software</i>	<i>ClassVP 5.03 (Shimadzu)</i>

AA, EPA, DPA and DHA metabolites were dissolved in absolute ethanol before separation on RP-HPLC. 150000 dpm of the sample was used for quantitative determination of metabolite content.

Metabolites were separated using a linear gradient from acetonitrile/water/acetic acid (50/50/0.1; vol/vol/vol) to acetonitrile/acetic acid (100/0.1; vol/vol) over 40 min at a flow rate of 1 ml/min.

2.3.3 Separation of EPA, DPA and DHA epoxy-regioisomers by NP-HPLC

EPA, DPA and DHA epoxy-regioisomers were separated on Normal Phase High Performance Liquid Chromatography (NP-HPLC) using Nucleosil 100-5 column (250 x 4 mm, Macherey & Nagel).

Epoxy product peaks of EPA, DPA and DHA with retention times of 20-22 min, 25-27 min and 23-26 min, respectively, were collected from RP-HPLC, evaporated under nitrogen and dissolved in absolute ethanol. Radioactivity of sample was counted on scintillation counter and amounts between 30-150000 dpm were loaded on NP-HPLC.

Regioisomers were separated isocratically using hexane/isopropanol/acetic acid (for EDP: 99.8/0.2/0.1, EETeTr: 99.7/0.3/0.1 and EDTeTr: 99.8/0.2/0.1; vol/vol/vol), over 40 min at a flow rate of 1.5 ml/min.

Separated peaks were collected and identified by gas chromatography–mass spectrometry (in collaboration with Dr. H. Honeck, MDC).

2.3.4 Separation of 17,18-EETeTr enantiomers by chiral HPLC

17(R),18(S)-EETeTr and 17(S),18(R)-EETeTr enantiomers were resolved by Chiral-HPLC using Chiralcel OB column (250 x 4,6 mm, Daicel). 17,18-EETeTr was collected from RP-HPLC, evaporated under nitrogen and dissolved in 200 µl absolute ethanol. Sample radioactivity was counted on scinticounter and 150000 dpm was used for further quantification. Sample was esterified with 100 µl diazomethane to methylester and then resolved over 40 min, using

hexane/isopropanol (99.7/0.3 (vol/vol)) linear gradient to hexane/isopropanol (98/2 (vol/vol)). Before separation, 1 h equilibration of the column using hexane/isopropanol (99.7/0.3 (vol/vol)) was conducted.

The identity of stereoisomers was determined by comparing retention times with chemically synthesized 17,18-EETeTr methylester racemic mixture, and 17,18-EETeTr prepared by recombinant human CYP1A1 and bacterial P450BM3. CYP1A1 produces 17(R),18(S)-EETeTr with 97 % specificity (Schwarz et al., 2004) and CYPBM3 (Capdevila et al., 1996) 17(S),18(R)-EETeTr with 98 % specificity.

2.4. Experiments with hypertensive rats

2.4.1 Experimental animals

Animal experiments described below were done in collaboration with Dr. D.N. Müller and his coworkers who were responsible for growing and treating animals for this study. dTGR were ordered from RCC Ltd. (Füllinsdorf, Germany). Animals used for this study were age-matched, 4 week old male rats, dTGR untreated (n=20), dTGR fenofibrate-treated (n=11, 30mg/kg/day in diet from week 4 to week 7) and Sprague-Dawley rats (SD) (n=7; Tierzucht, Schönwalde, Germany). To investigate effects of fenofibrate in nonpathological conditions, SD rats were used (n=6 in both groups, control and fenofibrate-treated). The same treatment protocol was used for SD fenofibrate-treated group as for treatment of dTGR rats.

2.4.2 Renal microsomal preparation

Renal microsomes were prepared from freshly dissected kidneys. Homogenization was performed using 50 mM Tris-HCl buffer (pH 7.4) containing 0,25 mM sucrose, 150 mM KCl, 2 mM EDTA, 2 mM dithiothreitol, and 0,25 mM PMSF in a motor-driven Teflon-glass Potter Elvehjem homogenizer. Microsomes were isolated by differential centrifugation (10 min, 1000 g; 20 min, 10000 g; 90 min, 100000 g) and

resuspended in 50 mM Tris-HCl (pH 7.7) containing 20 % glycerol, 5 mM EDTA, and 1 mM dithiothreitol. Aliquots were snap frozen in liquid nitrogen and stored at -80°C. The protein content was determined by the standard Lowry method.

2.4.3 Renal microsomal metabolism

Renal microsomes (80 µg of protein in a total volume of 0.1 ml) were incubated in 50 mM Tris/HCl buffer, pH 7.5, with 10 nmol ¹⁴C radiolabeled AA (0.55 x10⁶ dpm; final concentration, 100 µM) in the presence of NADPH (0.5 mM) for 20 min at 37°C. The reactions were terminated by acidification to pH 3.5 to 4.0 with 0.4 mM citric acid. The reaction products were extracted into ethyl acetate and resolved by RP-HPLC as described in 2.3.2.

AA hydroxylase activities were determined as the sum of 19- and 20-HETE and AA epoxygenase activities as the sum of EETs and corresponding DHETs produced per minute and mg of microsomal protein.

To analyze the formation of secondary AA metabolites, renal microsomes were incubated under the standard reaction conditions described above using AA (56 mCi/mmol) and primary metabolites (19-HEET, 20-HETE, EETs, and DHETs) in a final concentration of 20 µM.

In immunoinhibition experiments, microsomes were preincubated for 30 min at 37°C with 100 µg/ml of rabbit IgG (125 µg IgG/mg microsomal protein) before substrate and NADPH were added. The concentration of anti-CYP2C23 IgG were varied between 0 and 100 µg/ml whereas the total amount of IgG was kept constant by appropriate additions of control rabbit IgG.

2.4.4 Statistical analysis

Data are presented as means ± SEM. Statistically significant differences in mean values were tested by analysis of variance, repeated measures when appropriate, and the Scheffe' test. A value of P<0.05 was considered statistically significant. The data were analyzed using Statview statistical software.

3. Results

3.1 Regulation of renal AA-metabolism in a rat model of angiotensin II-induced hypertension and end-organ damage

CYP-dependent renal AA metabolism is strongly downregulated in dTGR. These rats represent an animal model of ANG II-induced hypertension and inflammatory end-organ damage (1.1.7). Our hypothesis was that hypertension and end-organ damage can be ameliorated by directly influencing the renal CYP-dependent AA metabolism. To test this hypotheses, dTGR and Sprague-Dawley (SD) control rats were treated for three weeks with the PPAR α activator fenofibrate (2.4.1). Fenofibrate treatment resulted in:

- reduction of mortality and blood pressure and prevention of albuminuria in dTGR*
- a significant increase in renal microsomal EET production in dTGR and SD rats (3.1.2.1)*
- a strong induction of CYP2C23 at the protein and enzyme activity level (3.1.2.3)*
- a significant increase in renal microsomal HEET production in dTGR and SD rats (3.1.3)*

3.1.1 Effects of fenofibrate on mortality, blood pressure and renal damage

In this part of the investigation, we studied the effect of the PPAR α activator fenofibrate on mortality, blood pressure, renal function and CYP-dependent renal microsomal AA metabolism. This was a joint study with colleagues from Franz-Volhard Clinic, Berlin-Buch (D.N. Müller, F.C. Luft and coworkers) who did all animal treatments, blood pressure and albuminuria measurements. Animals were treated for 3 weeks as described in 2.4.1. Blood pressure and albuminuria 7-week-old animals were compared.

In untreated male dTGRs, 10 of 20 rats died before sacrifice, whereas fenofibrate treatment reduced mortality to zero. No nontransgenic SD rat died before the end of the study.

As shown in Figure 3.1A, blood pressure was progressively increased in untreated dTGRs and exceeded that of SD control rats more than 100 mm Hg at week 7 (213 ± 3 mm Hg versus 107 ± 3 mm Hg; $P < 0.001$). Fenofibrate treated dTGRs remained normotensive and had blood pressure values of 120 ± 3 mm Hg at week 7 not different from SD control rats (Figure 3.1A).

Urinary albumin excretion was markedly higher in dTGRs than in SD rats: 29.3 ± 3.1 mg/day versus 0.19 ± 0.04 mg/day ($P < 0.001$). Feno-treated dTGRs did not develop significant albuminuria (0.7 ± 0.26 mg/day; Figure 3.1B).

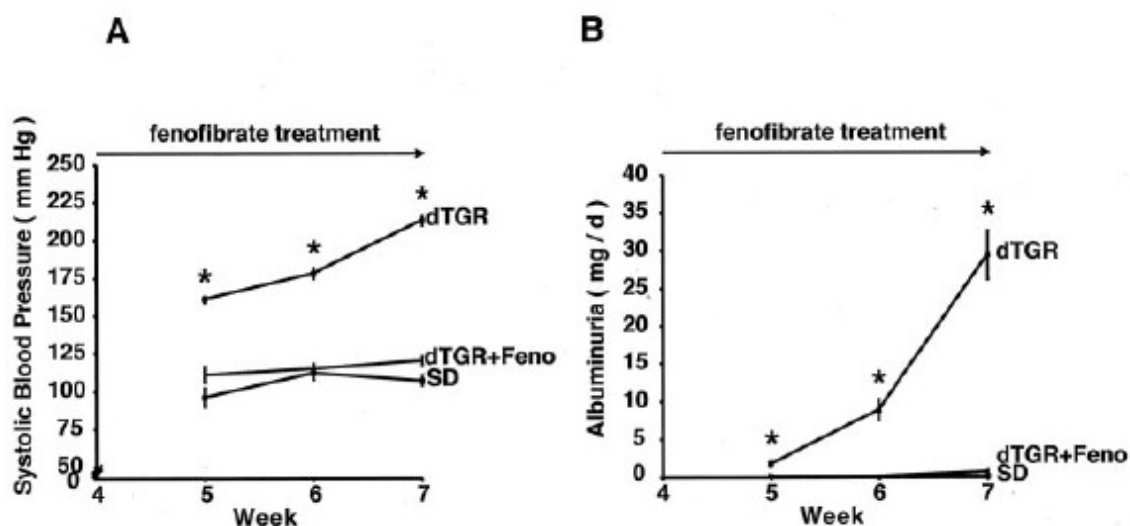


Figure 3.1 Fenofibrate treated dTGRs are compared to untreated dTGRs and SD controls. A: Systolic blood pressure was higher ($P < 0.001$) in untreated dTGRs than in fenofibrate treated dTGRs and in SD. B: Untreated dTGRs showed increased 24-hour albuminuria compared to SD ($P < 0.001$), whereas fenofibrate treated dTGRs were not different from SD (Muller et al., 2004).

3.1.2 Effects of fenofibrate on CYP-dependent AA metabolism under pathological conditions

3.1.2.1 Fenofibrate treatment strongly increases renal AA-epoxygenase but no AA-hydroxylase activity in dTGR

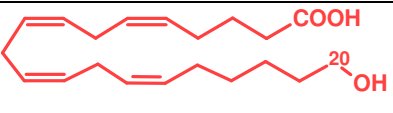
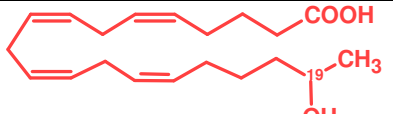
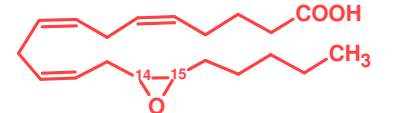
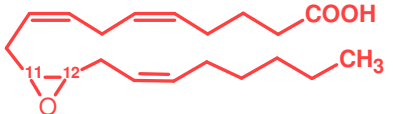
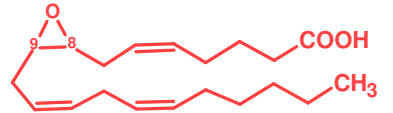
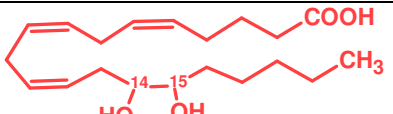
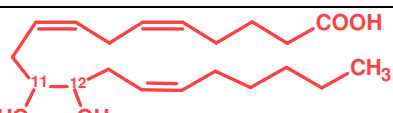
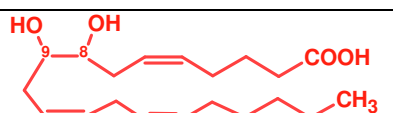
As shown in previous chapter, fenofibrate treatment recovered hypertension and end-organ damage in dTGR. We were further interested to see what is effect of fenofibrate on CYP metabolism in dTGR. In order to test that, renal microsomes of fenofibrate treated and control dTGR as well as SD rats were prepared as described in 2.4.2. AA-epoxygenase and AA-hydroxylase activities were determined by conversion of radiolabeled AA (2.4.3).

To distinguish the origin of the different AA metabolites produced by renal microsomes (listed in Table 3.1) we use the following definitions:

- EETs and 19/20-HETE are primary products of CYP-dependent AA epoxidation and hydroxylation, respectively.
- Products formed in a CYP-dependent reaction from EETs and HETEs are designated as secondary products. These involve, in particular, the hydroxy-epoxy-derivatives of AA, the so-called HEETs. These compounds are produced either by CYP-dependent epoxidation of HETEs or by CYP-dependent hydroxylation of EETs.
- All epoxy derivatives can be subject to hydrolysis resulting in the formation of the corresponding diols. This reaction is catalyzed by soluble epoxide hydrolase (sEH) and produces DHETs from EETs and HDHETs (hydroxy-dihydroxy-eicosatrienoic acid) from HEETs.

Figure 3.2 compares the epoxidation activities determined for renal microsomes of dTGR, fenofibrate-dTGR and SD rats. DTGR had in average AA-epoxygenase activity of 130 ± 21 pmol/min/mg, which was 61 % of AA-epoxygenase activity of SD control (214 ± 15 pmol/min/mg). Renal AA-epoxygenase activities of fenofibrate-treated dTGR animals were strongly induced to 249 ± 19 pmol/min/mg, and thus reached values almost two times higher than in untreated dTGR animals and higher than the activity of SD controls.

Table 3.1 List of renal microsomal metabolites of AA with retention times and structural formulas. For the secondary products (HEETs and DHETs) see Table 3.2

<i>AA metabolite</i>	<i>Retention time RP-HPLC</i>	<i>Structure</i>
20-HETE	15,4 min	
19-HETE	15,4 min	
14,15-EET	23,4 min	
11,12-EET	24,8 min	
8,9-EET	25,3 min	
14,15-DHET	12,3 min	
11,12-DHET	13,4 min	
8,9-DHET	14,3 min	

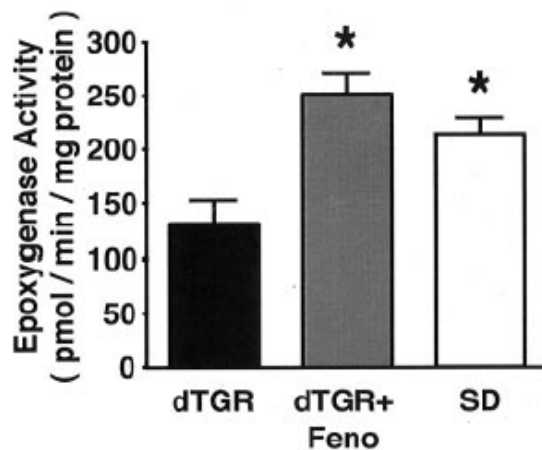


Figure 3.2 Effect of fenofibrate on renal AA-epoxygenase activity. AA epoxygenase activity of dTGR renal microsomes was significantly lower compared to fenofibrate-treated dTGR and SD control (*, $P < 0.01$). Values are mean \pm SEM, $n=6-8$ per group.

Both, dTGR and fenofibrate-treated dTGR renal microsomes showed significantly lower AA-hydroxylase activity compared to SD control (Figure 3.3). In contrast to AA-epoxygenase activity, dTGR renal AA-hydroxylase activity was not increased by fenofibrate treatment.

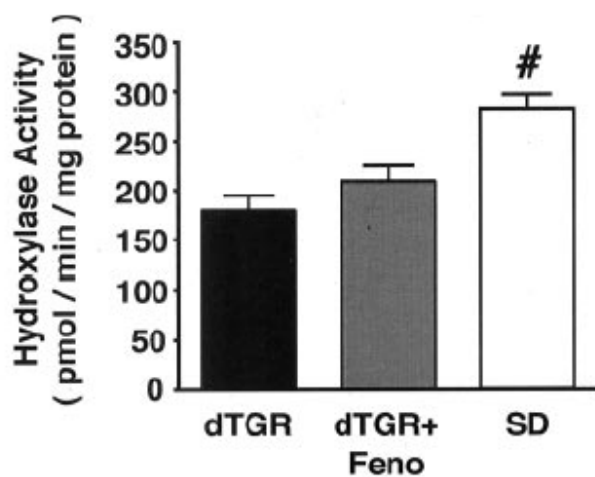


Figure 3.3 Effect of fenofibrate on renal AA-hydroxylase activity. AA hydroxylase activities were not induced by fenofibrate and remained below SD levels. Results are mean \pm SEM (#, $P < 0.05$ SD versus dTGR and fenofibrate-dTGR).

Taken together these studies show that fenofibrate had a marked effect on renal CYP-dependent AA metabolism in pathophysiological conditions. Interestingly,

only AA-epoxygenase but not AA-hydroxylase activity was significantly increased by the treatment with this PPAR α activator.

3.1.2.2. CYP2C23 is the major AA-epoxygenase in the kidney of dTGR and fenofibrate-treated dTGR.

To get insight into the mechanism by which fenofibrate induces renal AA epoxygenase activity, it was necessary to determine the main renal epoxygenase in both, dTGR and fenofibrate-treated dTGR. Antibody directed against CYP2C23 was used to inhibit CYP2C23 activity in renal microsomes. Anti-CYP2C23 was used in concentrations of 10, 25, 50 and 100 $\mu\text{g/ml}$.

Epoxygenase activity was inhibited by the anti-CYP2C23 antibody in a dose-dependent manner. Microsomes were incubated with the antibody as described in 2.4.3. At a concentration of 100 $\mu\text{g/ml}$ of anti-CYP2C23 antibody, AA-epoxygenase activity was almost completely inhibited in both groups (remaining activity less than 10 %). Hydroxylase activities were not affected by any concentration of anti-CYP2C23 antibody used (Figure 3.4).

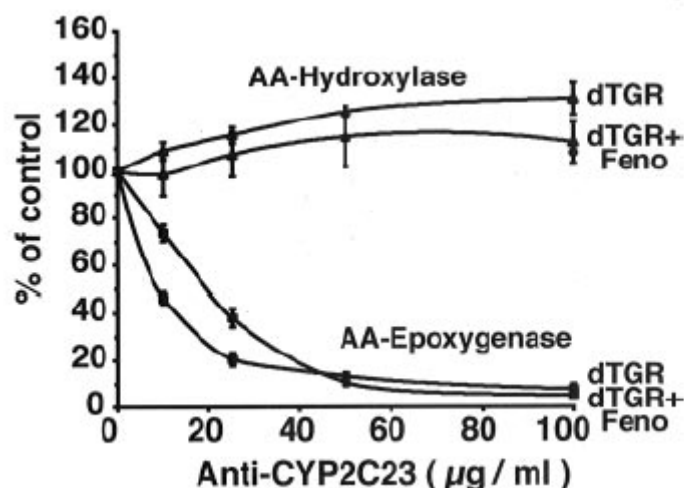


Figure 3.4 Inhibition of renal AA-epoxygenase activity by an antibody directed against CYP2C23. Anti-CYP2C23 IgG inhibited CYP-dependent AA-epoxidation but not AA-hydroxylation in renal dTGR and fenofibrate-treated dTGR microsomes ($n = 4$ in both groups). The activity of the respective sample containing only control IgG was set at 100 %.

This part of the study shows that CYP2C23 is the major renal epoxygenase in both dTGR and fenofibrate-treated dTGR. Therefore, our finding that fenofibrate induces AA epoxygenase activity should be directly due to corresponding increase in CYP2C23 expression and activity.

3.1.2.3 Renal protein expression of CYP2C23 is increased by fenofibrate treatment

As shown in chapter 3.1.2.1, renal AA-epoxygenase activity was strongly induced by fenofibrate treatment in dTGR. Moreover, we demonstrated that CYP2C23 is the major AA-epoxygenase in the kidney of the dTGR (3.1.2.2). Therefore, we were interested to find out whether fenofibrate treatment changes the renal level of CYP2C23 protein in dTGR animals.

Figure 3.5 shows results of Western blot analysis (2.2.8) of renal protein expression in dTGR, fenofibrate-treated dTGR and SD control rats.

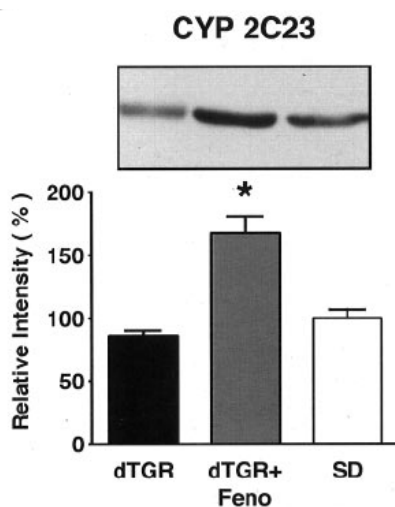


Figure 3.5 Comparison of renal CYP2C23 protein expression in dTGR, fenofibrate treated dTGR and SD animals. Western blot analysis of renal microsomes showed that CYP2C23 protein level was augmented in fenofibrate-treated dTGRs (n= 9) compared to untreated dTGRs (n = 6) and SD (n = 8) (*, P<0.001). Results are mean \pm SEM and given as percentage of SD.

Renal microsomes of dTGR showed a slight reduction of CYP2C23 protein level compared to SD controls, but in renal microsomes of fenofibrate-treated dTGR, protein expression was increased to 167 ± 13 % of SD control.

After demonstration that fenofibrate treatment increased protein level of CYP2C23 in the rat kidney, we were interested whether this increase in protein level is consequence of change in transcription. To this end, Taqman analysis was performed in collaboration with Dr. Maren Wellner (MDC). Results showed that the level of CYP2C23 mRNA expression was similar in dTGR, fenofibrate-treated dTGR and SD controls ($1,1 \pm 0,2$; $0,9 \pm 0,1$; $1,0 \pm 0,1$ arbitrary units, respectively) suggesting a posttranslational regulation CYP2C23.

In order to determine whether induction of CYP protein level by fenofibrate is unique for the expression of CYP2C23, we tested protein expressions of CYP2C11 and CYP4As (Figure 3.6 and Figure 3.7).

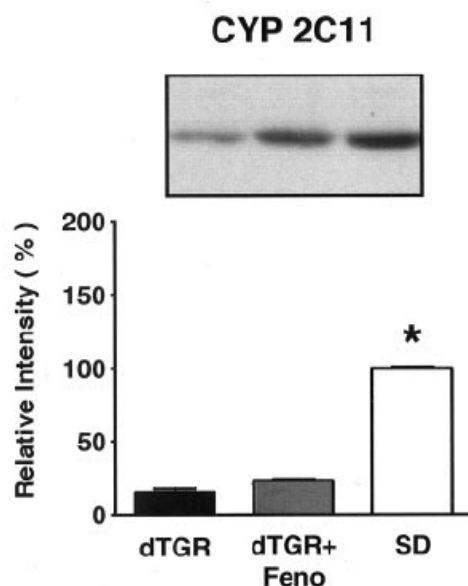


Figure 3.6 Comparison of renal CYP2C11 protein expression in dTGR, fenofibrate-treated dTGR and SD animals. Western blot analysis of renal microsomes showed that CYP2C11 protein level was significantly reduced in untreated dTGR and remained below the SD level after fenofibrate treatment (*, $P < 0.001$). Results are mean \pm SEM and given as percentage of SD.

Protein expression of CYP2C11, another potential AA-epoxygenase in rat (1.3.2) was strongly downregulated in dTGR, to 15 ± 2 % of SD controls.

In contrast to CYP2C23, fenofibrate treatment had only a weak effect on the recovery of the CYP2C11 (Figure 3.6).

Figure 3.7 shows protein expression of AA-hydroxylases, CYP4As, in dTGR, fenofibrate-treated dTGR and SD rats. CYP4A1 antibody was used for protein

detection. This antibody recognizes all CYP4A isoforms, therefore it was not possible to distinguish between single members of CYP4A subfamily. We can discuss here only about total CYP4A protein expression. There was no decrease in protein expression of CYP4A in dTGR compared to SD controls. Fenofibrate treatment of dTGR animals showed clear induction of CYP4A expression. Protein expression of CYP4A in fenofibrate-treated dTGR animals reached 180 % of untreated dTGR.

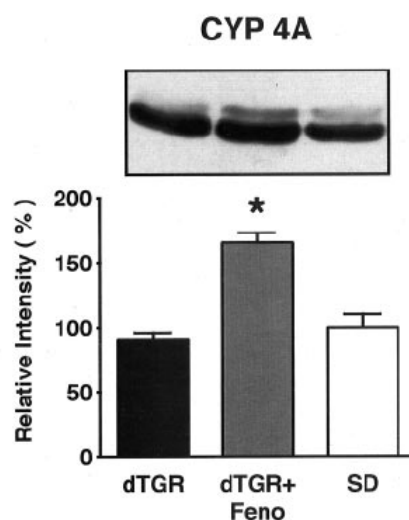


Figure 3.7 Comparison of renal CYP4A protein expression in dTGR, fenofibrate-treated dTGR, and SD animals. Fenofibrate treatment of dTGRs resulted in increased levels for CYP4A. (*, $P < 0.001$, dTGR-fenofibrate vs. dTGR and SD). Results are mean \pm SEM and percentage of SD.

Taken together, the studies described above (3.1.2.1-3.1.2.3) show that fenofibrate treatment strongly induces renal microsomal epoxygenase activities (almost two-fold) and CYP2C23 protein levels without effecting however CYP2C23 mRNA levels. Moreover, fenofibrate treatment increased CYP4A protein level whereas CYP2C11 expression remained unchanged.

3.1.3 Effects of fenofibrate on CYP dependent AA metabolism under physiological conditions

Previous data (3.1.2.1) showed a clear increase of CYP2C23 activity in fenofibrate-treated dTGR. This finding was surprising since a similar effect of PPAR α activation on CYP2C23 expression has been never reported before. In particular,

PPAR α activators were described as inducers of CYP4A but not CYP2C isoforms in rat, mouse and human. Therefore the question arose whether the effect we observed in dTGR was related to the specific pathological conditions in dTGR or can be considered as a general phenomenon which also occurs under physiological conditions. To address this question a second animal study was performed where we studied fenofibrate effects on normal SD rats.

Subsequent analysis of renal microsomal activities revealed that fenofibrate treatment of SD rats was even more effective compared to dTGR. Renal AA-epoxygenase activity in fenofibrate-treated SD rats was dramatically increased and reached 530 ± 25 pmol/minute/mg vs. 190 ± 11 pmol/minute/mg of untreated SD rats (Figure 3.8A). AA-hydroxylase activity did not increase after fenofibrate treatment (237 ± 12 pmol/min/mg vs. 204 ± 17 pmol/min/mg); Figure 3.8B.

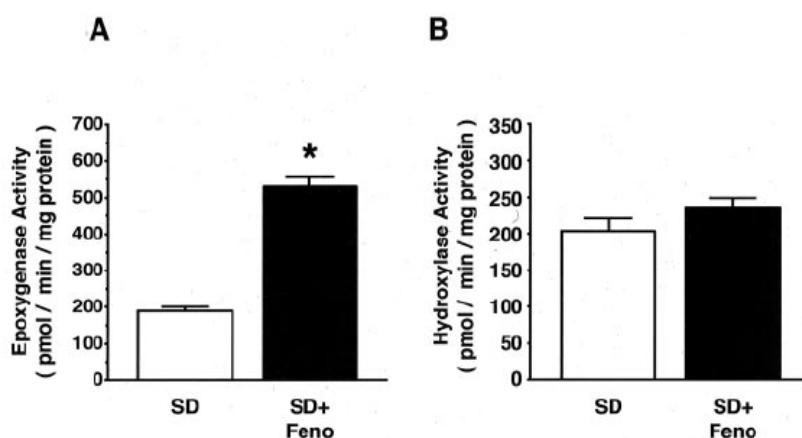


Figure 3.8 Effect of fenofibrate on renal AA-epoxygenase (A) and AA-hydroxylase (B) activity of SD rats. Epoxygenase activity was induced in fenofibrate-treated SD whereas hydroxylase activity stayed unchanged. Results are mean \pm SEM ($n = 6$ each; *, $P < 0.05$ SD versus fenofibrate-treated SD).

Protein expression of CYP2C23, CYP2C11 and CYP4A, in kidney of fenofibrate-SD rats, was significantly increased compared to untreated SD rats (to 161 ± 13 %; 150 ± 17 %, and 256 ± 46 % of SD controls, respectively; Figure 3.9).

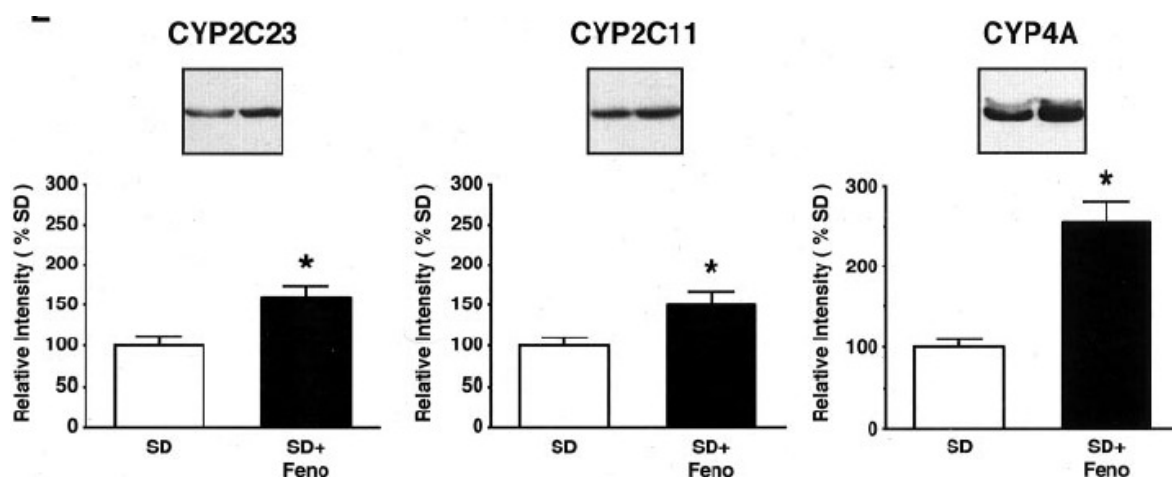


Figure 3.9 *Effect of fenofibrate treatment of renal CYP protein production in SD rats.* Western blotting revealed increased microsomal CYP2C23, CYP2C11, and CYP4A protein levels after fenofibrate treatment. Results are mean \pm SEM and are percent of untreated SD (*, $P < 0.05$ SD versus fenofibrate-treated SD).

Taken together, fenofibrate treatment had essentially the same effects under physiological and pathophysiological conditions. In both conditions, the fenofibrate effect was most pronounced on the CYP2C23 activity level whereas the CYP2C23 protein was only moderately increased and there was no effect on mRNA level. Moreover, it was interesting to note that fenofibrate induced CYP4A proteins which are generally considered to be PPAR α -dependent in their expression, but did not significantly enhance CYP4A-dependent renal microsomal AA hydroxylase activities.

3.1.4 Effect of fenofibrate on the generation of secondary AA metabolites

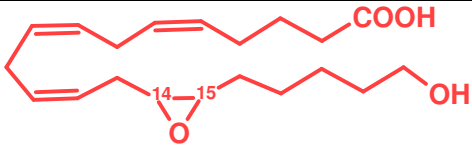
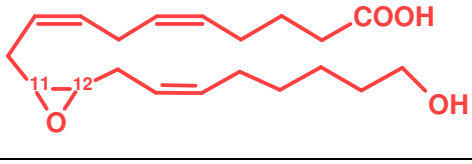
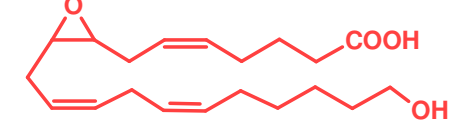
3.1.4.1 Fenofibrate strongly induces secondary product formation

As shown in chapters 3.1.2.1 and 3.1.3, fenofibrate treatment significantly increased epoxidation of AA to primary products in both dTGR and SD. In this part of the study it was tested whether or not the formation of secondary AA metabolites in dTGR and SD rats was affected in the same manner by fenofibrate treatment.

As already described in 3.1.2.1, renal microsomes can further metabolize primary AA products to secondary products. HEETs are secondary products, which can be synthesized by both CYP-dependent hydroxylation of EET and epoxidation of HETEs (3.3.1). DHETs and HDHETs are products of EET and HEET hydrolysis by

sEH. Secondary products of AA with their RP-HPLC retention times and structural formulas are listed in the Table 3.2.

Table 3.2 CYP-dependent secondary AA metabolites.

<i>Secondary AA metabolite</i>	<i>Retention time (RP-HPLC)</i>	<i>Structural formula</i>
20,14,15-HEET	9 min	
20,11,12-HEET	9 min	
20,8,9-HEET	9 min	

For testing the formation of secondary products, we used 20 μM of AA per reaction. This low substrate concentration was used to favor further conversion of primary products by CYP enzymes. In contrast, substrate concentrations of 100 μM were used in experiments for determination of AA-hydroxylase and AA-epoxygenase activities.

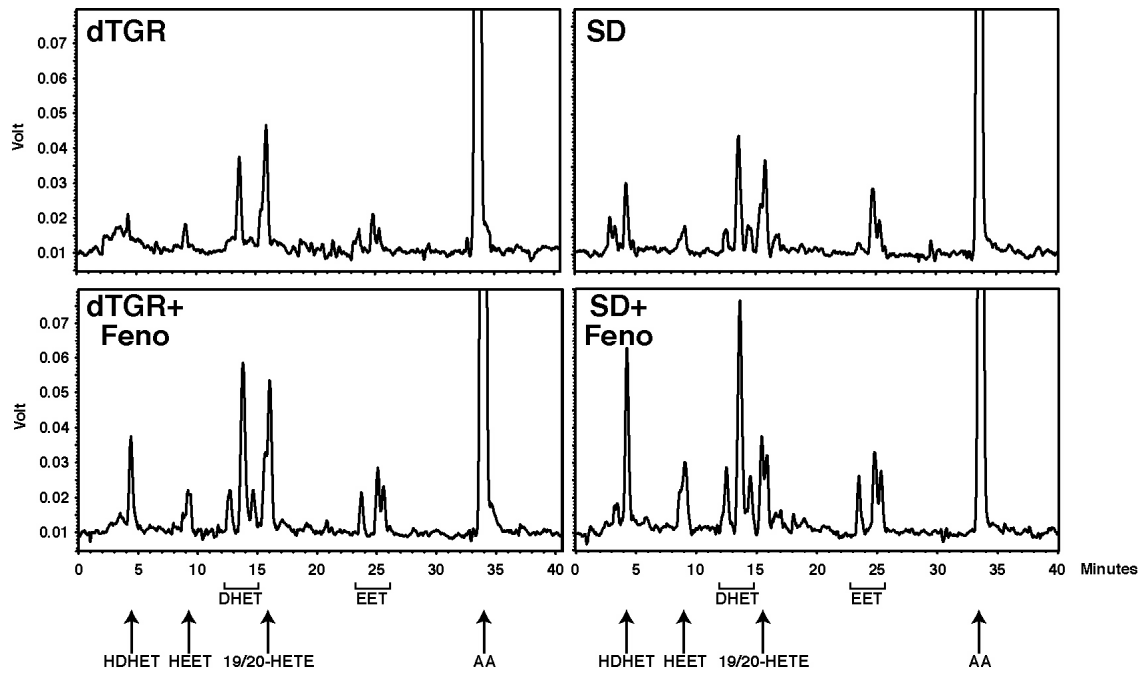


Figure 3.10 Chromatograms of primary and secondary products of CYP-dependent renal microsomal AA metabolism. Representative RP-HPLC chromatograms showing the conversion of AA (20 μ M) by renal microsomes isolated from the different animal groups indicated.

Decrease in AA secondary product generation by dTGR in comparison to SD renal microsomes was much more pronounced than in case of AA primary product generation (Figure 3.10, Figure 3.11). dTGR renal activity in secondary product formation was almost five times lower compared to SD controls. Fenofibrate treatment strongly induced conversion to secondary products (HEET + HDHET) in dTGR and SD compared to untreated dTGR and SD animals (6-fold and 3,5-fold, respectively, Figure 3.11).

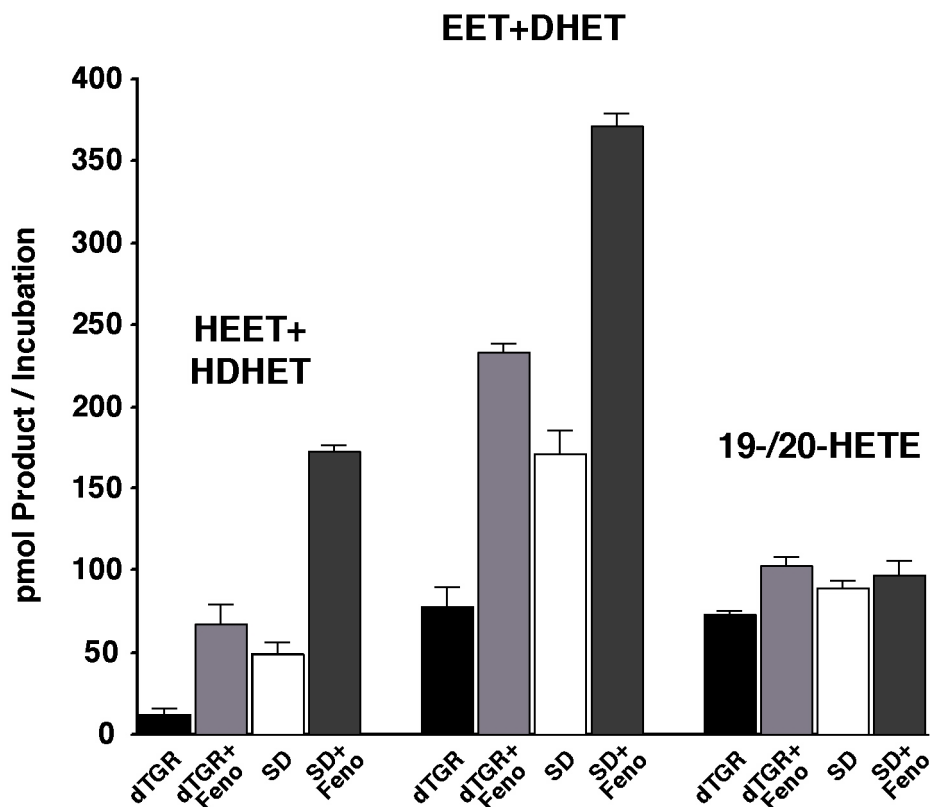


Figure 3.11 Primary and secondary products of CYP-dependent renal microsomal AA metabolism. Results obtained by resolving on RP-HPLC products of CYP-dependent AA metabolism are summarized ($n = 5$ per group). The data represent the total amounts (in pmol) of individual product classes formed during 20 minutes incubation of $20 \mu\text{M}$ AA using $80 \mu\text{g}$ of microsomal protein in 0.1 ml reaction mixtures.

3.1.4.2 HEET production from both 20-HETE and 11,12-EET is strongly induced by fenofibrate treatment

In theory, hydroxy-EETs can originate from EETs or 19/20-HETE. In this part of the study, we were interested to determine whether HEETs originate from EETs or HETE in SD control and fenofibrate-treated SD animals. We analyzed the metabolism of 20-HETE and of EETs by renal microsomes of SD and fenofibrate-treated SD rats. Both, 20-HETE and 11,12-EET were directly converted to HEET. 20-HETE epoxygenase and 11,12-EET hydroxylase activities were strongly induced in fenofibrate-treated SD animals ($394 \pm 17 \text{ pmol/min/mg}$ versus $128 \pm 8 \text{ pmol/min/mg}$ and $364 \pm 5 \text{ pmol/min/mg}$ versus $183 \pm 4 \text{ pmol/min/mg}$, respectively; Figure 3.12).

Taken together, renal microsomes produce HEETs as secondary products of AA metabolism. HEET originate from both 20-HETE epoxidation and EET hydroxylation and both HEET producing pathway are strongly induced. The role of CYP2C23 in formation of HEETs is shown in chapter 3.3.

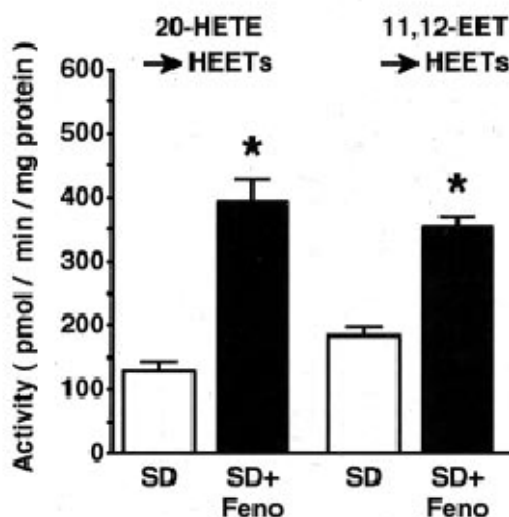


Figure 3.12 Secondary product formation by renal microsomes of SD rat. Both 20-HETE and 11,12-EET are equally good substrates for HEET production in kidney of SD rat. Both pathways of HEET formation are strongly induced by fenofibrate.

3.2 Heterologous expression of CYP enzymes

The aim of this part of the study was to produce enzymatically active CYP isoforms for subsequent analysis of their substrate specificities. To this end, the baculovirus-Sf-9 insect cell system was used. This system allowed to establish active microsomal enzyme systems consisting of a selected CYP isoforms and the human hCPR CYP isoforms successfully produced in this way included human CYP2C8 and CYP2C9, rat CYP2C11 and CYP2C23 and mouse Cyp4a12a and Cyp4a12b.

3.2.1 Recombinant baculovirus

All baculoviruses used in this study are listed in Table 3.3. All CYP baculoviruses except CYP2C23 virus were already prepared and their expression in Sf9 cells was established in our laboratory.

Table 3.3 List of baculoviruses used in this study

<i>CYP virus</i>	<i>Provided by:</i>
<i>CYP2C8</i>	Dr. E. Barbosa-Sicard
<i>CYP2C9</i>	B. Christ
<i>CYP2C11</i>	Dr. E. Barbosa-Sicard
<i>CYP2C23</i>	part of this work
<i>Cyp4a12a</i>	Dr. W-H Schunck
<i>Cyp4a12b</i>	Dr. W-H Schunck
<i>hCPR</i>	D. Schwarz

As a part of this study, CYP2C23 baculovirus was prepared, in order to get enzymatically active CYP2C23 enzyme (Figure 3.13).

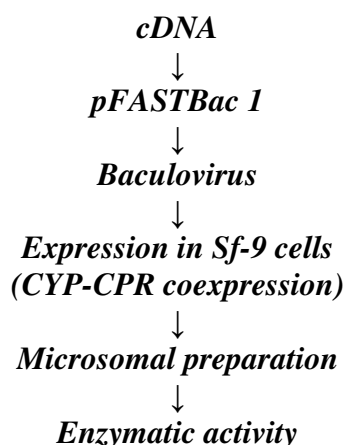


Figure 3.13 *The experimental way from cloning of a selected CYP cDNA to testing of its enzymatic activity. cDNA of selected CYP was cloned into pFASTBac 1, which was transformed into DH10Bac cells where recombination with bacmid occurs. Positive bacmid was used for production of CYP-carrying virus. Sf-9 cells were infected with CYP- and CPR- carrying baculovirus and those cells were used for microsomal preparation. Microsomes coexpressing CYP and hCPR were used for radiolabeled substrate conversion.*

cDNA of CYP2C23 was cloned into pFASTBac I plasmid (provided by Dr. Barbosa-Sicard) which was used for bacmid production (2.1.2). Baculovirus was produced as described in 2.1.7. After baculovirus preparation it was necessary to test whether it expresses CYP2C23. Sf-9 cells were infected and after 48 h, cells were harvested and COD spectra (2.2.3) were measured using the cell lysate (Figure 3.14). COD spectra showed absorption maximum at 450 nm that thus clearly confirming the expression of spectrally intact CYP protein (1.1.1).

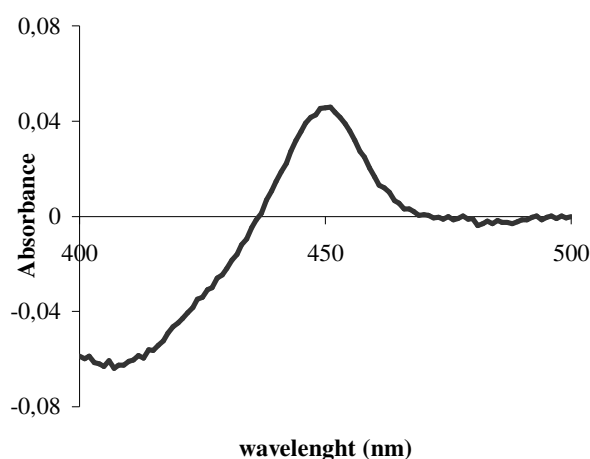


Figure 3.14 *COD spectrum showing the expression of recombinant CYP2C23 in insect cells. Insect cell culture expressed about 180 nmol/l.*

3.2.2 Expression of selected CYP isoforms in Sf-9 cells

Sf-9 microsomes co-expressing a selected CYP and hCPR were used for analysis of CYP enzymatic activities. In order to optimize CYP/hCPR expression, firstly was determined optimal MOI for CYP virus expression. In Table 3.4 is shown example for optimization of CYP2C23 expression. CYP2C23 virus had virus titar $\sim 2 \times 10^9$ /ml Insect cells were infected with different MOIs of CYP2C23 virus. Infection of 10 ml of insect cells with 75 μ l of virus yielded the highest expression of CYP2C23. In the next step, optimization of CYP/hCPR coexpression was conducted. Insect cells were co-infected with 75 μ l of CYP2C23 virus and various MOIs of hCPR virus (Table 3.5).

Table 3.4 *Establishing of optimal conditions for expression of CYP2C23. 10 ml of insect cells were infected with 10-100 μ l of CYP2C23 virus. Cells were harvested after 48 h and COD spectra were measured using cells lysates.*

CYP2C23 virus	nmol/ml
10 μ l	0.31
30 μ l	0.43
50 μ l	0.69
75 μl	0.74
100 μ l	0.76

Table 3.5 *Establishing of optimal conditions for co-expression of CYP2C23 and hCPR 10 ml of insect cells were infected with 75 μ l of CYP2C23 virus and 10-100 μ l of hCPR virus. Cells were harvested after 48 h and COD spectra and hCPR activity were measured using cells lysates.*

	+10 μl hCPR virus	+30 μl hCPR virus	+50 μl hCPR virus	+75 μl hCPR virus	+100 μl hCPR virus
CYP(nmol/ml)	0.2	0.2	0,14	0.12	0.09
hCPR (U/ml)	0.25	0.3	0.28	0.31	0.34

Cells were harvested after 48h and cell lysates were used for determination of CYP and CPR content (Figure 3.15 and Figure 3.16).

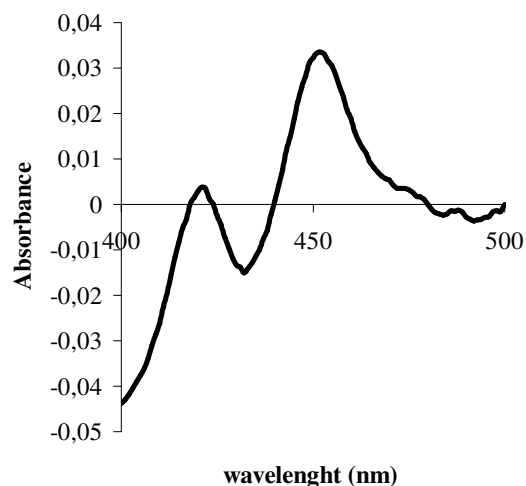


Figure 3.15 CO spectrum of lysate of Sf-9 cells co-expressing CYP2C23 and CPR.

The best CYP/CPR baculovirus ratio (Table 3.5, in bold) was used for further microsome preparations. Microsomes used in this study were prepared as described in 2.2.5. Ratios of CYP: CPR concentrations of microsomes prepared and used in this study are shown in Table 3.6.

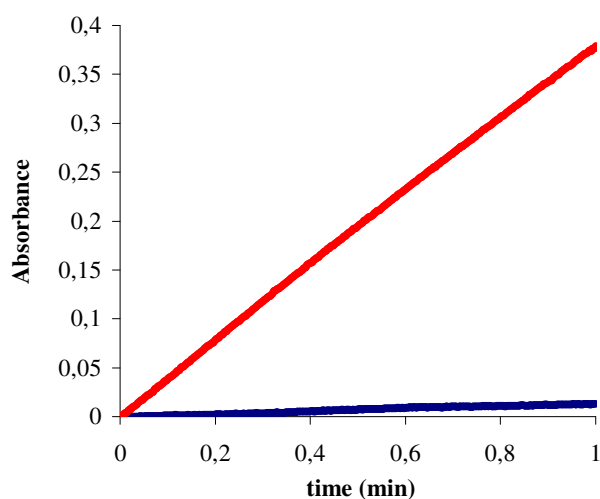


Figure 3.16 CPR activity of lysate from Sf-9 cells co-expressing CYP2C23 and hCPR. On this figure are shown CPR activities of lysates of Sf-9 cells co-expressing CYP2C23 and hCPR (in red) and Sf-9 cells expressing CYP2C23 only (in black).

Table 3.6 CYP: CPR ratios in microsomes used in this study.

<i>CYP P450</i>	<i>CYP: CPR ratio</i>
CYP2C8	0.8
CYP2C9	0.65
CYP2C11	0.75
CYP2C23	1.36
Cyp4a12a	0.9
Cyp4a12b	2

3.3. CYP-dependent formation of secondary AA metabolites, HEETs

EETs and HETEs are described as physiologically important AA metabolites (1.1.6), but there are AA secondary metabolites hydroxy-EETs (HEETs), which are also described as bioactive. HEETs are synthesised by CYP4A-dependent hydroxylation of EETs. They are potential endogenous PPAR α activators (Coward et al., 2002). In this part of the study, we described a novel pathway of HEET formation, which consists in the CYP2C-dependent epoxidation of 20-HETE. Moreover, we showed that this novel pathway is the main pathway of HEET formation in rat kidney. We were also interested in whether recombinant CYP2Cs (human CYP2C8 and CYP2C9, rat CYP2C11 and CYP2C23) and Cyp4as (Cyp4a12a and Cyp4a12b) have higher activities in formation of primary or secondary products.

3.3.1 CYP2C23-dependent formation of HEET in renal microsomes

As mentioned before, Coward et al. discovered the first pathway of HEET formation in 2002. This pathway involves CYP2C-dependent epoxidation of AA to EETs, followed by CYP4A-dependent hydroxylation of EETs. In this part of the study, we investigated whether also the opposite order of reactions, that means AA hydroxylation to 19/20-HETE followed by 19/20-HETE epoxidation, can form HEETs.

To address this question we selected CYP4A1 as a major 20-HETE synthase and CYP2C23 as a major EET-synthase present in the rat renal microsomes and tested their ability to hydroxylate EETs and to epoxidize 20-HETE, respectively (Figure 3.17). As expected, CYP4A1 converted 8,9-EET to HEETs ($R_t = 9$ min). Interestingly, a metabolite with the same R_t was produced by CYP2C23 converting 20-HETE. This reaction was dependent on the presence of CYP2C23 in the microsomes since the microsomes prepared from control cells expressing only hCPR were totally inactive.

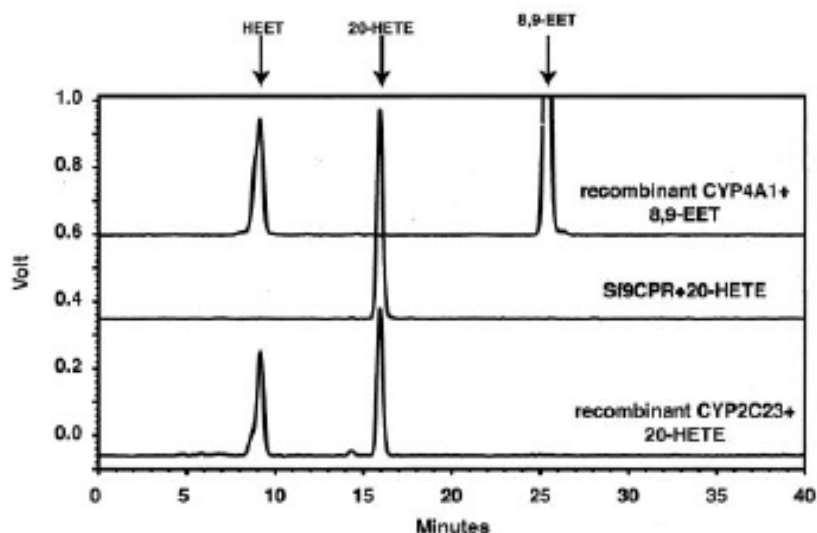


Figure 3.17 RP-HPLC analysis of HEET formation catalyzed by recombinant CYP enzymes. HEETs were produced either by CYP4A catalyzed hydroxylation of 8,9-EET (upper chromatogram) or by CYP2C23 catalyzed epoxidation of 20-HETE (lower chromatogram). 20-HETE was not converted by insect cell microsome expressing only hCPR.

As shown in the previous chapter (3.1.3), rat renal microsomes form HEET via CYP4A and CYP2C23 pathway (Figure 3.12). To test the efficiency of both pathways, 11,12-EET and 20-HETE were used as respective substrates. As shown in Figure 3.18, 11,12-EET was converted to 11,12-DHET (by sEH) contaminating the renal microsomes, HEETs (by CYP4A-dependent hydroxylation and HDHET (by hydrolysis of HEETs or hydroxylation of 11,12-DHET). 20-HETE was efficiently epoxidized to HEETs which were further hydrolyzed to HDHETs. 11,12-DHET conversion yielded a single product corresponding to HDHET.

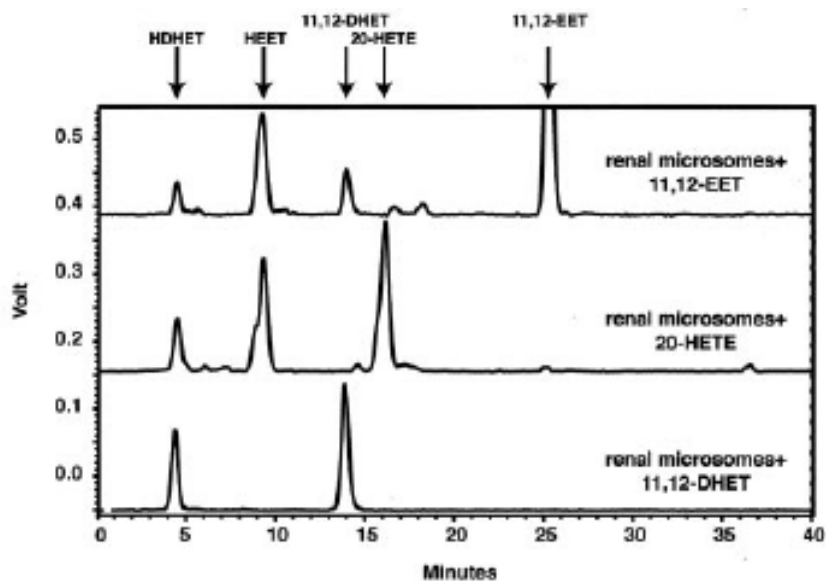


Figure 3.18 RP-HPLC analysis of HEET and HDHET formation by rat kidney microsomes using 11,12-EET, 20-HETE and 11,12-DHET as substrates.

In a further set of experiments, we were interested to find out whether HEET formation proceeds with a certain regioselectivity. To address this question we analyzed fractions from three different sources: a) from AA conversion by rat renal microsomes, b) from 20-HETE epoxidation by CYP2C23 and c) from 20-HETE conversion by renal microsomes.

HEET fractions were collected from RP-HPLC and resolved into regioisomers on NP-HPLC (Figure 3.19). For preparation of standard compounds, we took advantage of the high regioselectivity of CYP4A1. The metabolites produced by ω -hydroxylation of 8,9-, 11,12- and 14,15-EET by recombinant CYP4A1 showed retention times of 44.9 minutes (20-hydroxy-8,9-EET, 20,8,9-HEET), 44.0 minutes (20,11,12-HEET), and 53.7 minutes (20,14,15-HEET) in NP-HPLC.

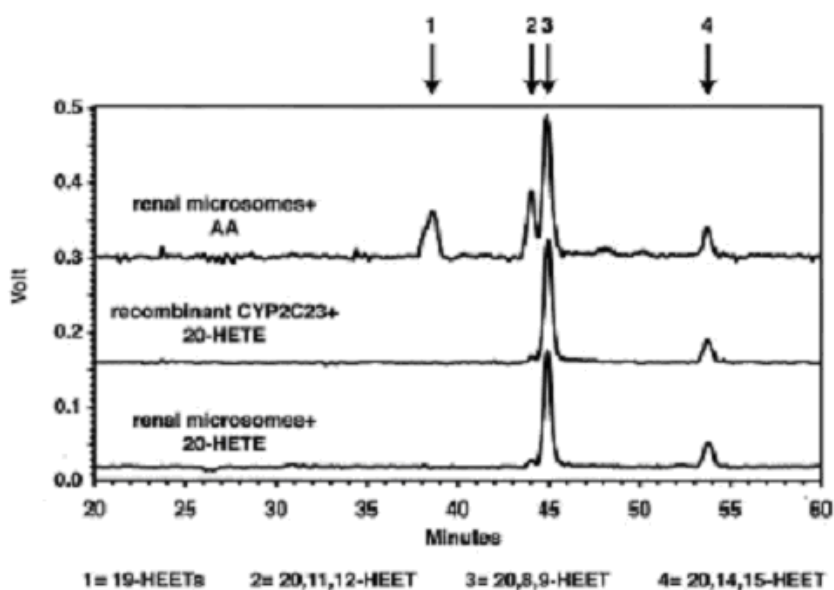


Figure 3.19 NP-HPLC analyses of HEETs produced by renal microsomes and CYP2C23.

The HEET fraction after AA conversion with rat renal microsomes was resolved into four product peaks migrating at 38.5 minutes (19-hydroxy-EETs; 21 % of total product), 44.0 minutes (20,11,12-HEET; 21 %), 44.9 minutes (20,8,9-HEET; 50 %), and 53.7 minutes (20,14,15-HEET; 8 %). These data showed that 20,8,9-HEET was the main product. Epoxidation of 20-HETE by recombinant CYP2C23 resulted in a major product co-migrating with 20,8,9-HEET (~80 % of total product) and a minor product co-migrating with 20,14,15-HEET. 20,11,12-HEET occurred only in trace amounts (less than 3 % of total product). A very similar HEET pattern with 20,8,9-HEET as the predominant metabolite was obtained after incubation of renal microsomes with 20-HETE.

To summarize, 20,8,9-HEET was the main HEET regioisomer formed in renal microsomal AA metabolism. CYP2C23 converted 20-HETE also mainly to 20,8,9-HEET. We can conclude that CYP2C23-dependent 20-HETE epoxidation is a major route of HEET production in rat kidney.

3.3.2 Metabolism of EETs and 20-HETE by recombinant CYP isoforms

As described in the previous chapter there are two routes of HEET formation, namely CYP4A-dependent EET hydroxylation and CYP2C23-dependent 20-HETE

epoxidation. In this part of the study, we analyzed the enzymatic efficiencies of human and rat CYP2Cs and mouse Cyp4as towards 20-HETE and EETs as substrates for HEET formation. As a measure of efficiency we determined for each isoform the conversion rates of AA and compared it to that of EET (Cyp4as) and 20-HETE (CYP2Cs).

All tested recombinant CYP2Cs (CYP2C8, CYP2C9, CYP2C11 and CYP2C23) converted 20-HETE with similar or higher activities compared to AA (Figure 3.20). CYP2C8, CYP2C11 and CYP2C23 dependent conversion of 20-HETE resulted in the formation of a single product peak on RP-HPLC ($R_t = 9$ min). In contrast, CYP2C11 produced several additional product peaks ($R_t = 2-7$ min) where HEETs represented 40 % of total product. All CYP2Cs converted 20-HETE with higher activity compared to that of AA. CYP2C9 converted 20-HETE with an activity that was only 35 % higher than that of AA (3.4 vs. 2.5 nmol/nmol/min, respectively). Conversion of 20-HETE by CYP2C11 resulted in 9.3 nmol/nmol/min what represents 164 % of AA conversion (5.7 nmol/nmol/min).

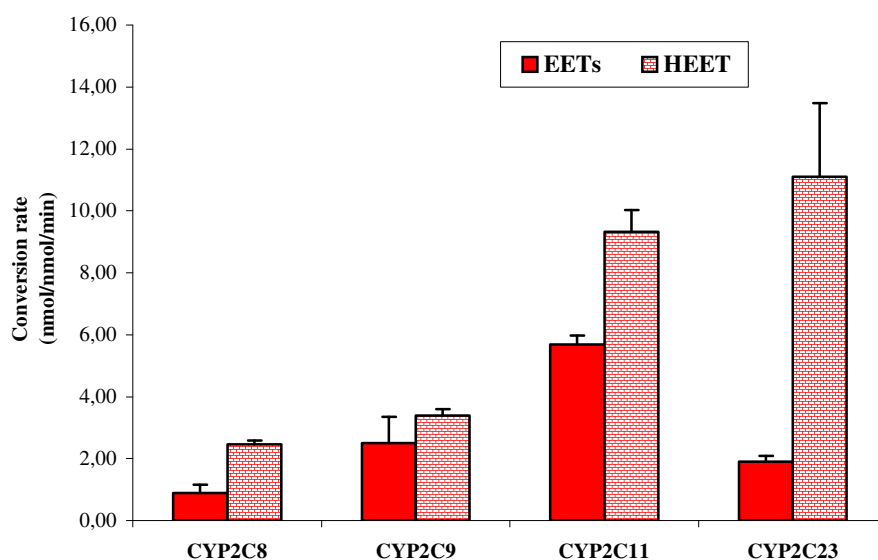


Figure 3.20 *Enzymatic activities of CYP2C8, CYP2C9, CYP2C11 and CYP2C23 towards AA and 20-HETE. Substrates were used in 10 μ M concentrations and were converted in presence of NADPH, for 3 minutes by 10 pmol of recombinant microsomes. Metabolites were resolved on RP-HPLC. All reactions were done in triplicate.*

CYP2C8 showed much higher preference towards 20-HETE than to AA. Conversion of 20-HETE yielded 2,5 nmol/nmol/min, or 280 % of that for AA. The

most extreme example was conversion by CYP2C23. This enzyme converted 20-HETE with an almost 6-fold higher activity than AA (11.1 vs. 2 nmol/nmol/min, respectively).

Results of 20-minute conversions of 14,15-, 11,12- and 8,9-EET by Cyp4a12a and Cyp4a12b are shown in Figure 3.21. Both recombinant enzymes showed the highest activity towards 11,12-EET. Activities were more than two-fold higher compared to that of AA conversion (2.4-fold higher for Cyp4a12a and 2.2-fold higher for Cyp4a12b). The activities towards 14,15- and 8,9-EET were similar to that of AA.

These results show that CYP2C enzymes (CYP2C8, CYP2C9, CYP2C11 and CYP2C23) and Cyp4a enzymes (Cyp4a12a and Cyp4a12b) convert EETs and 20-HETE with activities that were equal or even higher compared to that of AA. We can conclude that CYP2Cs and Cyp4as do not only have a role in primary (EETs and 20-HETE) but also in secondary product formation (HEETs).

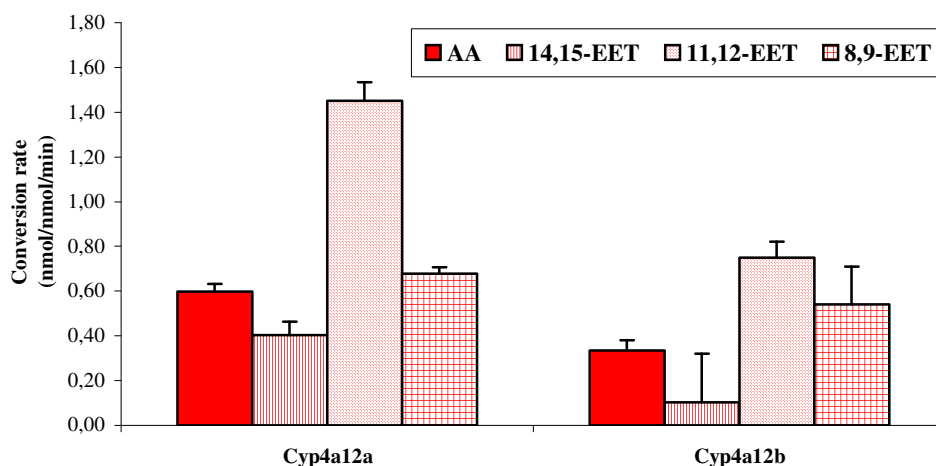


Figure 3.21 Enzymatic activities of Cyp4a12a and Cyp4a12b towards AA, 14,15-, 11,12- and 8,9-EET. 10 μ M concentration of substrate was converted in presence of NADPH, for 20 minutes by 10 pmol of recombinant microsomes. Metabolites were resolved on RP-HPLC. All reactions were done in triplicate.

3.4 CYP-dependent metabolism of ω -3 fatty acids

ω -3 fatty acids show antiinflammatory, antiproliferative, antihypertensive, anticoagulative and antiarrhythmic effects. Our hypothesis was that competition between AA and ω -3 fatty acids could modulate production of CYP-dependent metabolites, which could contribute to these beneficial cardiovascular effects of ω -3 fatty acids. Here we tested whether EPA, DPA and DHA can serve as alternative substrates for CYPs. We analyzed conversions of ω -3 fatty acids by renal microsomes of mouse, rat and human and human liver microsomes. In order to determine the engagement of different CYP isoforms in ω -3 fatty acid metabolism, we also tested conversions of EPA, DPA and DHA by recombinant CYP isoforms including AA epoxygenases from human (CYP2C8 and CYP2C9), and rat (CYP2C11 and CYP2C23) and AA hydroxylases from human (CYP4A11 and CYP4F2), and mouse (Cyp4a12a and Cyp4a12b).

The main results were as follows:

- Renal and liver microsomes and recombinant CYPs converted EPA, DPA and DHA with enzymatic efficiencies equal or higher compared to AA (3.4.2, 3.4.3.1, 3.4.4.1)*
- All studied CYP2C isoforms produced epoxy-derivatives when converting EPA, DPA and DHA. The pattern of regioisomeric epoxyeicosatetraenoic acids (EETeTrs), epoxydocosatetraenoic acids (EDTeTrs) and epoxydocosapentaenoic acids (EDPs) was isoform specific. Moreover the regiospecificity was substrate-dependent. For example, CYP2C23 epoxidized AA preferentially at the 11,12-; EPA at the 17,18-; DPA at the 10,11- and DHA at 10,11- and 19,20-double bond*
- Typical AA hydroxylases (CYP4As and CYP4F2) catalyzed the ω - and ω -1 hydroxylation of EPA, DPA and DHA and showed epoxygenase activity directed against the ω -3 double bond.*

3.4.1 Resolution and identification of epoxy- and hydroxy- derivatives of EPA, DPA and DHA

The aim of this part of this study was to identify all CYP-dependent metabolites of ω -3 fatty acids. Recombinant enzymes were co-expressed in Sf-9 insect cells together with human recombinant CPR (2.2.3). Insect cell microsomes were prepared (2.2.6) and used for conversion of AA, EPA, DPA and DHA; all substrates were tested at 10 μ M concentration and were converted by 10 pmol of CYP in a reaction time of 10 minutes. CYP4A11, Cyp4a12a and Cyp4a12b were incubated with cytochrome b5 in a 1: 1 molar ratio in order to increase CYP activity. Commercially available CYP4F2, which was used in this study already contained cytochrome b5. After 5 min of pre-incubation, the reactions were started with 0,5 mM NADPH and after 10 minutes of reaction time, stopped with 20 mM citric acid (2.3.1). Metabolites were extracted with ethylacetate. Samples were analyzed using RP-HPLC as described in 2.3.2 (Figure 3.22).

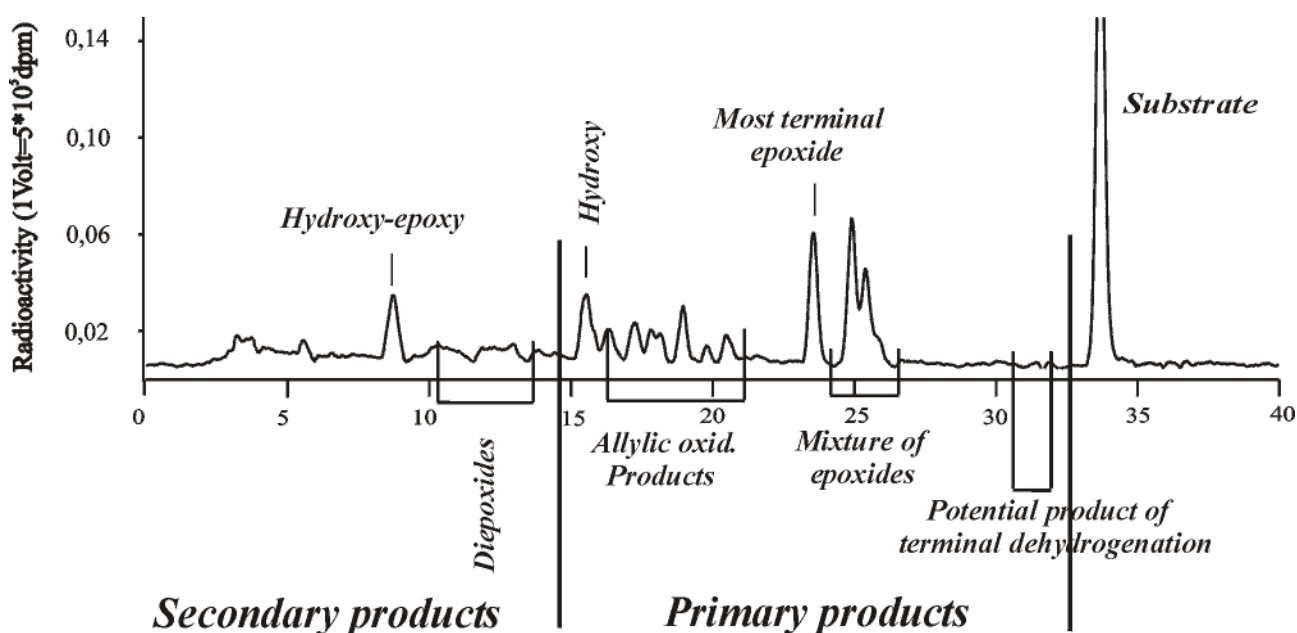
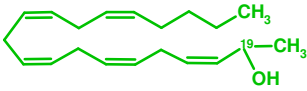
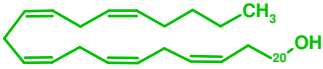
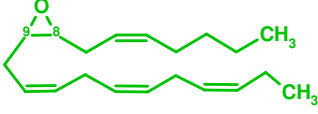
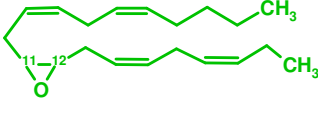
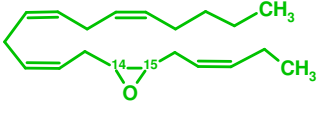
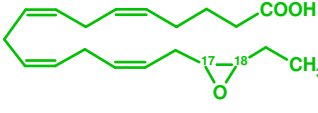
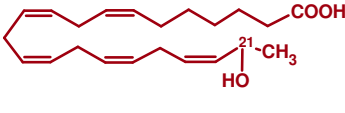

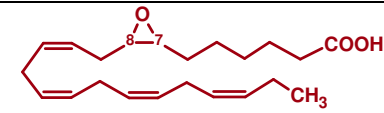
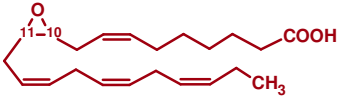
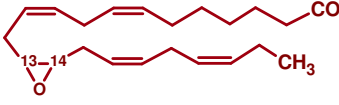
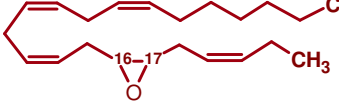
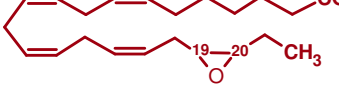
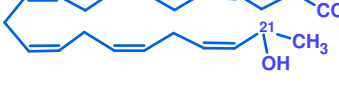
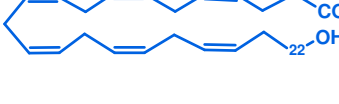
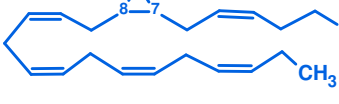

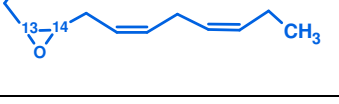
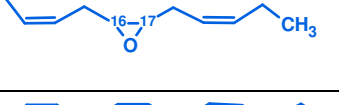
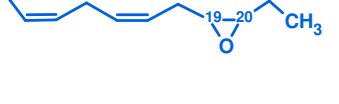


Figure 3.22 General scheme of the resolution of CYP-dependent PUFA metabolites on RP-HPLC. The figure shows metabolite pattern produced by CYP2C9 from AA as an example.

In order to further separate different regioisomers, metabolites were resolved on NP-HPLC (2.3.3). Single metabolites were identified by GC-MS (Dr. H. Honeck and C. Andrée). All CYP-dependent metabolites of EPA, DPA, and DHA and their retention times in RP- and NP-HPLC are summarized in Table 3.7.

Table 3.7 Structural formulas of epoxy- and hydroxy-derivatives of EPA, DPA and DHA. * *Rt*- retention time

Metabolite	Rt* (RP-HPLC)	Rt* (NP-HPLC)	Formula
19-OH-EPA	14.2 min	19.5 min	
20-OH-EPA	14.2 min	21.1 min	
8,9-EETeTr	21.2 min	21.8 min	
11,12-EETeTr	21.2 min	16.5 min	
14,15-EETeTr	21.2 min	14.5 min	
17,18-EETeTr	20 min	18,8 min	
21-OH-DPA	15.6 min	21.2 min	
22-OH-DPA	15.6 min	26.5 min	
7,8-EDTeTr	25.6 min	43.4 min	

10,11-EDTeTr	25.6 min	26.2 min	
13,14-EDTeTr	25.6 min	23.2 min	
16,17-EDTeTr	25.6 min	21.7 min	
19,20-EDTeTr	24.4 min	-	
21-OH-DHA	18.4 min	14.8 min	
22-OH-DHA	18.4 min	20.9 min	
7,8-EDP	25.2 min	29.7 min	
10,11-EDP	25.2 min	23.2 min	
13,14-EDP	25.2 min	19.5 min	
16,17-EDP	25.2 min	17.4 min	
19,20-EDP	24.15 min	-	

3.4.2 Metabolism of ω -3 fatty acids by mouse, rat and human renal microsomes and human liver microsomes

Kidney and liver are described as organs with intensive CYP-dependent AA metabolism. Therefore, we were interested to find out whether ω -3 fatty acids (EPA, DPA and DHA) can compete with AA as substrates for CYP-dependent metabolism in these organs. To this end, AA, EPA, DPA and DHA were converted by mouse renal, rat renal, human renal and human liver microsomes.

Analysis of AA, EPA, DPA and DHA conversion by renal and liver microsomes was performed essentially as described in 2.4.4, using however substrate concentration of 10 μ M and reaction time of 30 min. Results are presented in Figure 3.23. This figure shows comparison of total activities towards the different PUFAs of mouse, rat and human renal microsomes expressed in pmol/mg/min.

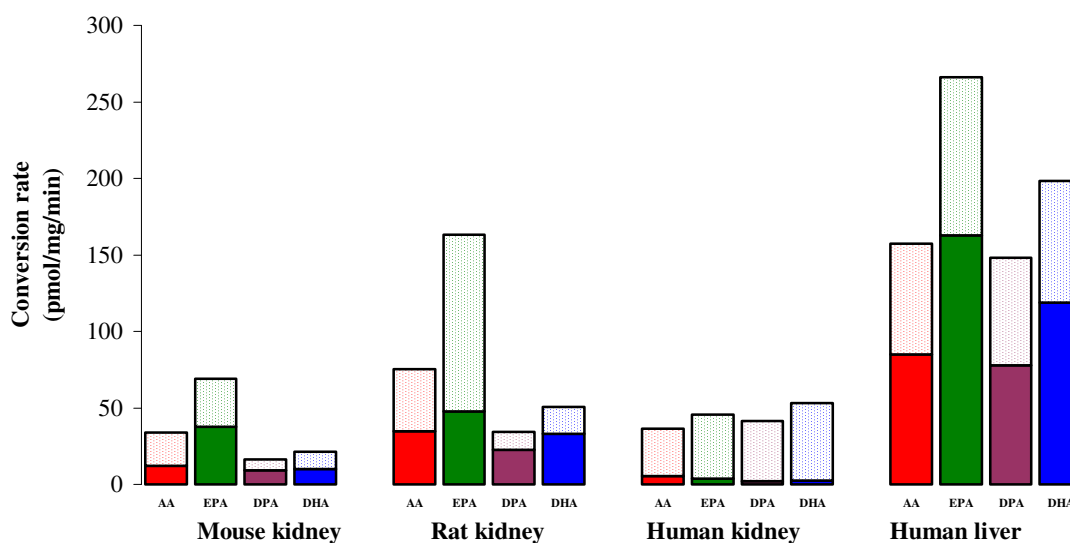


Figure 3.23 *Enzymatic activities of renal mouse, rat, human microsomes and human liver microsomes towards AA, EPA, DPA and DHA. Microsomal activities were determined using reaction mixtures of 0.4 ml containing 320 μ g of microsomal protein and substrate at concentration of 10 μ M (AA, EPA, DPA and DHA). Reactions were started with NADPH and stopped after 30 min. Lower part of the bar (bold) represents epoxygenase activity and upper part of the bar (empty) represents hydroxylase activity. Data are mean \pm SE values of experiments done in triplicate (mouse and rat renal microsomes) or using four different microsomal samples (human renal and liver microsomes).*

Mouse renal microsomes were prepared from 10-12 weeks old NMRI mice. These microsomes showed a clear preference for EPA. The conversion rates of EPA were two-fold higher compared to that of AA (69 vs. 33.8 pmol/mg/min). DPA and DHA were metabolized with significantly lower rates, which reached about 50 and 60 % of those determined with AA (16,4 and 21,3 pmol/mg/min, respectively). The ratio of AA-epoxygenase and AA-hydroxylase products was ~1: 2. Interestingly, there was a clear shift of the epoxy: hydroxy ratio in conversion of ω -3 fatty acids. Conversions of EPA, DPA and DHA yielded equal amounts of epoxy and hydroxy products, whereas AA was converted almost exclusively to hydroxy products (Figure 3.23).

Rat renal microsomes were prepared from kidneys of 7 weeks old SD rats. Microsomes converted ω -3 fatty acids to a similar product pattern as mouse microsomes. The conversion rate of EPA was two-fold higher compared to that of AA (163 vs. 75.5 pmol/mg/min) whereas conversions of DPA and DHA represented 46 % and 67 %, of AA conversion, respectively. There was a significant shift in epoxygenase: hydroxylase product ratio. AA was converted to epoxy and hydroxy products in an approximately 1: 1 ratio (1: 1.2). In contrast, EPA was mainly hydroxylated. The ratio of EPA-epoxidation to hydroxylation was nearly 1: 2.5. Conversion of both DPA and DHA resulted in two-times more epoxy product compared to level of hydroxy product (Figure 3.23).

Human renal and liver microsomes were obtained from eight different patients. Human liver microsomes were kindly provided by Dr. U. Zanger, Dr. Margarete Fisher-Bosch Institute for Clinical Pharmacology, Stuttgart. Human renal microsomes were prepared in our laboratory from biopsies kindly provided by Dr. A. Fiebler in collaboration with Clinic of Urology, Berlin-Buch. Biopsies originated from four different human subjects. Renal microsomal samples differed in the level of conversion but the pattern of enzymatic activities towards substrates was the same. All four samples of renal microsomes converted ω -3 fatty acids with similar or higher rates than AA (Figure 3.24). On average, EPA, DPA and DHA were metabolized with rates corresponding to 126, 117 and 147 % that of AA. ω -3 fatty acids were predominantly hydroxylated (Figure 3.24). Average ratio of epoxy to

hydroxy formation was shifted from 1: 5 for AA to 1: 12, 1: 19 and 1: 20 for EPA, DPA and DHA, respectively.

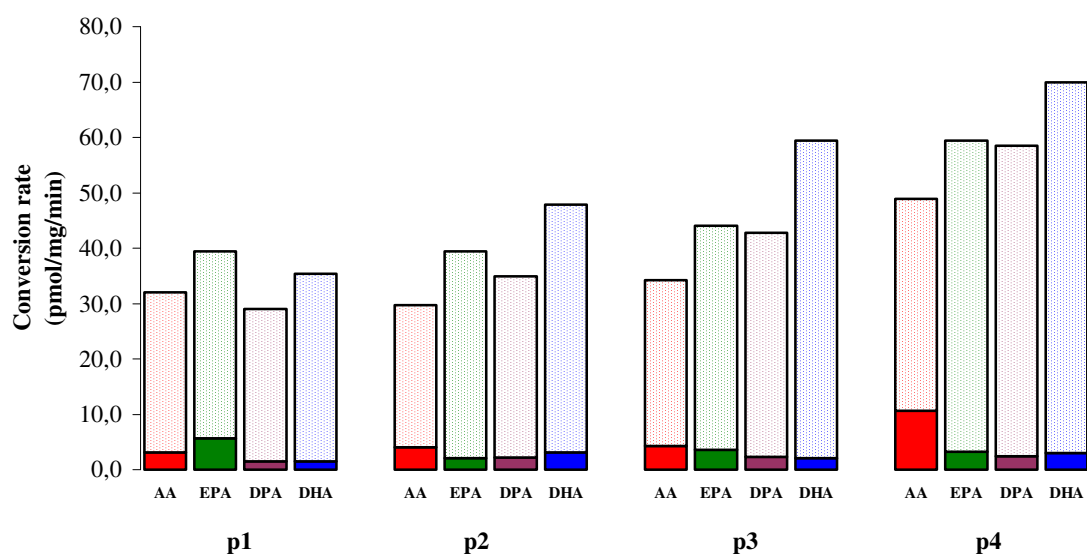


Figure 3.24 Enzymatic activities of human renal microsomes of four different human subjects towards AA, EPA, DPA and DHA. Microsomal activities were determined using reaction mixtures of 0.4 ml containing 320 μg of microsomal protein and substrate at concentration of 10 μM (AA, EPA, DPA and DHA). Reactions were started with NADPH and stopped after 30 min. Lower part of the bar (bold) represents epoxygenase activity and upper part of the bar (empty) represents hydroxylase activity. P1-4 stands for human subject 1-4.

Human liver microsomes (Figure 3.25) derived from four patients showed different individual enzymatic activities. However they had the same type of substrate preference. EPA was clearly the best substrate and was converted on average with rates reaching ~170 % of that of AA. DPA and DHA conversion rates were 94 and 126 % of that of AA, respectively. Interestingly, there was no shift in the ratio of epoxy and hydroxy products. Epoxidation was the slightly preferred reaction. Ratios of hydroxy and epoxy metabolites were in the range from 1: 1.1 to 1: 1.5 (Figure 3.25).

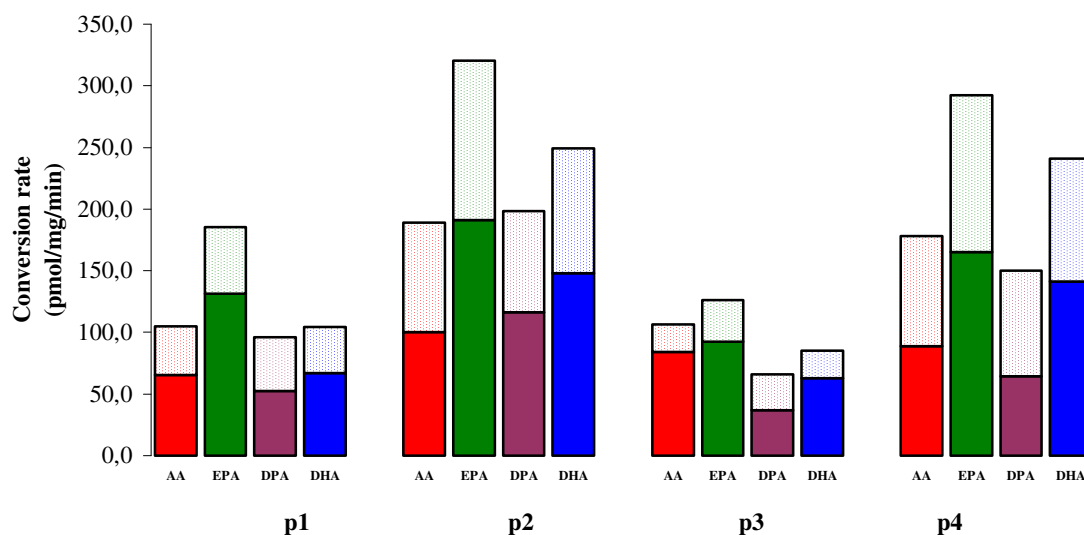


Figure 3.25 *Enzymatic activities of human liver microsomes of four different human subjects towards AA, EPA, DPA and DHA. Microsomal activities were determined using reaction mixtures of 0.4 ml containing 320 μ g of microsomal protein and substrate at concentration of 10 μ M (AA, EPA, DPA and DHA). Reactions were started with NADPH and stopped after 30 min. Lower part of the bar (bold) represents epoxygenase activity and upper part of the bar (empty) represents hydroxylase activity. P1-4 stands for human subject 1-4.*

3.4.3 Metabolism of ω -3 fatty acids by recombinant epoxygenases

Results of conversions of ω -3 fatty acids by mouse, rat and human renal and human liver microsomes were shown in the previous chapter (3.4.2). The aim of this part of the study was to examine the metabolism of EPA, DPA and DHA by recombinant CYP isoforms that are highly expressed in the kidney and the liver in order to determine the involvement of particular isoforms in tissue-specific CYP-dependent metabolism. We compared enzymatic activities towards EPA, DPA and DHA by AA epoxygenases from human (CYP2C8 and CYP2C9), and rat (CYP2C11 and CYP2C23) and AA hydroxylases from human (CYP4A11 and CYP4F2), and mouse (Cyp4a12a and Cyp4a12b). Moreover, we determined the CYP-dependent metabolite pattern for each of the ω -3 fatty acids studied.

3.4.3.1 Comparison of enzymatic activities towards AA, EPA, DPA and DHA

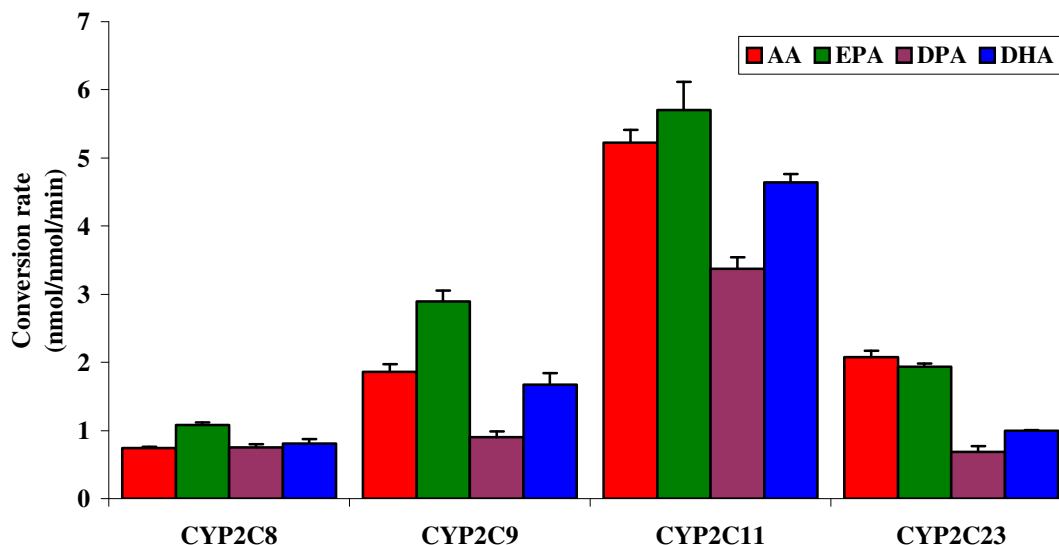


Figure 3.26 Enzymatic activities of CYP2C8, CYP2C9, CYP2C11 and CYP2C23 towards AA, EPA, DPA and DHA. Microsomal activities were determined using reaction mixtures of 0.1 ml containing 10 pmol of microsomal protein and substrate at concentration of 10 μ M (AA, EPA, DPA and DHA). Reactions were started with NADPH and stopped after 10 min. Data are mean \pm SE values of experiments done in triplicate.

The activities of recombinant AA-epoxygenases towards EPA, DPA and DHA were analyzed as described in 3.4.1. Figure 3.26 shows enzymatic activities of the enzymes tested and activities are presented in nmol/nmol/min.

CYP2C8 converted EPA with 50 % higher activity compared to AA (1.08 vs. 0.74 nmol/nmol/min). Activities of DPA and DHA conversion were similar to the activity of AA conversion (0.75 for DPA and 0.81 nmol/nmol/min for DHA, respectively).

CYP2C9, similarly to CYP2C8, converted EPA as a preferred substrate (2.9 compared to 1.86 with AA nmol/nmol/min). DPA was converted with rates that reached only about 50 % of AA conversion (0.9 vs. 1.86 nmol/nmol/min). DHA conversion was in the same range as that of AA (1.67 vs. 1.86 nmol/nmol/min).

CYP2C11 was much more active than the other AA-epoxygenases tested in this study. Therefore, the reaction time was shortened to 5 min. EPA was converted with an activity similar to that of AA (5.7 vs. 5.23 nmol/nmol/min). Conversion of DPA

was lower compared to that of AA and EPA (3.37 nmol/nmol/min). DHA was converted with activity similar to that of AA (4.64 nmol/nmol/min).

CYP2C23 converted AA and EPA with almost equal rates (2.08 vs. 1.93 nmol/nmol/min, respectively). The activity towards DPA and DHA relatively low: 33 % (0.69 vs. 2.08 nmol/nmol/min) and 50 % (0.99 vs. 2.08 nmol/nmol/min) of AA conversion rate.

Taken together, this part of the study clearly demonstrates that AA epoxygenases from human (CYP2C8 and CYP2C9) and rat (CYP2C11 and CYP2C23) accept the ω -3 fatty acids, EPA, DPA and DHA as efficient alternative substrates. EPA appeared to represent a slightly preferred substrate, however, even the conversion rates of DPA and DHA reached at least 50 % of that of AA.

3.4.3.2 CYP2C isoform-specific metabolite patterns

3.4.3.2a Metabolite pattern of EPA, DPA and DHA produced by CYP2C8

As already described in Introduction (1.1.4.1), CYP2C8 is the main CYP isoform in human kidney but it is also highly expressed in human liver. CYP2C8 metabolizes AA to 14,15-EET and 11,12-EET as major products. These epoxides are formed in similar quantities (48: 52) (Dai D. et al., 2001).

Results from this study confirmed that 14,15-EET and 11,12-EET are major products of AA conversion by CYP2C8 (Figure 3.27). After 10 minutes of reaction, in addition to two major epoxy products, several minor products were additionally detected. The peak with a retention time of ~9 minutes represented HEET, a secondary AA product. The minor peak with retention time of 15,4 min represented 19/20-HETE. Another group of minor metabolites had retention times from 16 to 21 min and most probably represented allylic oxidation products. These peaks show typical absorption maximum at 253 nm as known for compounds having a hydroxy group adjacent to conjugated double bonds

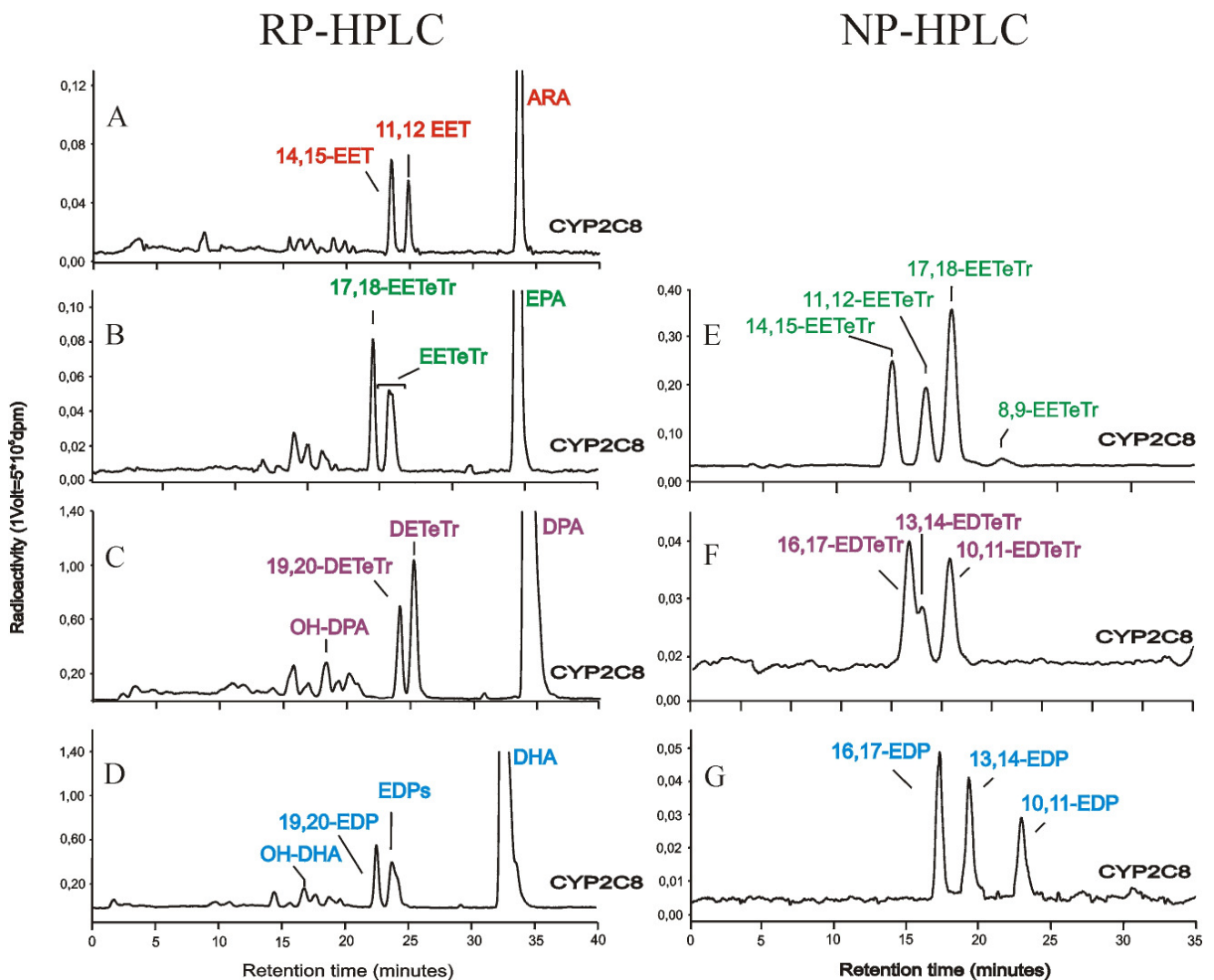


Figure 3.27 HPLC analyses of AA, EPA, DPA and DHA metabolites produced by CYP2C8. 10 pmol of CYP2C8 was incubated with 10 μ M of substrate (AA, EPA, DPA and DHA). Reactions were started with NADPH and stopped after 10 min. Metabolites were extracted and resolved on HPLC. A, B, C and D chromatograms represent examples of RP-HPLC resolved CYP2C8-dependent metabolites of AA, EPA, DPA and DHA, respectively. E, F and G chromatograms show the resolution of epoxy metabolites, which were not clearly separated on RP-HPLC (EETeTr, DETeTr and EDP, respectively) by using subsequent NP-HPLC.

CYP2C8 converted **EPA** mainly to epoxy products (Figure 3.27). They represent about 70 % of total product. Epoxy products appeared on RP-HPLC as two peaks. 17,18-EETeTr migrated from the column with a retention time of 20 minutes. That was the major epoxy metabolite accounting for almost 50 % of total epoxy product. The second peak eluting at 21,2 minute retention time represented a mixture of unresolved epoxy metabolites, which were collected and further analyzed at the NP-HPLC. Further analysis showed that 11,12-EETeTr and 14,15-EETeTr represented

22 % and 30 %, of the total epoxy product. 8,9-EETeTr was a minor epoxy product with only 3 % (Table 3.9). There was a small amount of product with retention time of 14.2 minutes that co-migrated with 19/20-OH-EPA, as well as group of small products with retention times between 15 and 17 minutes, which most likely represent hydroxyeicosapentaenoic acids (HEPEs) with dienol functionality.

DPA metabolite pattern resembled that of EPA (Figure 3.27). Epoxidation was the main reaction. RP-HPLC resolved the epoxy products into 19,20-EDTeTr (single product peak at 23 min retention time) and a mixture of unresolved epoxy metabolites (peak from 24-26 min retention time). The ω -3 double bond was the preferred site of reaction. The corresponding product, 19,20-EDTeTr, represented 35 % of total epoxy product. The mixture of other epoxy products was further resolved on NP-HPLC into 10,11-EDTeTr, 14,15-EDTeTr and 16,17-EDTeTr representing 25 %, 11 % and 29 % of total epoxy product, respectively. The 7,8 double bond was not attacked (Figure 3.27, Table 3.9).

DHA was converted similar to the other substrates mainly by epoxidation (Figure 3.27). The main product was 19,20-EDP with 43 % of total epoxy product. 10,11-EDP, 13,14-EDP and 16,17-EDP represented 15 %, 19 % and 23 %, respectively (Table 3.9). In addition to epoxy metabolites, DHA was converted to minor amounts of OH-DHA with retention time of 15.6 min, and a group of products eluting at 17.5-19 minutes, which are again most probably allylic oxides.

Furthermore, in this study it was directly tested how EPA and AA compete for the conversion by CYP2C8. As shown in Table 3.8 CYP2C8 converted preferentially EPA if both substrates were present in equimolar concentrations (10 μ M each). Under these conditions CYP2C8 produced nearly 3-fold more EPA- than AA-epoxides.

Table 3.8 AA and EPA competition for conversion by CYP2C8. 10 μ M AA, a mixture of 5 μ M AA+5 μ M EPA or 10 μ M EPA were incubated for 10 min with 10 pmol of CYP2C8. Metabolites were resolved on RP-HPLC. All reactions were done in triplicate. Total amounts of AA and EPA epoxy products are given in pmol. Standard deviations were less than 10 % of mean.

CYP2C8	AA product	EPA product
10 μ M AA	57,9	0
5 μ M AA+5 μ M EPA	28,5	69,2
10 μ M EPA	0	101,5

3.4.3.2b Metabolite pattern of EPA, DPA and DHA produced by CYP2C9

As already introduced in chapter 1.1.4.1, CYP2C9 is the major human liver AA-epoxygenase but also highly expressed in kidney. Compared to CYP2C8, the regioselectivity of CYP2C9 was less pronounced. CYP2C9 metabolizes AA to 8,9-EET, 11,12-EET and 14,15-EET. 14,15-EET is the major product with approximately 50 % of total epoxy product. 8,9-EET and 11,12-EET are generated in ratio close to 1: 2 (Daikh et al., 1994).

The AA conversion data of this study correspond to these published results on CYP2C9 regioselectivity. After 10 minutes of reaction, the main epoxy products were 11,12-EET and 14,15-EET. In addition, minor amounts of 19/20-HETE were detected. Moreover three product peaks with retention times from 19.7 to 21.5 were formed, which most probably represented allylic oxidation metabolites (Figure 3.28).

EPA was converted to 14,15-EETeTr as the main metabolite (45 % of total epoxy product). 8,9-EETeTr and 11,12-EETeTr were produced in a ratio of about 1: 1.5. 17,18-EETeTr represented the minor product (7 % of total epoxidation) (Table 3.9). In addition to this predominant epoxidation, hydroxylation and allylic oxidation were catalyzed to minor extent. Products of hydroxylation and allylic oxidation had retention times of 14,5 min and 16-18 min (Figure 3.28).

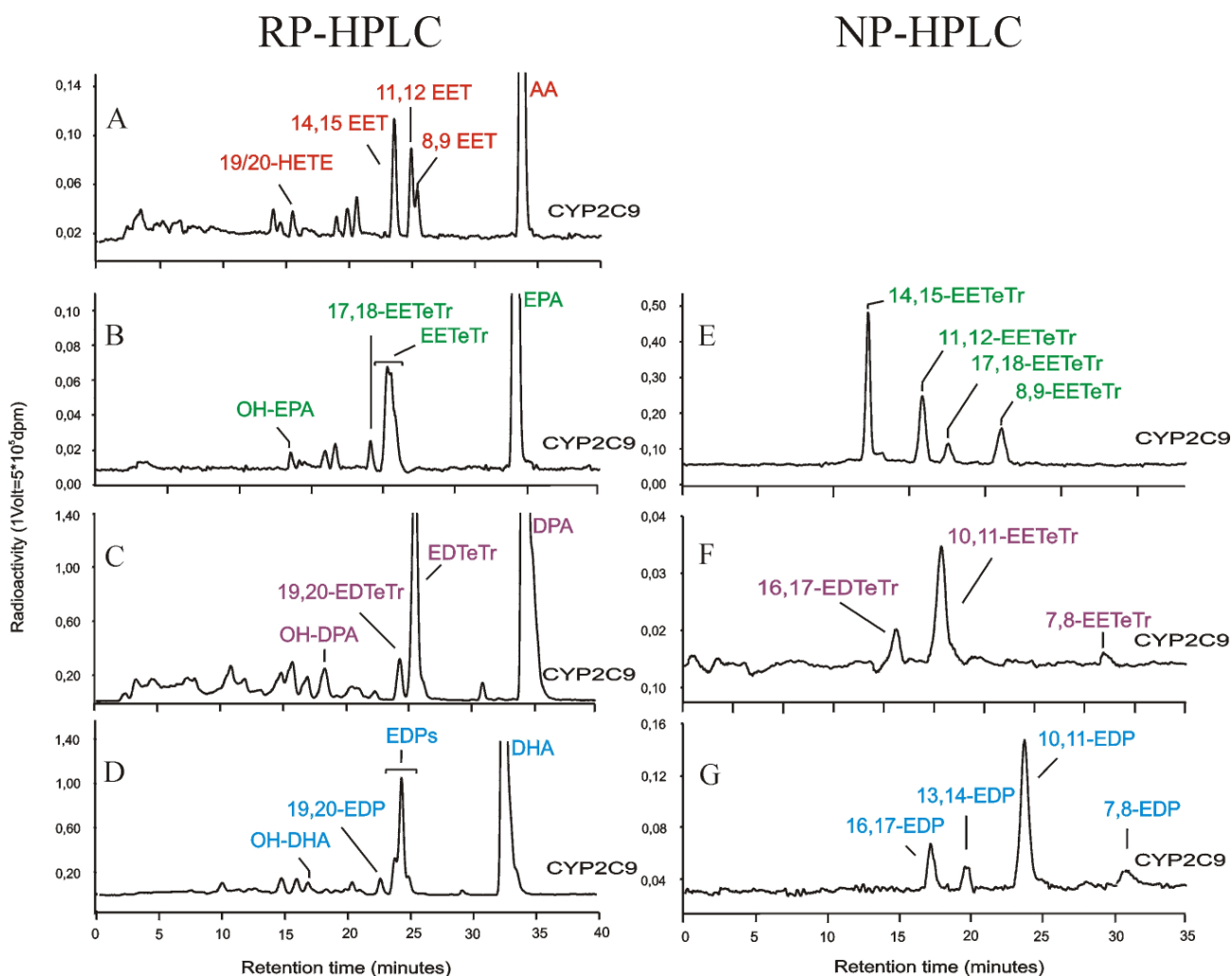


Figure 3.28 HPLC analyses of AA, EPA, DPA and DHA metabolites produced by CYP2C9. 10 pmol of CYP2C9 was incubated with 10 μ M of substrate (AA, EPA, DPA and DHA). Reactions were started with NADPH and stopped after 10 min. Metabolites were extracted and resolved on HPLC. A, B, C and D chromatograms represent examples of RP-HPLC resolved CYP2C9-dependent metabolites of AA, EPA, DPA and DHA, respectively. E, F and G chromatograms show the resolution of epoxy metabolites, which were not clearly separated on RP-HPLC (EETeTr, DETeTr and EDP, respectively) by using subsequent NP-HPLC.

DPA was mainly converted to epoxy products. Series of minor products appeared with retention times ranging from 12 to 17 min. These products were not further analyzed. The peak with retention time of 18.5 min corresponded to OH-DPA. Epoxy metabolites of DPA were resolved on RP-HPLC into 19,20-EDTeTr peak and a fraction of other epoxy metabolites (retention time of 26 min). This peak was resolved using NP-HPLC (Figure 3.28). The main product was 10,11-EDTeTr, which represented 66 % of total product. 7,8-EDTeTr, 16,17-EDTeTr and 19,20-EDTeTr were generated in ratio 1: 1.7: 1 (Figure 3.28, Table 3.9).

DHA was converted to epoxides and to a minor extent also to OH-DHA peak. 10,11-EDP was the predominant metabolite (62 % of total epoxidation); Figure 3.28. The other epoxy products, 7,8-EDP, 13,14-EDP, 16,17-EDP and 19,20-EDP, reached only 6 %, 10 %, 12 % and 10 % of total epoxy-product (Table 3.9).

3.4.3.2c Metabolite pattern of EPA, DPA and DHA produced by CYP2C11

CYP2C11 is the main AA-epoxygenase in the rat liver and is also highly expressed in the rat kidney. As already described in Introduction (1.1.4.2), CYP2C11 metabolizes AA to 14,15-, 11,12- and 8,9-EET. 11,12- and 14,15-EET were formed in similar quantities (~30 % of total epoxy product); Holla et al., 1999.

In agreement with previous studies, recombinant CYP2C11 used in present study metabolized AA to 14,15-, 11,12- and 8,9-EET. 14,15-, 11,12- and 8,9-EET were formed in a ratio of about 1: 2: 2 (Table 3.9). Significant amount of HETEs (about 20 % of the total product) were formed as well as a range of products, which considering their absorption at 253 nm most probably represent allylic oxidation products. There was a significant formation of HEETs, secondary AA product, which migrated with a retention time of 9 minutes.

CYP2C11 converted **EPA** mainly to epoxy products. All four epoxides, 8,9-, 11,12-, 14,15-, 17,18-EETeTr were synthesized in similar amounts, representing 20: 20: 27: 33 of total epoxidation product, respectively (Table 3.9) but 17,18-EETeTr was the major product. The peak at 14.9 min co-migrated with OH-EPA. The group of products with retention times between 14.5-18 minutes most probably presented different isomers of HEPEs. Minor peaks occurred at 8-9 min and 12.1 min. The peak at 12.1 min most likely represented secondary product, involving diepoxides resulting from further epoxidation of primary EETeTrs (Figure 3.29).

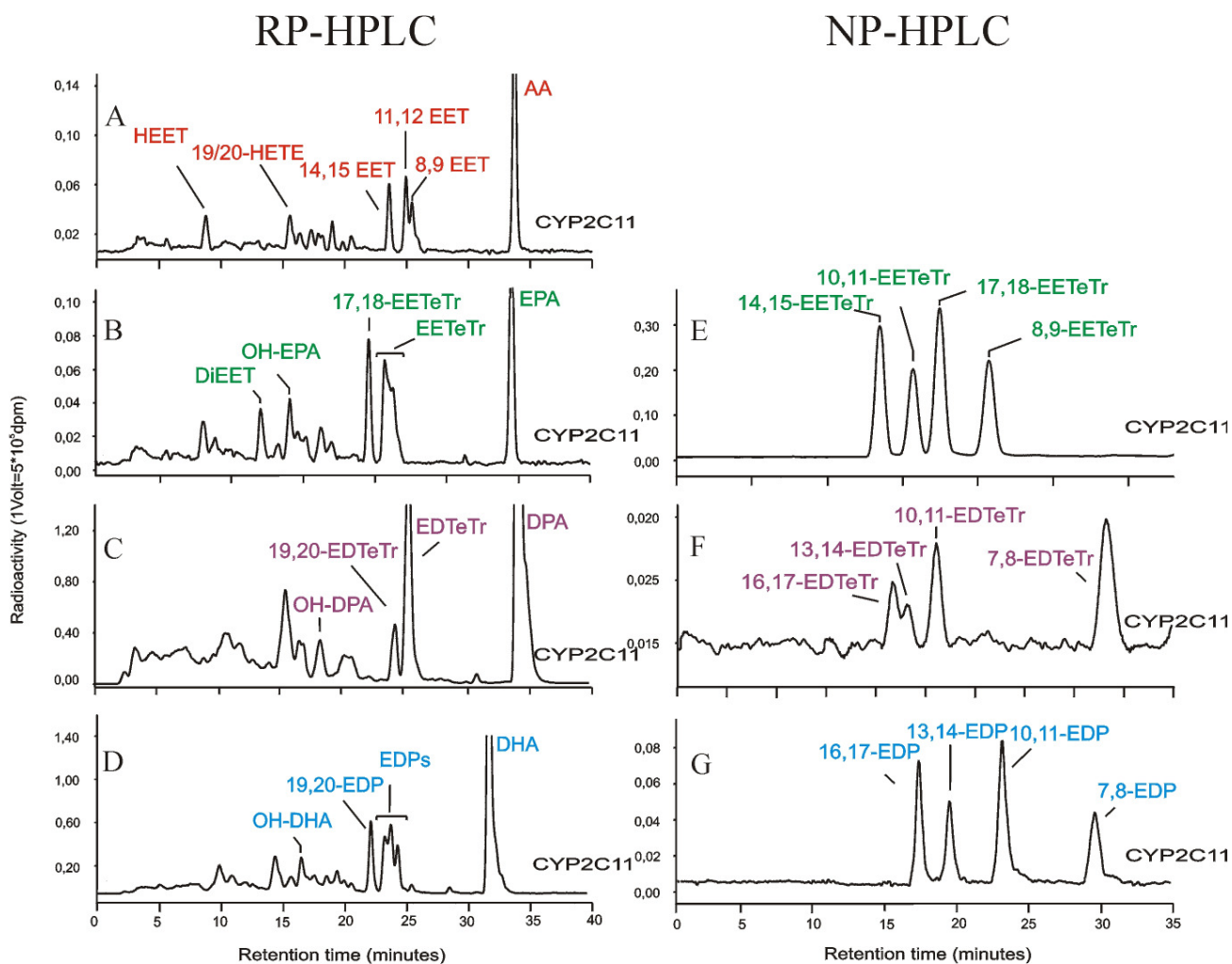


Figure 3.29 HPLC analyses of AA, EPA, DPA and DHA metabolites produced by CYP2C11. 10 pmol of CYP2C11 was incubated with 10 μ M of substrate (AA, EPA, DPA and DHA). Reactions were started with NADPH and stopped after 5 min. Metabolites were extracted and resolved on HPLC. A, B, C and D chromatograms represent examples of RP-HPLC resolved CYP2C11-dependent metabolites of AA, EPA, DPA and DHA, respectively. E, F and G chromatograms show the resolution of epoxy metabolites, which were not clearly separated on RP-HPLC (EETeTr, DETeTr and EDP, respectively) by using subsequent NP-HPLC.

DPA was metabolized to all possible regioisomeric epoxides. 7,8-EDTeTr, 10,11-EDTeTr, 13,14-EDTeTr, 16,17-EDTeTr and 19,20-EDTeTr were formed in a ratio of 37: 18: 8: 13: 23 (Table 3.9). Other products included metabolites with retention times of 15.5 and 16.5 min, which were probably diepoxides. Formation of identical products occurred when using chemical oxidation for synthesizing DPA epoxides if the oxidizing agent was used in excess. The metabolite with a retention time of 18 min was OH-DPA. The mixture of metabolites with retention times between 3 and 15 minutes was not further analyzed (Figure 3.29).

DHA was epoxidized to 7,8-EDP, 10,11-EDP, 13,14-EDP, 16,17-EDP and 19,20-EDP in a ratio of 15: 26: 13: 20: 26 (Figure 3.29, Table 3.9). Minor hydroxy metabolites and an unknown product with a retention time of 14.5 min were also detected.

3.4.3.2d Metabolite pattern of EPA, DPA and DHA produced by CYP2C23

As already described in introduction (1.1.4.2), CYP2C23 is main rat kidney AA epoxygenase. It metabolizes AA mainly to epoxides (8,9-EET, 11,12-EET and 14,15-EET) and to the lesser extend to HETEs. 11,12-EET is the major product with 54 % of total product whereas 8,9-EET and 14,15-EET represent 27 and 14 % of total product, respectively (Karara, 1993).

Results of the present work are equivalent to regioselectivity of CYP2C23 as described above. Our recombinant CYP2C23 epoxidized **AA** mainly to 11,12-EET, which represented 59 % of total epoxide production. 8,9-EET and 14,15-EET corresponded to 25 % and 16 % of total epoxidation (Table 3.9). Under the conditions used, formation of secondary AA product, HEET, represented ~3 % of total metabolites. A minor 19/20-HETE peak was also present (Figure 3.30).

EPA was also epoxidized with high regioselectivity. The 17,18-double bond was the clearly preferred site of epoxidation (about 60 % of total EETeTrs), and 8,9-, 11,12-, and 14,15-EETeTr were produced in almost equal quantities (13 %, 14 %, and 15 % of total EETeTrs) (Table 3.9). CYP2C23 produced minor amounts of 19/20-OH-EPA. The peak with a retention time of 12.1 min, most probably represented diepoxy product as already described for CYP2C11.

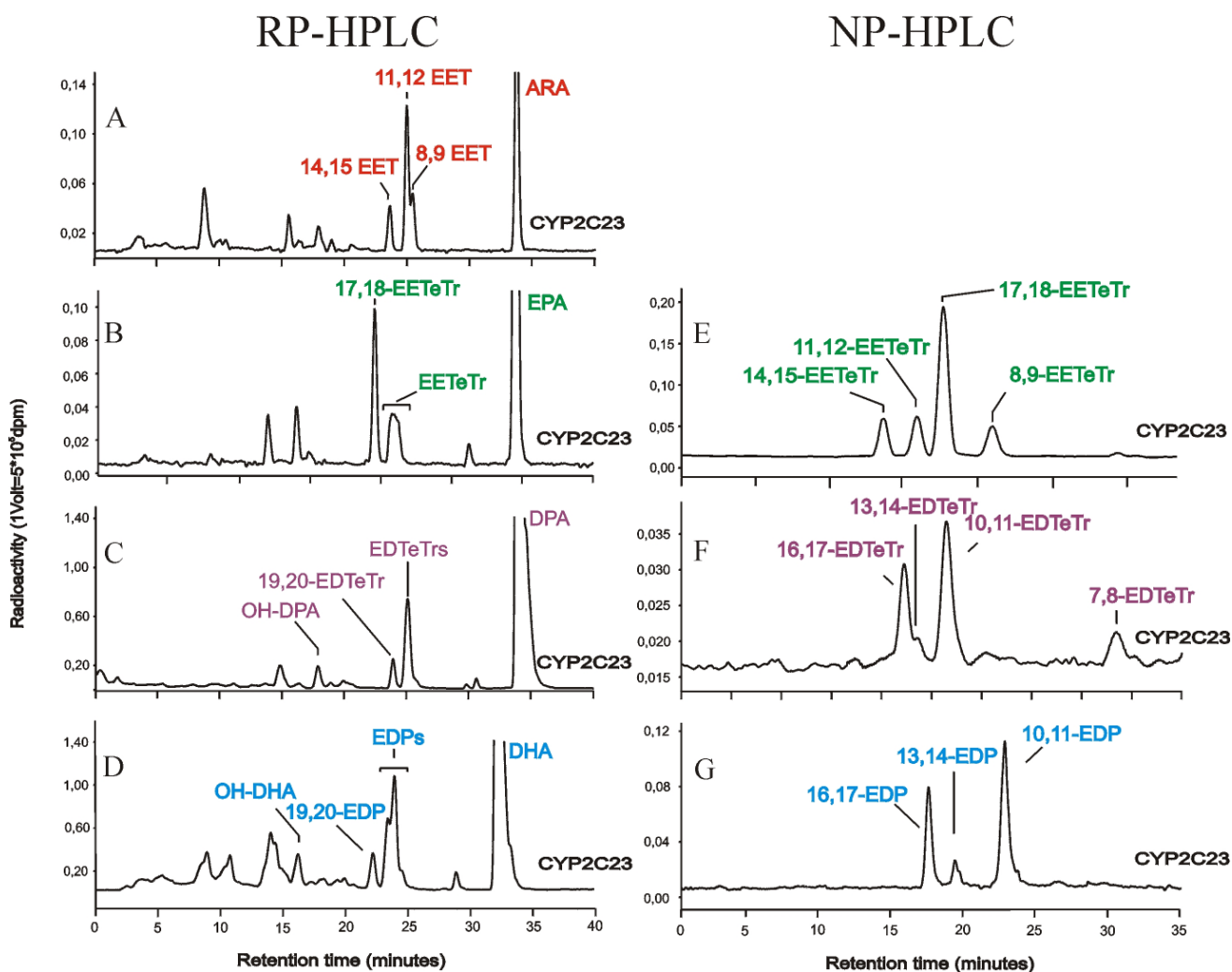


Figure 3.30 HPLC analyses of AA, EPA, DPA and DHA metabolites produced by CYP2C23. 10 pmol of CYP2C23 was incubated with 10 μ M of substrate (AA, EPA, DPA and DHA). Reactions were started with NADPH and stopped after 10 min. Metabolites were extracted and resolved on HPLC. A, B, C and D chromatograms represent examples of RP-HPLC resolved CYP2C11-dependent metabolites of AA, EPA, DPA and DHA, respectively. E, F and G chromatograms show the resolution of epoxy metabolites, which were not clearly separated on RP-HPLC (EETeTr, DETeTr and EDP, respectively) by using subsequent NP-HPLC.

To characterize the stereoselectivity of CYP2C23 in 17,18-epoxidation, the 17,18-EETeTr was collected from RP-HPLC and further resolved using chiral-HPLC. As shown in Figure 3.31, CYP2C23 predominantly formed 17(R), 18(S)-EETeTr which represented 70 % of total 17,18-EETeTr. CYP2C8 displayed the opposite stereoselectivity and produced predominantly 17(S),18(R)-EETeTr (72 % of total 17,18-EETeTr) whereas bacterial CYP101 (BM3) showed almost absolute stereospecificity in favor of producing 17(S),18(R)-EETeTr. Stereoselectivity

experiments with CYP2C8 and CYPBM3 towards 17,18-epoxidation were done by Dr. Barbosa-Sicard in our laboratory.

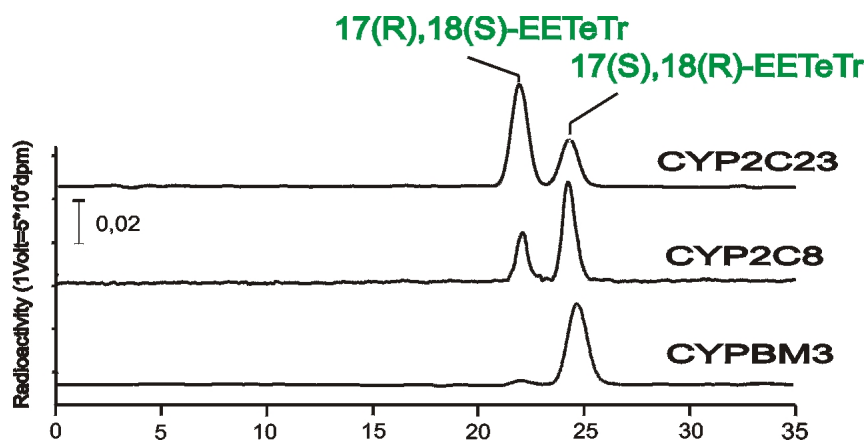


Figure 3.31 Chiral-HPLC analysis of 17,18-EETeTr produced by CYP2C23. CYP2C23-dependent EPA metabolites were extracted and resolved on RP-HPLC. 17,18-EETeTr was collected and reacted with diazomethane to synthesize methylester. 17,18-EETeTr-methylester was resolved on chiral -HPLC.

DPA was not converted with such a high regioselectivity as AA and EPA. The major product was 10,11-EDTeTr (41 % of total epoxidation). 7,8-: 13,14-: 16,17-: 19,20-EDTeTr represented 13 %, 5 %, 25 %, and 16 % of total epoxidation, respectively (Table 3.9). OH-DPA was present with the ~3 % of total metabolism. The minor peak with retention time of 15 min was most probably a diepoxide. We observed the formation of identical products when using chemical oxidation for synthesizing DPA epoxides if the oxidizing agent was used in excess (Figure 3.30).

DHA was epoxidized to 10,11-EDP, 13,14-EDP, 16,17-EDP and 19,20-EDP in a ratio of 38: 4: 21: 37. The 7,8-double bond was not attacked. In addition to epoxidation, DHA hydroxylation also occurred. The products migrating with retention times of 9, 11 and 14 min were produced by all tested CYP2Cs. However, the formation was most pronounced with CYP2C23. We assumed that this reflects extensive secondary product formation by CYP2C23, which was obviously able to further epoxidize and hydroxylate the primary epoxy products (Figure 3.30).

As summarized in Table 3.9, this part of the study shows that AA-epoxygenases were able to efficiently metabolize ω -3 fatty acids. All substrates were mainly converted to epoxides. The pattern of metabolites was isoform specific. Moreover, regiospecificity was substrate-dependent. For example, CYP2C23 epoxidized AA

preferentially at the 11,12-, EPA at the 17,18-, DPA at the 10,11- and DHA at 10,11- and 19,20-double bonds. All epoxygenases except CYP2C9 preferentially attacked the ω -3 double bonds of EPA and DHA.

Table 3.9 Regioselectivity of CYP2C isoforms in the epoxidation of AA, EPA, DPA and DHA. Substrates were converted by CYPs under identical conditions (as described in 2.3.1) and different regioisomeric epoxides were resolved by combination of RP-HPLC and NP-HPLC (compare with Figures 3.27, 3.28, 3. 29 and 3.30). Values are presented as a percentage of total amount of epoxy product. The respective main products are marked by colour.

Epoxygenases

	AA			EPA				DPA					DHA				
	8,9-EET	11,12-EET	14,15-EET	8,9-EETeTr	11,12-EETeTr	14,15-EETeTr	17,18-EETeTr	7,8-EDTeTr	10,11-EDTeTr	13,14-EDteTr	16,17-EDTeTr	19,20-EDTetr	7,8-EDP	10,11-EDP	13,14-EDP	16,17-EDP	19,20-EDP
CYP2C8	0	52	48	3	22	30	45	0	25	11	29	35	0	15	19	23	43
CYP2C9	18	30	52	20	28	45	7	9	66	0	15	9	6	62	10	12	10
CYP2C11	19	42	39	20	20	27	33	37	18	8	13	23	15	26	13	20	26
CYP2C23	25	59	16	13	14	15	58	13	41	5	25	16	0	38	4	21	37

3.4.4 Metabolism of ω -3 fatty acids by recombinant hydroxylases

As shown in 3.4.2, kidney and liver microsomes are highly active in hydroxylating EPA, DPA and DHA. The aim of this part of the study was to identify major CYP isoforms involved in this metabolism. To this end, we compared enzymatic activities of human (CYP4A11, CYP4F2) and mouse (Cyp4a12a and Cyp4a12b) AA hydroxylases towards AA, EPA, DPA and DHA and we also determined the CYP-specific metabolite pattern for each of studied ω -3 fatty acids.

3.4.4.1 Comparison of enzymatic activities towards AA, EPA, DPA and DHA

The activities of recombinant AA-hydroxylases towards EPA, DPA and DHA were analyzed as described in 3.4.1. Figure 3.32 shows the enzymatic activities of the enzymes tested. Activities are given in nmol/nmol/min.

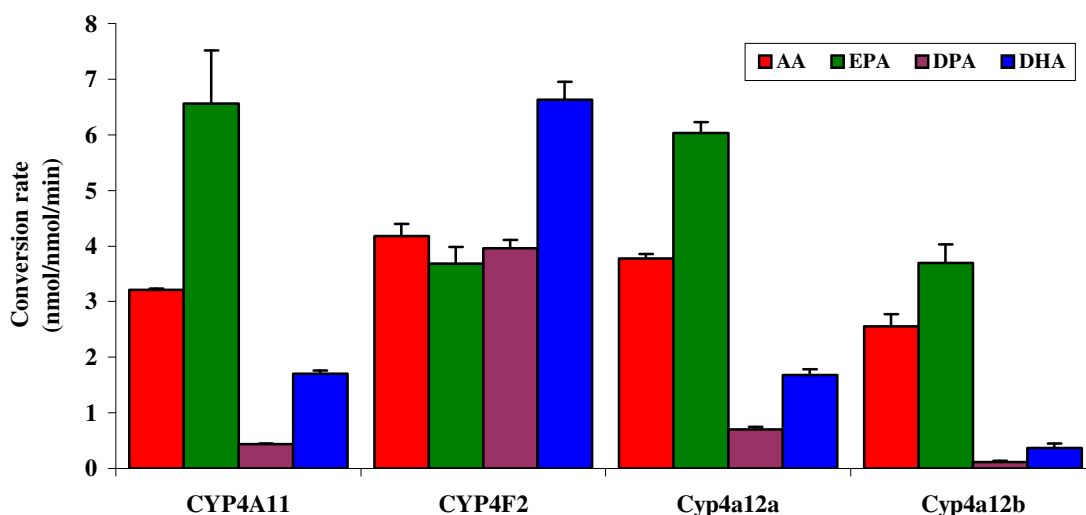


Figure 3.32 *Enzymatic activities of CYP4A11, CYP4F2, Cyp4a12a and Cyp4a12b towards AA, EPA, DPA and DHA. Microsomal activities were determined using reaction mixtures of 0.1 ml containing 10 pmol of microsomal protein and substrate at concentration of 10 μ M (AA, EPA, DPA and DHA) Reactions were started with NADPH and stopped after 10 min. Data are mean \pm SE values of experiment done in triplicate.*

CYP4A11 converted EPA with an activity two-fold higher compared to that of AA (6.5 vs. 3.2 nmol/nmol/min). DPA conversion was extremely low (~ 0.5 nmol/nmol/min) whereas activity towards DHA reached 50 % of that of AA.

Interestingly, **CYP4F2** showed different substrate specificity towards ω -3 fatty acids compared to CYP4A11, Cyp4a12b and Cyp4a12b. CYP4F2 had similar activities towards AA, EPA and DPA (4, 3.7, and 4 nmol/nmol/min, respectively). However, the DHA conversion rate by CYP4F2 was much higher compared to that of all other hydroxylases tested. CYP4F2-dependent DHA conversion reached a rate of ~7 nmol/nmol/min which was at least 3-fold higher compared to the activities of other isoforms.

Cyp4a12a converted AA with an activity (3.77 nmol/nmol/min) similar to that of CYP4A11 and CYP4F2 (3.2 and 4 nmol/nmol/min). The conversion rate of EPA was almost two-fold higher compared to that of AA. DPA was converted with much lower rate than AA (1 vs. 3.77 nmol/nmol/min) whereas conversion of DHA reached 50 % of AA conversion rate.

Cyp4a12b showed a substrate preference similar to that of Cyp4a12a and CYP4A11. That means that EPA was the preferred substrate. The conversion rate of EPA was about 50 % higher than that of AA (2.5 vs. 3.7 nmol/nmol/min). In contrast, DPA and DHA were poor substrates (0.2 and 0.4 nmol/nmol/min, respectively).

Taken together, these results demonstrated that CYP isoforms known before only as AA-hydroxylases are also able to efficiently convert ω -3 fatty acids such as EPA, DPA and DHA. Each of the CYP isoforms studied shows a unique substrate preference. EPA was the preferred substrate of CYP4A11, Cyp4a12a and Cyp4a12b. DPA and DHA were preferred substrates of CYP4F2.

3.4.4.2 CYP4A/4F isoform-specific metabolite patterns

3.4.4.2a Metabolite pattern of conversion of EPA, DPA and DHA by CYP4A11

As already described in Introduction (1.1.5.3), CYP4A11 is together with CYP4F2 the major AA-hydroxylase in human kidney. This enzyme metabolized AA mainly to 20-HETE (Lasker et al., 2000).

Results of the present study confirm this already published CYP4A11-dependent AA metabolite pattern. Recombinant CYP4A11 converts AA to 19/20-HETE. 20-HETE and 19-HETE were formed in ratio 78: 22 under our conditions.

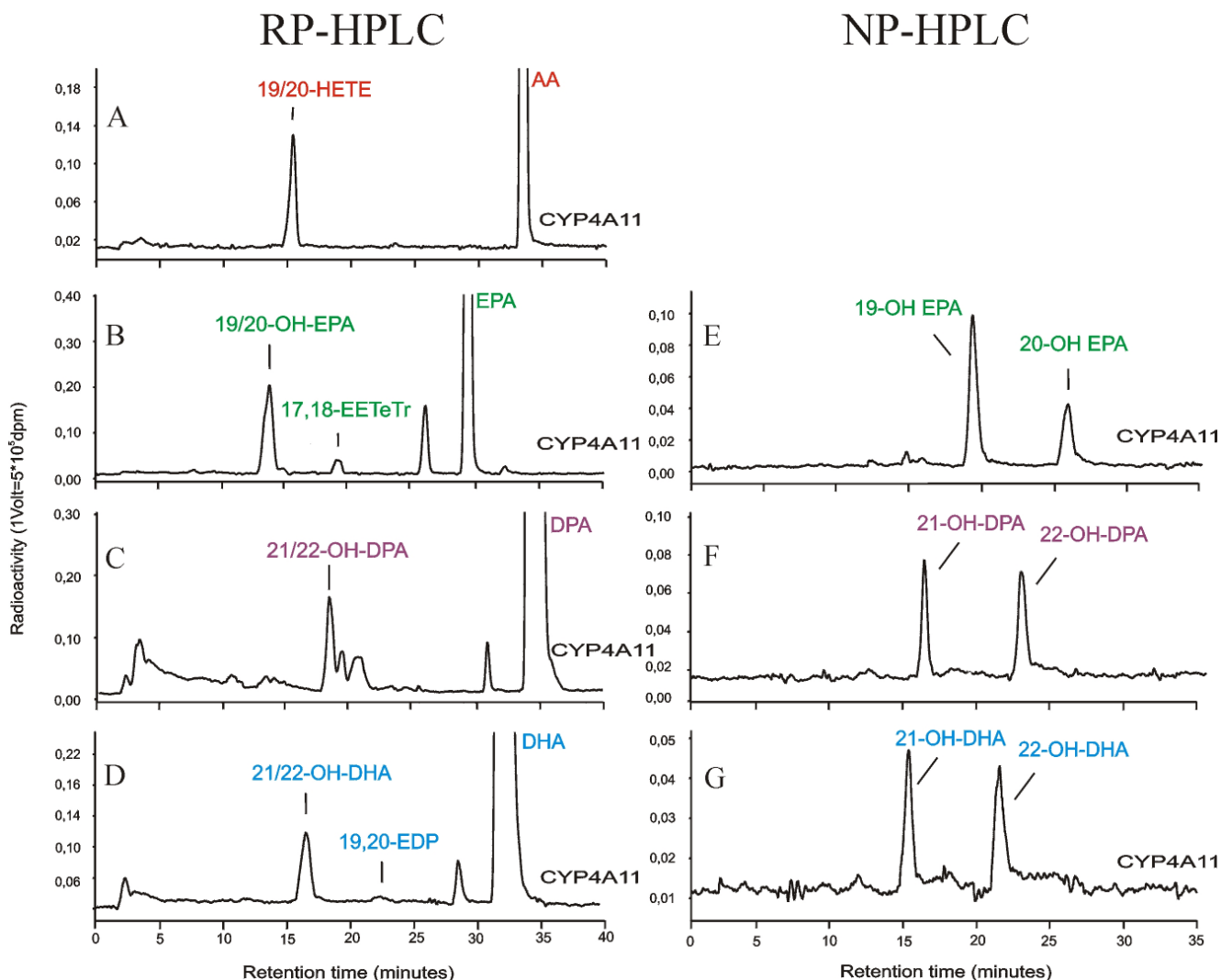


Figure 3.33 HPLC analyses of AA, EPA, DPA and DHA metabolites produced by CYP4A11. 10 pmol of CYP4A11 was incubated with 10 μ M of substrate (AA, EPA, DPA and DHA). Reactions were started with NADPH and stopped after 10 min. Metabolites were extracted and resolved on HPLC. A, B, C and D chromatograms represent examples of RP-HPLC resolved CYP4A11-dependent metabolites of AA, EPA, DPA and DHA, respectively. E, F and G chromatograms show the resolution of epoxy metabolites, which were not clearly separated on RP-HPLC (19/20-OH-EPA, 21/22-OH-DPA, 21/22-OH-DHA, respectively) by using subsequent NP-HPLC.

Interestingly, separation of **EPA** metabolites showed that CYP4A11 was not only acting as a hydroxylase but also as an epoxygenase. The epoxy product eluted at 18.7 minutes, which was equal to the retention time of authentic 17,18-EETeTr (Figure 3.33). The ratio between the products of hydroxylation and epoxidation was 9: 1 (Table 3.11). In contrast to hydroxylation of AA, where 20-HETE was the major product, CYP4A11 hydroxylated EPA mainly to 19-OH-EPA, which represented 69 % of the total hydroxylation product. There was a prominent

unidentified metabolite with a retention time of 25.6 min. This metabolite is the potential product of terminal dehydrogenation of EPA. This type of reaction has been first reported for CYP4A11 catalyzed 11,12-desaturation of lauric acid. Further studies are necessary, however to prove the respective identity of our EPA metabolite.

CYP4A11 converted **DPA** to 21/22-OH-DPA. The regiospecificity of this reaction was not further determined. Due to low conversion rate it was not possible to collect sufficient amounts of OH-DPA for further determination of regiospecificity (Figure 3.33). Moreover, an unidentified peak migrating at $R_t = 31$ min was observed which is potential product of terminal dehydrogenation of DPA.

DHA was converted to 21/22-OH-DHA and to a minor extent to 19,20-EDP (Figure 3.33). These two reactions occurred in a ratio of 11: 1. ω - and ω -1 hydroxy-metabolites were produced in almost equal quantities 21-OH-DHA: 22-OH-DHA = 48: 52 (Table 3.11). An unknown peak with $R_t = 29$ min appeared in significant amounts. This peak resembled unidentified EPA and DPA metabolites described above and it is potential product of terminal dehydrogenation of DHA.

3.4.4.2b Metabolite pattern of conversion of EPA, DPA and DHA by CYP4F2

As already described in Introduction (1.1.5.1), CYP4F2 is the major human liver AA-hydroxylase. This enzyme is also expressed in kidney. Similar to CYP4A11, CYP4F2 metabolizes AA mainly to 20-HETE.

Results from this work confirmed that 20-HETE is the major product of CYP4F2-dependent AA hydroxylation. 20-HETE represented 98 % of total hydroxylation product (Figure 3.33, Table 3.11).

EPA was converted to 19/20-OH-EPA and to traces of 17,18-EETeTr. 20-OH-EPA was the main product with 83 % of total hydroxylation (Table 3.11). There were also traces of an unknown metabolite with a retention time of 25.6 min, which appeared also with CYP4A11-dependent conversion of EPA and it is potential product of terminal dehydrogenation of EPA (Figure 3.33).

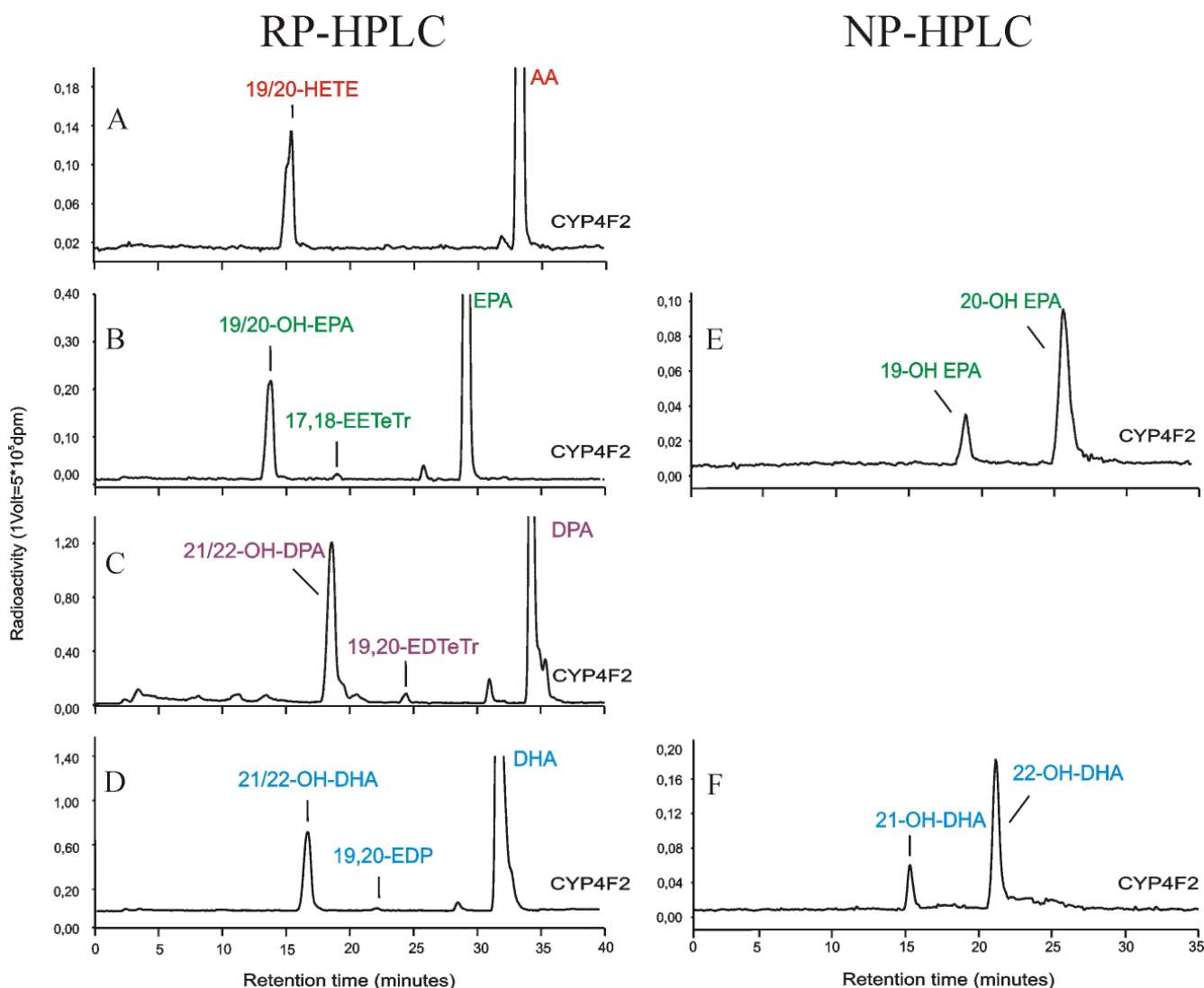


Figure 3.34 HPLC analyses of AA, EPA, DPA and DHA metabolites produced by CYP4F2. 10 pmol of CYP4F2 was incubated with 10 μ M of substrate (AA, EPA, DPA and DHA). Reactions were started with NADPH and stopped after 10 min. Metabolites were extracted and resolved on HPLC. A, B, C and D chromatograms represent examples of RP-HPLC resolved CYP4F2-dependent metabolites of AA, EPA, DPA and DHA, respectively. E and F chromatograms show the resolution of epoxy metabolites, which were not clearly separated on RP-HPLC (19/20-OH-EPA, 21/22-OH-DPA, 21/22-OH-DHA, respectively) by using subsequent NP-HPLC.

DPA was hydroxylated to 21/22-OH-DPA. 22-OH-DPA represented 70 % of the total hydroxy product. Traces of epoxidation were also detectable (Figure 3.34). An unidentified metabolite with retention time of 31 minute was present as already described by CYP4A11.

As with EPA and DPA, **DHA** was hydroxylated and there were also traces of epoxy product. Epoxidation represented 1 % of total metabolism (Figure 3.34). The major

product was 22-OH-DHA with 82 % of total hydroxy product (Table 3.11). Traces of an unidentified 27-minute peak were present. As already described previously by CYP4A11, this peak is potential product of terminal dehydrogenation.

Analogous to direct competition between AA and EPA for conversion with CYP2C8 (Table 3.8), in this study was examined to what extent AA and DHA compete for the conversion by CYP4F2. As shown in Table 3.10, DHA was clearly preferred substrate if present together with AA in equimolar amount. DHA metabolites were formed with 3-fold higher activity compared to AA metabolites.

Table 3.10 AA and DHA competition for conversion by CYP4F2. 10 μ M AA, a mixture of 5 μ M AA+5 μ M DHA or 10 μ M DHA were incubated for 10 min with 10 pmol of CYP4F2. Metabolites are resolved on RP-HPLC. All reactions were done in triplicate. Total amounts of AA and DHA hydroxy products were given in pmol.

CYP4F2	AA product (pmol)	DHA product (pmol)
10 μ M AA	35,2	0
5 μ M AA+5 μ M DHA	12	33
10 μ M DHA	0	64,2

3.4.5.2c Metabolite pattern of conversion of EPA, DPA and DHA by Cyp4a12a

Cyp4a12a and Cyp4a12b were described as the most active mouse AA-hydroxylases by our laboratory (1.1.5.2). Cyp4a12a is highly expressed in the kidney and liver where it forms 20-HETE.

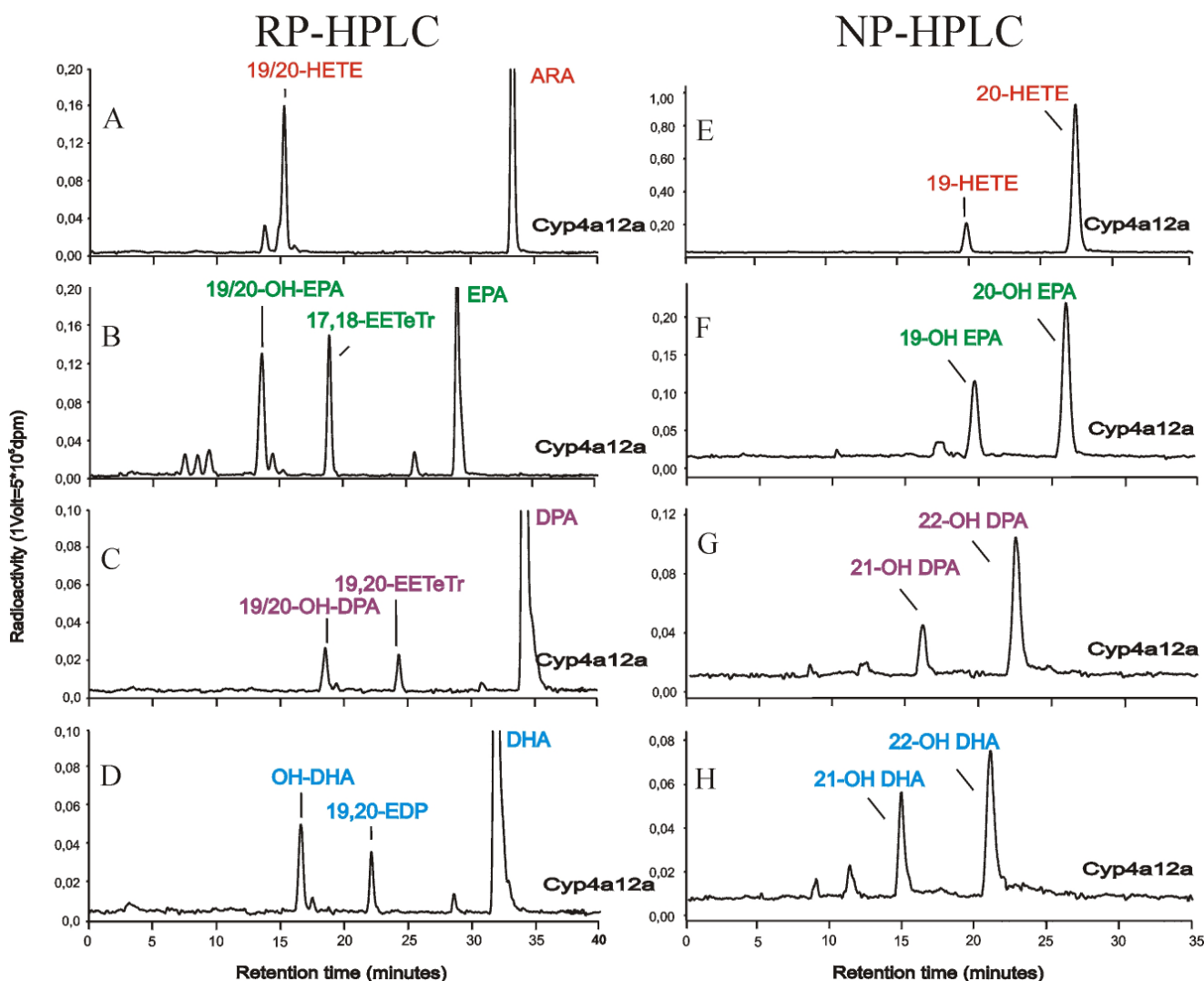


Figure 3.35 HPLC analyses of AA, EPA, DPA and DHA metabolites produced by *Cyp4a12a*. 10 pmol of *Cyp4a12a* was incubated with 10 μ M of substrate (AA, EPA, DPA and DHA). Reactions were started with NADPH and stopped after 10 min. Metabolites were extracted and resolved on HPLC. A, B, C and D chromatograms represent examples of RP-HPLC resolved *Cyp4a12a*-dependent metabolites of AA, EPA, DPA and DHA, respectively. E, F, G and H chromatograms show the resolution of epoxy metabolites, which were not clearly separated on RP-HPLC (19/20-OH-EPA, 21/22-OH-DPA, 21/22-OH-DHA, respectively) by using subsequent NP-HPLC.

This study also showed that 20-HETE is the major *Cyp4a12a*-dependent AA metabolite. *Cyp4a12a* hydroxylated AA to a 19- and 20-HETE, in a ratio of 14 % to 86 %. An additional peak with a retention time of 13.7 min appeared. This peak strongly increased upon prolonged incubation. Using GC-MS (Dr. H. Honeck, MDC) and LC-MS (Dr. M. Rothe, FILT GmbH) analysis, this peak was identified as dicarboxylic acid (α,ω -icosatetraenoic acid). It represents a secondary product

of AA-hydroxylation metabolism and originates from further oxidation of 20-HETE (Figure 3.35).

EPA was converted to both 19/20-OH-EPA and 17,18-EETeTr. In contrast to EPA conversion by CYP4A11 and CYP4F2, epoxidation was the major reaction. Amount of 17,18-EETeTr produced by Cyp4a12a was 1.4-fold higher compared to that of hydroxy-metabolites. 19-OH-EPA and 20-OH-EPA were formed in a ratio of 33: 67 (Table 3.11). A potential product of terminal dehydrogenation with a retention time of 25.6 min occurred with Cyp4a12a as with other CYP4a isoforms (Figure 3.35).

DPA was also both hydroxylated and epoxidized by Cyp4a12a. The ratio between these two reactions was in favor of hydroxylation, which was 1.7-fold higher. The main product was 22-OH-DPA, which represented 70 % of total hydroxylation (Figure 3.35). A potential product of terminal dehydrogenation eluted at 31 min was present like in the case of previously tested AA-hydroxylases (Figure 3.35).

DHA was metabolized to hydroxy- and epoxy-metabolites in a ratio of 2.2: 1 (Table 3.11). An unidentified peak, a potential product of terminal dehydrogenation, already described by other CYP4As, with a retention time of 28.6 min was present (Figure 3.35). Cyp4a12a metabolized DHA mainly to 22-OH-DHA. It represented 65 % of total hydroxylation.

3.4.5.2d Metabolite pattern of conversion of EPA, DPA and DHA by Cyp4a12b

As already described in Introduction (1.1.5.2), Cyp4a12a and Cyp4a12b differ in only 11 amino acids. Despite this very high degree of sequence identity, similarity between Cyp4a12b and Cyp4a12a is very high; these two isoforms produce different patterns of metabolites. Cyp4a12b hydroxylised **AA** to 19/20-HETE (Rt= 15.4 min) and to a minor amount of 18-HETE (Rt =16 min). 19- and 20-HETE were formed in ratio of 11: 89 (Figure 3.36).

As already described for Cyp4a12a variant, Cyp4a12b also catalyzed epoxidation and hydroxylation of **EPA**. Epoxidation represented the major reaction. Cyp4a12b formed 2.6-fold more 17,18-EETeTr than 19/20-OH-EPA (Table 3.11). NP-HPLC showed that 20-OH-EPA represented the major hydroxy product. The 19-: 20-OH-EPA ratio was 37: 64. In addition to the expected metabolites (19-OH-EPA and 20-

OH- EPA), there were 2 other minor peaks detected in NP-HPLC (Figure 3.36). Those two peaks were not identified.

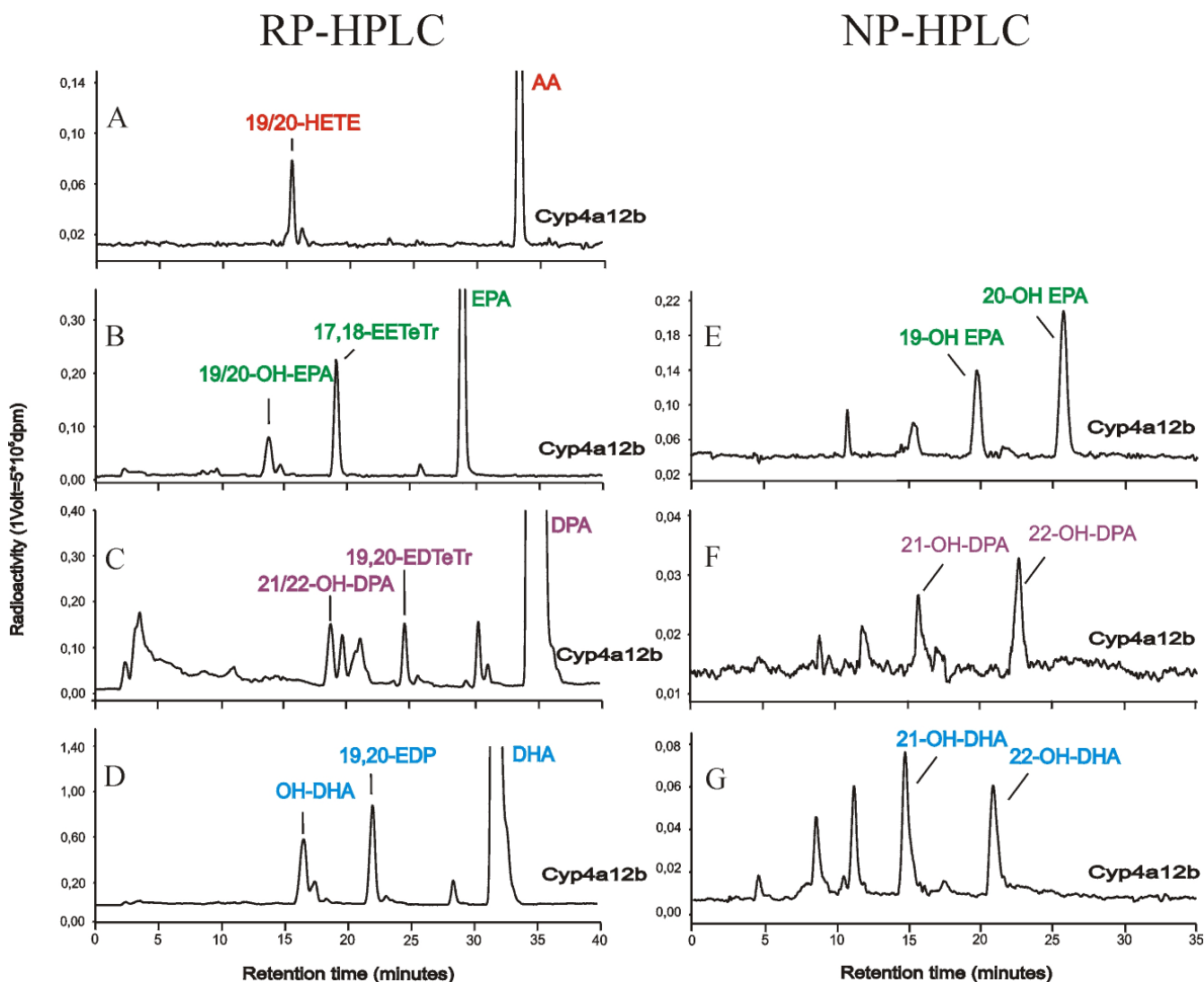


Figure 3.36 HPLC analyses of AA, EPA, DPA and DHA metabolites produced by Cyp4a12b 10 pmol of Cyp4a12b was incubated with 10 μ M of substrate (AA, EPA, DPA and DHA). Reactions were started with NADPH and stopped after 10 min. Metabolites were extracted and resolved on HPLC. A, B, C and D chromatograms represent examples of RP-HPLC resolved Cyp4a12b-dependent metabolites of AA, EPA, DPA and DHA, respectively. E, F and G chromatograms show the resolution of epoxy metabolites, which were not clearly separated on RP-HPLC (19/20-OH-EPA, 21/22-OH-DPA, 21/22-OH-DHA, respectively) by using subsequent NP-HPLC.

Cyp4a12b poorly metabolized **DPA**. Hydroxy- and epoxy-products were present in 1: 1 ratio. Moreover, Cyp4a12b converted DPA to three unknown metabolites with retention times of 20 min, 22 min and 31 min. Third unknown metabolite (Rt=31min) was already described as the potential product of terminal

dehydrogenation. The peak with a retention time between 2-5 minutes probably represented products of strong substrate autooxidation (Figure 3.36).

DHA was converted by Cyp4a12b to 19,20 EDP and 21/22-OH-DHA. Epoxidation was the major reaction. The amount of 19,20-EDP formed was 1.5 times higher compared to 21/22-OH-DHA. 21/22-OH-DHA was collected from RP-HPLC and further resolved in NP-HPLC. 5 peaks were detected. Peaks with retention times 15 and 21 minute represented 21-OH-DHA and 22-OH DHA, respectively. The other 3 peaks with retention times 4.3, 9.1 and 12 minutes were not further identified (Figure 3.36). Interestingly, Cyp4a12a-dependent conversion of DHA yielded also similar unexpected product peaks. 21-: 22-OH-DHA were formed in ratio of 55 % to 45 % respectively (Table 3.11).

Table 3.11 Reaction specificity and regioselectivity of CYP4A/4F in conversion of AA, EPA, DPA and DHA. Substrates were converted by CYPs under identical conditions (as described in 2.3.1). Hydroxy and epoxy products were quantified using RP-HPLC (hydroxy: epoxy ratio in first column of the table). Different regioisomeric hydroxy products were further resolved by NP-HPLC (compare with Figures 3.33, 3.34, 3.35 and 3.36) Values are presented as a percentage of total amount of hydroxy product.

Hydroxylases

	AA			EPA			DPA			DHA		
	Hydroxy: Epoxy	19-HETE	20-HETE	Hydroxy:Epoxy	19-OH-EPA	20-OH-EPA	Hydroxy : Epoxy	21-OH-DPA	22-OH-DPA	Hydroxy : Epoxy	21-OH-DHA	22-OH-DHA
CYP4a12A	1:0	14	86	1:1,4	33	67	1,7:1	27	73	2,2:1	35	65
CYP4a12B	1:0	11	89	1:2,6	37	64	1:1	N.d.	N.d.	1:1,5	55	45
CYP4A11	1:0	22	78	9:1	69	31	1:0	N.d.	N.d.	11:1	48	52
CYP4F2	1:0	2	98	24:1	17	83	29:1	30	70	99:1	18	82

Taken together, this part of the study demonstrated that the CYP4A and CYP4F enzymes, which preferentially function as AA ω -hydroxylases, were less regioselective when metabolizing the ω -3 fatty acids. Moreover, it was remarkable that the CYP4A and CYP4F enzymes functioned solely as hydroxylases when converting AA but showed additional epoxygenase activity towards ω -3 fatty acids. This property was most pronounced with mouse Cyp4a isoforms (Table 3.11).

4. Discussion

4.1 CYP-dependent EET/HEET-formation as a novel target for the treatment of high blood pressure

The present study focuses on dTGR as a model of ANG II-induced hypertension and renal damage, and shows that this disease state can be strongly ameliorated by treating the animals with PPAR α activator fenofibrate. Fenofibrate treatment restored CYP-dependent renal EET/HEET formation.

As already outlined in Introduction (1.1.7), dTGR show significantly lower renal microsomal epoxygenase and hydroxylase activities as well as reduced activities of several potential epoxygenases (CYP2C11, CYP2C23, and CYP2J) These alterations of are associated with developing of hypertension and renal damage in this model (Kaergel et al., 2002).

A similar relationship between hypertension and altered CYP metabolism seems to exist in various animals suggesting that results of the present study maybe at least in part generalized.

Hypertension in these animal models could be caused by (Table 4.1):

- decreased renal EET.
- increased vascular 20-HETE.
- decreased tubular 20-HETE.

The following discussion will focus on such animal models of hypertension, which show decreased EET levels similar to our dTGR.

As already described in Introduction (1.1.6) and summarized in the Figure 4.1, EETs have antihypertensive properties. Decrease in EET level may lead to sodium retention and vasoconstriction and both conditions may cause hypertension.

EET levels can be reduced due to:

- diminished expression level and/or activity of CYP epoxygenases
- increased activity of sEH, which hydrolyzes EETs to corresponding inactive vic- DHETs.

Table 4.1 List of animal models, which develop hypertension and renal damage in association with alterations in CYP-dependent metabolism.

Animal model of hypertension	Alteration in CYP-dependent metabolism	Reference
<i>ANG II/salt treated rats</i>	Decreased EET level/ inability to upregulate EET level	Zhao et al., 2003a
<i>Salt sensitive Dahl rat</i>		Makita et al., 1994
<i>dTGR</i>		Kaergel. et al., 2002
<i>Rats fed high fat diet</i>		Wang. et al., 2003
<i>Young SD rats-salt treated</i>		Sankaralingam. et al., 2006
<i>ANG II infusion</i>	Increase in vascular 20-HETE level	Muthalif et al., 2000
<i>SHR</i>		McGiff and Quilley, 1999
<i>DOCA/salt-treated</i>		Oyekan et al., 1997
<i>CYP4a14 knock out mouse</i>		Holla et al., 2001
<i>Cyclosporin A-treated rats</i>		Seki et al., 2005
<i>Salt sensitive Dahl rat</i>	Decrease in tubular 20-HETE level	Ma et al., 1994
<i>HET0016/salt-treated</i>		Hoagland et al., 2003

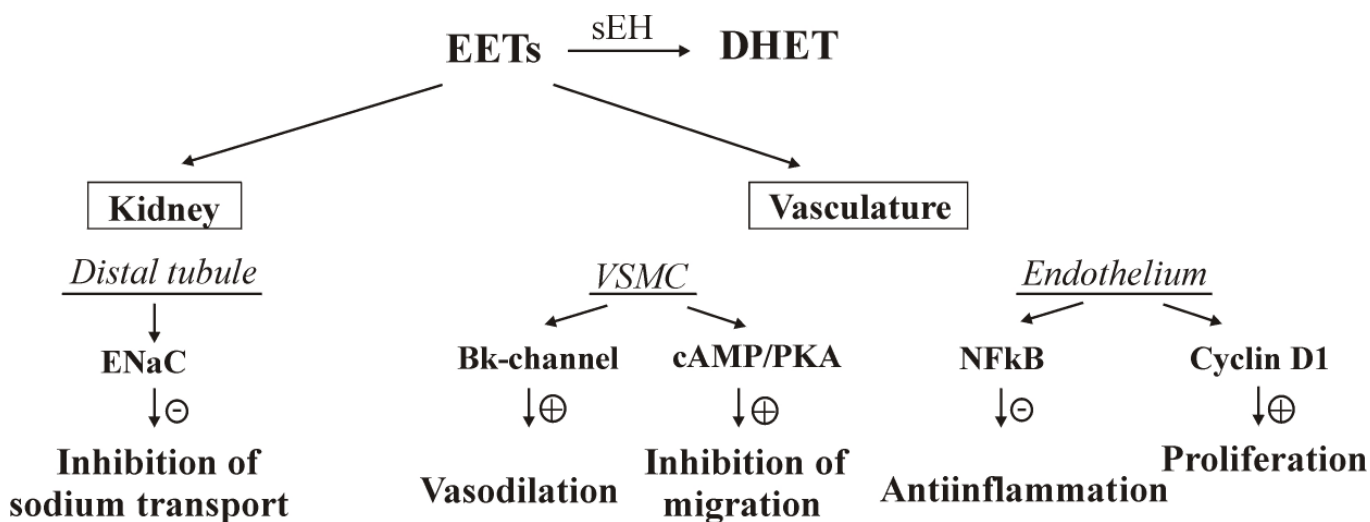


Figure 4.1 Scheme of EET actions in kidney and vasculature.

4.1.1. Downregulation of EET/HEET formation in animal models of hypertension

Salt intake

Capdevila et al. (1992) demonstrated in rat that high salt intake increases the renal microsomal epoxygenase activity. Urinary excretion of epoxygenase metabolites was 10-20-fold increased by salt induction. High salt intake did not have significant effect on the microsomal hydroxylase activity. The major AA epoxygenase in the rat kidney is CYP2C23 and that is the renal CYP2C isoform, which is upregulated by excess dietary salt intake (Holla et al, 1999). Treatment of rats on a high salt diet with the epoxygenase inhibitor, clotrimazole, produces significant increases in mean arterial blood pressure. Furthermore, clotrimazole treatment causes significant reductions in the urinary excretion of epoxygenase metabolites and selective inhibition of the renal microsomal epoxygenase reaction. The prohypertensive effects of clotrimazole are reversed when either the salt or clotrimazole treatment is discontinued (Makita et al., 1994). Interestingly, CYP2C23 was also the major EET synthase in our dTGR model and its activity was strongly downregulated in association with ANG II induced hypertension and strongly upregulated with treatment with fenofibrate. As it will be discussed later on there is a further interesting parallel: salt, ANG II and fenofibrate effects on CYP2C23 activity are mediated at a posttranslational level.

Salt sensitive Dahl rat

The indication that a salt-inducible renal epoxygenase protects against hypertension, are supported by studies with the Dahl rat model of genetic salt-sensitive hypertension. Dahl resistant animals responded to excess dietary salt by inducing kidney microsomal epoxygenase activity and remain normotensive. In contrast, Dahl salt sensitive rats are unable to regulate epoxygenase activity in response to salt loading and suffer from severe hypertension (Makita et al., 1994).

ANG II/salt treated rats

Interestingly, combined administration of ANG II and a high salt diet significantly downregulates expression of CYP2C23, CYP2C11, and CYP2J protein in renal microvessels (Zhao et al., 2003a, Zhao. et al., 2003b). Elmarakby et al. (2006) showed that TNF-alpha contributes to downregulation of CYP2C23 in ANG II dependent high-salt hypertension. It appears that high ANG II levels prevent the normal induction of CYP2C23-dependent EET generation in response to salt loading. The combination of ANG II infusion and high salt provides rather nonphysiological condition since high salt normally reduces the activity of the renin-angiotensin system. The pathophysiological condition including decreased EET levels after ANG II infusion combination with high salt resembles that of our dTGR model.

Young SD rats

Young SD rats (five weeks old) develop high blood pressure after salt treatment whereas SD adults (53 weeks old) do not increase blood pressure under the same conditions. In adult rats, salt induces CYP4A and CYP2C mRNA level and therefore it increases level of eicosanoids important for sodium excretion. In contrast, in young rats CYP4A and CYP2C23 levels are diminished (Sankaralingam et al., 2006). Whether or not young and adult rats do respond differentially also to high ANG II levels is unknown. It is interesting to note however, that dTGR animals analyzed in the present study had an age of seven weeks. Animals in higher age could not be studied since untreated dTGR were died at the age of eight weeks.

High fat diet

Providing a further animal model that shares many features with our dTGR animals, Wang et al. (2003) showed that rats fed with high fat diet develop higher blood

pressure. These animals also show decrease of CYP-derived eicosanoid synthesis in the different renal zones (cortex, medulla, and papilla). The renal ω -hydroxylase activity is decreased by 46 % in cortex, 43 % in medulla, and 46 % in papilla of HF rats. The renal epoxygenase activity is decreased by 46 % in cortex, 31 % in medulla, and 56 % in papilla of HF rats. The changes in the rate of 20-HETE and EET formation in different renal zones are consistent with the levels of expression of CYP4A and CYP2C23 proteins, respectively.

Pregnancy

Pregnancy is also good model for studies of blood pressure regulation since it is associated with changes of blood pressure. Zhou et al. (2005) showed that EETs contribute to the control of blood pressure during pregnancy. During gestation in pregnant rats epoxygenase activity was elevated by 47-97 % depending of the gestation stage. This was associated with elevation of protein expression of AA epoxygenases CYP2C23, CYP2C11 and CYP2J2. Epoxygenase-specific inhibition by PPOH, which does not have an effect on hydroxylase activity, inhibits epoxygenase activity and leads to high blood pressure. Again the parallels to the dTGR are obvious. The most interesting finding with the pregnancy model was that inhibition of EET generation is sufficient to cause hypertension.

4.1.2 Increased EET hydrolysis in animal models of hypertension

As already mentioned above, the activity of CYP2C/2J is not the only factor that determines the level of biologically active EETs. SEH-dependent hydration of EETs is also a very important factor. Several studies show a correlation between high blood pressure and increased sEH activity. Below, SHR and ANG II treated rat are described as two models of hypertension, which show increased sEH activity.

SHR

EET hydrolysis was increased 5- to 54-fold in renal cortical S9 fractions from the SHR relative to the normotensive WKY rats. Increased EET hydrolysis was consistent with increased expression of sEH in the SHR renal microsomes and cytosol relative to the WKY samples. The urinary excretion of 14,15-DHET was 2.6-fold higher in the SHR than in the WKY rat, confirming increased EET

hydrolysis in the SHR in vivo. Blood pressure was significantly decreased 6 hours after treatment of SHRs with a selective sEH inhibitor and this treatment had no effect on blood pressure in the WKY rats (Yu et al., 2000).

ANG II treated rats

Inhibition of sEH lowers blood pressure in rats with ANG II hypertension as well. Renal cortical sEH protein expression was significantly higher in ANG II hypertension compared with normotensive animals. Administration of sEH inhibitors lowered systolic blood pressure in ANG II hypertensive animals (Imig et al., 2002). SEH inhibition has not only antihypertensive properties; it also improves renal vascular function and ameliorates hypertension induced renal damage. SEH protein expression was increased in renal microvessels from hypertensive rats. SEH inhibitor treatment significantly attenuated afferent arteriolar diameter responses to ANG II in hypertensive kidneys. Urinary albumin excretion, an index of renal damage, was also lower in CDU-treated hypertensive rats (Zhao et al., 2004).

Taken together, these studies suggest that elevation of EETs by induction of CYP enzymes and/or inhibition sEH could lower blood pressure and protect the kidney from ANG II-induced damage. In our dTGR model we did so far successful treatment to induced CYP-dependent EET generation and it will be an important task for future studies to analyze the potential beneficial effects of sEH inhibition.

4.2 Regulation of EET formation by PPAR α agonists

4.2.1 Effect of fenofibrate in different animal models

PPARs are ligand-activated transcription factors, which bind to PPAR-response elements in a gene promoter region. Some isoforms of CYP4A have this promoter region and can be induced by PPAR agonists. (Aldridge et al., 1995; Muerhoff et al., 1992). Fibrates, the lipid-lowering drugs, are selective agonists for PPAR α (Forman et al., 1997), and administration of these drugs induces CYP4A mRNAs and proteins in the liver and kidney of rats (Green, 1999; Hardwick et al., 1987; Sundseth and Waxman, 1992; Gibson, 1989). Resembling the results of the present study with dTGR model, fibrates prevent the development of hypertension in Dahl

salt-sensitive rats (Roman et al., 1993) and stroke-prone spontaneously hypertensive rats (Shatara et al., 2000). In the Table 4.2 summarizes data from several studies, which indicate that an essential step in the antihypertensive action of PPAR α agonists may be indeed induction of CYP-dependent EET metabolism.

Young SD rats show inability to increase expression of CYP2C and CYP4A in kidney under salt treatment, causing sodium retention and developing high blood pressure. In these rats, PPAR α agonist clofibrate increases level of renal CYP4A and CYP2C and prevents sodium retention and reduction of blood pressure to normal (Sankaralingam et al., 2006).

High fat diet induces high blood pressure in rats (4.1). Clofibrate treatment of rats fed high fat diet induces renal tubular CYP4A, and therefore 20-HETE production. This leads to regulation of sodium retention and blood pressure (Zhou et al., 2006).

Table 4.2 Reports on fibrate effects in animal models of hypertension

Animal model of hypertension	Effect of fibrate	Reference
<i>Salt sensitive Dahl rat</i>	↑ tubular 20-HETE	Zhao et al., 2003a
<i>SHR</i>	?	Makita et al., 1994
<i>Young SD rats-salt treated</i>	↑ renal CYP4A and CYP2C	Kaergel. et al., 2002
<i>Rats fed high fat diet</i>	↑ tubular 20-HETE	Wang. et al., 2003
<i>ANG II-induced hypertension</i>	↑ tubular 20-HETE and EETs	Sankaralingam et al., 2006
<i>Obese Zucker rats</i>	↑ EETs	Muthalif et al., 2000

Fenofibrate treatment prevents development of **ANG II-dependent hypertension** in C57BL/6J mice. Fenofibrate treatment markedly increases levels AA-hydroxylase and AA-epoxygenase activities and therefore increases 20-HETE and EET level in the kidney. Upregulation of 20-HETE and EET production in renal

tubules contribute to blood pressure lowering effects of fenofibrate (Vera et al., 2005).

Similar to our study, which is described in next chapter (4.2.2), Zhao et al. (2006) showed that renal levels of CYP2C11 and CYP2C23 are decreased in **obese Zucker rats** and that fenofibrate treatment restores their protein levels. In contrast to data presented in chapter 4.2.2, in obese Zucker rats, increase of CYP2C11 protein level by fenofibrate was significant. Moreover, fenofibrate treatment induced protein level of CYP2C11 in SD control rats (4.2.2), whereas it did not have any effect on epoxygenase activity in lean Zucker rats.

4.2.2 Effect of fenofibrate in dTGR

4.2.2.1 Effect of fenofibrate on inflammation and end-organ damage in dTGR

In collaboration with D.N. Müller, F.C. Luft and coworkers, we found that fenofibrate treatment reduced mortality of dTGR from 50 % for untreated animals to zero. The blood pressure was significantly reduced in treated animals and was similar to SD control rats. Fenofibrate prevented albuminuria and protected against matrix protein deposition (collagen IV and fibronectin); Muller et al., 2004.

NF- κ B DNA binding activity was markedly increased in dTGRs, whereas fenofibrate treatment reduced it to the low levels typical for healthy control animals. Infiltration of immune cells in the kidney was also suppressed by fenofibrate (Muller et al., 2002). We can conclude that fenofibrate treatment abolished inflammatory response in dTGR and protect against ANG II induced hypertension and end-organ damage.

4.2.2.2 Mechanisms of fenofibrate-induced prevention of inflammation in dTGR

The direct pathway of anti-inflammatory action of activated PPAR α involves interfering with activity of NF- κ B and AP-1 transcription factors by protein-protein interaction between PPAR α and p65 and c-Jun subunits of NF- κ B and AP-1,

respectively. PPAR α also induces the expression of the inhibitory protein I κ B α and therefore keeps NF- κ B in inactive complex (Figure 4.2).

An additional mechanism of anti-inflammatory PPAR α action may occur via CYP-dependent eicosanoid production. EETs are described as inhibitor of cytokine-induced I κ B kinase complex activation, a key step in the pathway leading to NF- κ B activation (Node K. et al., 1999). It is also reported that treatment of rats with a general P450 inhibitor sensitizes the animals to subsequent inflammatory stimuli (Carcillo et al., 1998). Since AA epoxygenase activity is reduced in dTGR (4.1), the assumption was that induction of AA epoxygenase activity and EET level can contribute to suppression

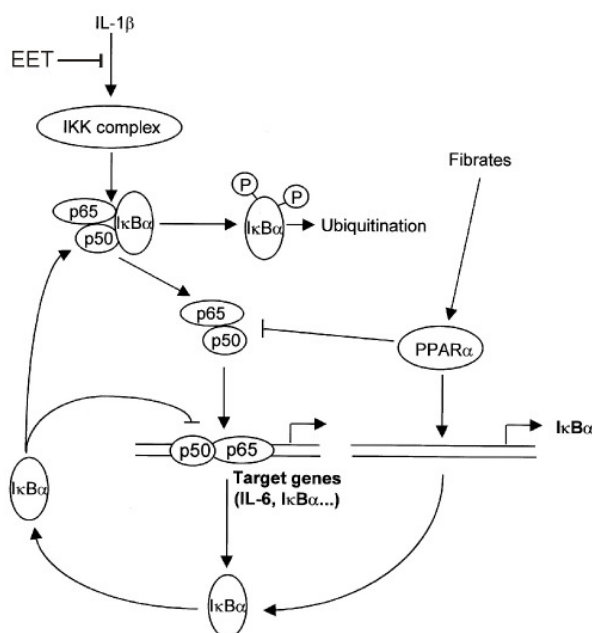


Figure 4.2 Model of inhibition of NF- κ B signalling pathway by PPAR α activators. According to Delerive P. et al., 2000 and extended by the role of EETs as an inhibitor of cytokine induced NF- κ B activation (Node et al., 1999).

of proinflammatory mechanisms triggered by NF- κ B. The data presented in the present study showed for the first time that fenofibrate significantly increased renal AA-epoxygenase but not AA-hydroxylase activity in dTGR and SD control rats. CYP2C23 was detected as a major renal AA-epoxygenase in dTGR and SD rats as well as in corresponding fenofibrate-treated groups. CYP2C23 epoxidizes AA mainly to 11,12-EET (Holla et al., 1999), which represents the regioisomer with the most potent anti-inflammatory properties (Node et al., 1999).

4.2.2.3 Effect of fenofibrate on renal EET formation in dTGR

4.2.2.3.1 Possible mechanism of downregulation of CYP expression and activity in dTGR

As already described in 1.1.7 and 4.1.1.1, dTGR show significantly lower renal microsomal epoxygenase and hydroxylase activities as well as reduced protein levels of several AA-epoxygenases (CYP2C11, CYP2C23, and CYP2J); Kaergel et al., 2002. The mechanism of CYP downregulation is still unclear in this model. Several studies described that different CYP isoforms are downregulated during inflammation (Iber et al., 1999). In contrast to findings in dTGR, hypertension induced by long-term infusion of ANG II in rat is not associated with reduced renal AA epoxygenase activities and decreased CYP2C23 and CYP2C11 levels (Imig et al., 2001). The main difference of dTGR model, compared to ANG II infusion, may be related to the fact that uncontrolled inflammation triggered by high local ANG II concentrations is responsible for renal damage in dTGR (Luft et al., 1999). Furthermore, the finding that dTGR show strongly reduced renal CYP2C11 levels correlate to results of downregulation of hepatic CYP2C11 expression in models of hepatic inflammation (Iber et al., 1999). Proposed mechanism that leads to hepatic CYP2C11 reduction includes NF- κ B binding negative regulatory element, which suppresses CYP2C11 transcription (Iber et al., 2000). Muller et al., (2002) described TNF- α as crucial factor for developing of inflammation in dTGR whereas Elmarakby et al., (2006) reported that TNF- α contributes to downregulation of mRNA level of CYP2C23 in salt-sensitive angiotensin hypertension.

Moreover, decrease in protein level can occur due to protein degradation. The crucial factor in redirecting CYP to proteasomal degradation is structural and functional damage of the enzyme. Impaired heme biosynthesis, heme deficiency or heme modification, results in damaged CYP enzyme. Reactive oxygen species or reactive metabolic products can attack the P450 heme and therefore damage the enzyme, which is a signal for enzyme rapid degradation (Wang et al., 1999; Correia et al., 2005). Reactive oxygen species were detected in glomeruli of dTGR animals (Theuer et al., 2005) but there is no evidence that it triggers proteasomal degradation of CYPs. Nitric oxide (NO) can bind to prosthetic heme group of CYP

and inhibit its enzymatic activity. A NO-dependent mechanism is described as responsible for decreasing endothelial CYP2C expression and for downregulation of the endothelium-derived hyperpolarizing factor in response to proinflammatory mediators (Kessler et al., 1999). Increased NO concentrations may be also responsible for inactivation of CYP4A enzymes (Oyekan et al., 1999). Inhibition of iNOS restores CYP2J4 protein content and CYP activity in acute pneumonia (Yaghi et al., 2004). NO synthase II is strongly activated in the kidney of dTGR and this could lead to conclusion that NO plays role in the downregulation of CYP expression in dTGR (Luft et al., 1999; Muller et al., 2000; Muller et al., 2001). Surprisingly, Theuer and coworkers (2005) demonstrated however, that inhibition of NO synthase does not improve renal CYP enzymatic activity in dTGR, although has partial effect on renal CYP4A and CYP2C11 protein expression (Figure 4.3).

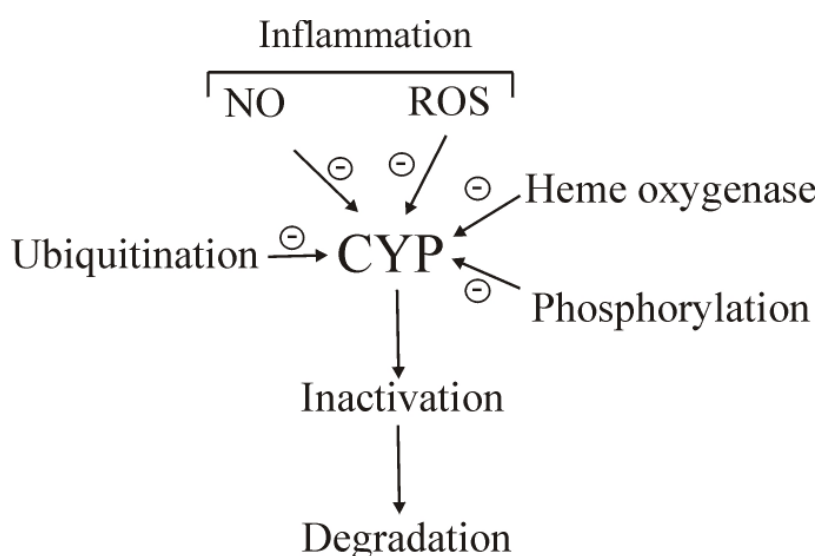


Figure 4.3 Possible triggers of CYP inactivation and degradation.

4.2.2.3.2 Effect of fenofibrate on CYP expression and activity in dTGR and SD rats

Fenofibrate treatment increased AA epoxygenase activity in both dTGR and SD rats whereas AA hydroxylase activity remained unchanged (3.1.1.1, 3.1.2). We have identified CYP2C23 as a major AA epoxygenase in the kidney of dTGR and SD (3.1.1.2). Fenofibrate treatment of both groups of animals induced protein level of CYP2C23 to ~160 % of that of non-treated SD animals (3.1.1.3, 3.1.2). Fenofibrate treatment did not alter protein level of CYP2C11 in dTGR, whereas under the same

conditions protein level in SD rats was increased to 150 % of nontreated SD rats (3.1.1.3, 3.1.2). Therefore, elevated level of AA epoxygenase activity in kidney of fenofibrate-treated dTGR can be attributed to increase of CYP2C23 activity. Direct transcriptional regulation of the CYP2C23 gene was excluded, since the promoter does not contain a typical PPAR α response element (Roussel et al., 1995). That was confirmed by comparison of renal CYP2C23 mRNA levels between dTGRs and SD rats (3.1.1.3). They did not differ and were not influenced by fenofibrate treatment. In both dTGR and SD rats, fenofibrate effect was most pronounced on the CYP2C23 activity level whereas the CYP2C23 protein expression was only moderately increased and there was no effect on mRNA level. These results correspond to several other studies, which report similar data. For example, high-salt intake of rats also induced CYP2C23 at protein level without change of mRNA level (Holla et al., 1999). Furthermore, Yu. et al. (2006) reported that borage oil rich diet increases AA epoxygenase activity and CYP2C23, CYP2C11, and CYP2J protein levels without effect on mRNA in SHR. These data lead to the conclusion that regulation of CYP protein expression and activity under fenofibrate treatment occurs at a post-translational level.

4.2.2.3.3 Potential mechanisms of regulation of CYP expression and activity by fenofibrate

From the data described in the previous chapter it can be concluded that regulation of CYP2C23 expression and activity is regulated at post-translational level. In general, relatively little is known about post-translational regulation of CYP enzymes. For example, CYP2E1 can be induced by ethanol that induces protein level but mRNA remains unchanged (Song et al., 1986; Song et al., 1987). CYP2E1 may provide an interesting example of how to investigate the regulation of CYP2C23 by fenofibrate. Ethanol induction of CYP2E1 is proposed to be due to an increase in translation rate and/or protein stabilization (Eliasson et al., 1988; Tsutsumi et al., 1993). Roberts et al. (1995) described protein stabilization as a primary mechanism. In this study, it was reported that the half-life of ethanol-stabilized CYP2E1 is 38 h what is significantly longer compared to control half-life of CYP2E1 of 6–7 h followed by a slower secondary phase. The mechanism underlying the rapid degradation of CYP2E1 appears to involve the ubiquitin-

proteasome proteolytic pathway. The pathway of rapid proteolytic degradation must be somehow altered by ethanol but the mechanism stays unclear. Moreover, Eliasson et al. (1990) reported that phosphorylation on Ser-129 of CYP2E1 is an important step which occurs prior proteolysis. Korsmeyer et al. (1999) indicated that CYP2B1 and CYP3A also underlie ubiquitination, which proceeded after their phosphorylation, but it remains to be determined whether, in common with several other cellular proteins, such P450 phosphorylation is indeed required for their degradation.

The effect of fenofibrate on CYP2C23 activity was much more pronounced than on CYP2C23 protein expression. Therefore, it can be concluded that those two processes are regulated independently. Phosphorylation is described as a very important process in the regulation of enzymatic activities of CYPs involved in biosynthesis of cholesterol and steroid hormones (Aguiar et al., 2005). Role of phosphorylation differs between different CYPs. For example for CYP51, it is reported that the phosphorylated form of the enzyme showed lower activity (Sonoda et al., 1995). On the other hand, activity of CYP11A1 is stimulated by posttranslational phosphorylation (Caron et al., 1975; Vilgrain I. et al., 1984). 17-20 lyase activity of human CYP17A1 was regulated in the same way. Cyp17A1 has bifunctional active site (Nakajin et al., 1881), which catalyzes 17-hydroxylation and cleavage of 17-20 steroid bond (lyase activity). Phosphorylation of serine and threonine residues by protein kinase A (PKA) increases 17-20-lyase activity, while dephosphorylation has an opposite effect (Zhang et al., 1995). Oesch-Bartolomowicz et al. (2001) reported on an important role of Ser-128 in rat liver CYP2B1. This site is phosphorylated by PKA resulting in instant decrease of enzymatic activity. Interestingly, that correlates with homologous Ser-129 of CYP2E1, which is reported as site of phosphorylation, which occurs prior proteolysis (Eliasson et al., 1990) CYP2C23 contains an Arg-Arg-X-Ser sequence, which is represents a recognition motif for PKA. Analogous to Ser-128 in CYP2B1 and Ser-129 in CYP2E1, CYP2C23 has Ser-131, which could be the site for phosphorylation (Figure 4.4). Possible phosphorylation of this site could be involved in regulation of CYP2C23.



Figure 4.4 Alignment of protein sequences of CYP2C23, CYP2E1 and CYP2B1 between amino acid position 100 and 150. The recognition motif for PKA is labelled by red square. The last amino acid in recognition motif is a serine, which represents site of phosphorylation in CYP2E1 and CYP2B1. Therefore we hypothesize that the corresponding serine in CYP2C23 (Ser-131) may play an important role in the regulation of CYP2C23 activity. Sequences were aligned in Clustal W program (EMBL-EBI).

4.2.3 CYP-dependent AA-metabolites as endogenous PPAR α activators

As already described in 3.1.1.1 and 3.1.3, CYPs convert AA to EETs and HETEs, as primary products, which can be further metabolized by CYP to AA secondary products, the HEETs. The ability of CYP4A enzymes to hydroxylate EETs to HEETs has been already reported (Coward et al., 2002). We found a novel pathway, in which HEETs are efficiently produced by CYP2C23-dependent epoxidation of 20-HETE. CYP2C23-dependent 20-HETE epoxidation is a major route of HEET production in rat kidney (Figure 4.5).

HEET generation via both pathways required an interaction of CYP4A and CYP2C enzymes. According to immunohistochemical analysis, CYP4A and CYP2C23 are co-localized in most medullary and certain cortical tubules and may thus indeed cooperate to produce HEETs (Muller et al., 2004).

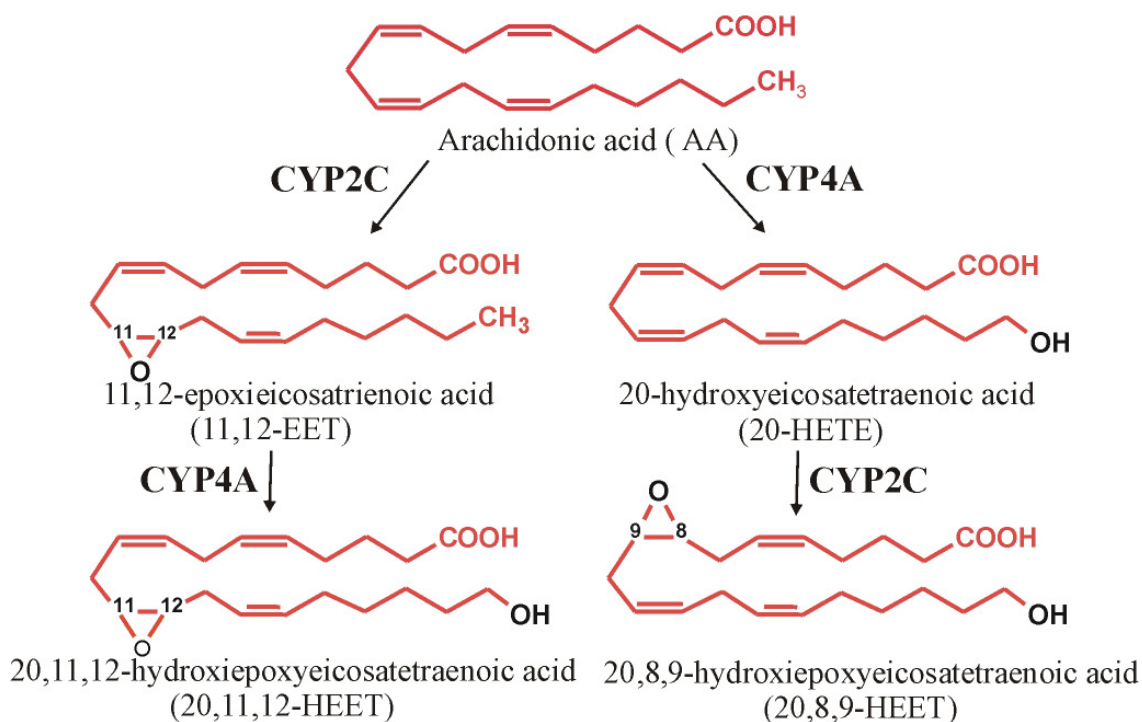


Figure 4.5 Mechanism of HEET syntheses. HEETs are synthesised in two-step reactions catalyzed by CYP2C and CYP4A isoforms. AA can be either firstly epoxidized to EET (11,12-EET as a major regioisomer produced by CYP2C23) and then further hydroxylated by CYP4A to HEET (20,11,12-HEET is a major product of this pathway). The second pathway is initiated by CYP4A-dependent hydroxylation to 20-HETE followed by CYP2C catalyzed epoxidation to HEET. Due to the unique regioselectivity of CYP2C23 in 20-HETE epoxidation, 20,8,9-HEET is a major product of this pathway in rat renal microsomes.

We also showed that CYP2C- and Cyp4A-dependent formation of HEET is not a minor side reaction but may be as important as primary product formation. In line with this assumption, the activities of CYP2C isoforms tested (CYP2C8, CYP2C9, CYP2C11 and CYP2C23) were higher towards 20-HETE compared to AA. For example, CYP2C23 metabolized 20-HETE about 5-fold better than AA. Cyp4as (Cyp4a12a and Cyp4a12b) showed also very good activities towards EETs. 11,12-EET was accepted as the best substrate among AA and EET regioisomers. Conversion of 11,12-EET was about 2-fold higher compared to that of AA (Figure 4.6 and Figure 4.7).

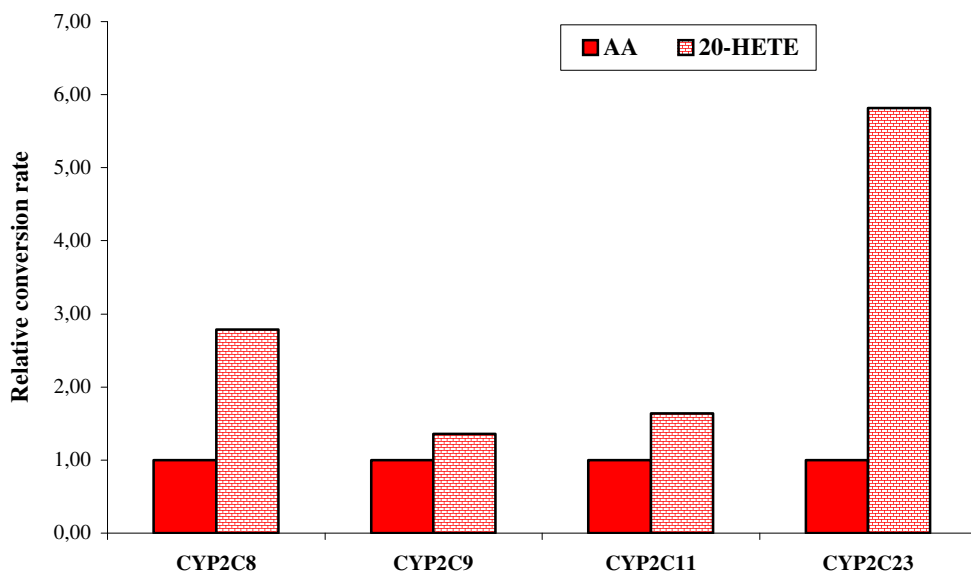


Figure 4.6 Conversion rates of AA and 20-HETE by CYP2C isoforms. Conversion rates are presented relative to that of AA, which was set to 1.

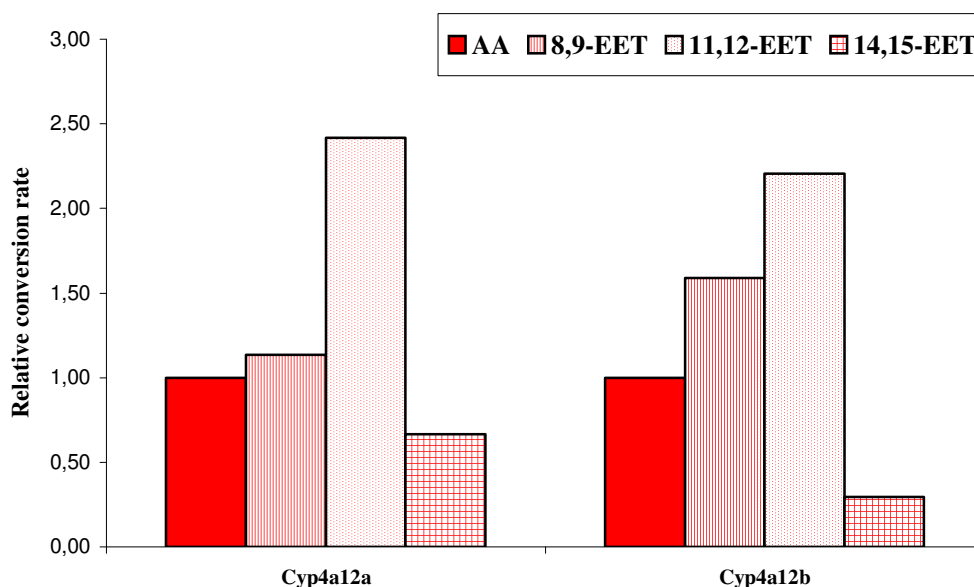


Figure 4.7 Conversion rates of AA, 8,9-, 11,12- and 14,15-EET by Cyp4a12a and Cyp4a12b. Conversion rates are presented relative to that of AA, which was set to 1.

Cowart and colleagues (2002) showed that HEETs function as high-affinity endogenous PPAR α activators. In dTGR, decreased CYP activity drastically affects AA secondary product generation. DTGR renal activity in secondary product formation was almost five times lower compared to SD controls (3.1.3). This decrease was much more pronounced compared to AA primary product generation.

The fenofibrate treatment resulted in marked increase of secondary product formation in dTGR (6-fold) and in SD rats (3.5-fold). Moreover, even though fenofibrate did not induce AA-hydroxylation in SD rats, hydroxylation of EETs to HEETs was almost two-fold induced. It remains unclear why AA secondary product formation was much more “sensitive” than formation of AA primary products in response to the disease state and fenofibrate treatment. We speculate that this fact is in part due to the necessity of at least two CYP isoforms for each HEET formation (CYP2C and CYP4A). Both are subject to regulation what may synergistically increase or decrease HEET generation. Second, it should be noted that the different CYP4A isoforms in rat (CYP4A1, 2, 3, 8) differ significantly in the abilities to hydroxylate AA (Nguyen et al., 1999) and EETs (Coward et al., 2002). Thus, fenofibrate probably induced a CYP4A isoform that shows low AA hydroxylase but high EET hydroxylase activity.

4.2.4 Hypothesis on the mechanism of fenofibrate action on high blood pressure and end-organ damage

In summary, the results of the present study propose the following mechanism for the involvement of CYP-dependent eicosanoids in the regulation of blood pressure and renal end-organ damage in the dTGR model. When released from membrane phospholipids, AA can be converted by CYP4As and CYP2Cs to 20-HETE and EETs, respectively. Both primary products can be further converted to HEET. For HEET synthesis, the activity of both CYP4A and CYP2C is necessary. In the kidney, both isoforms colocalized to most medullary and certain cortical tubules. In the kidneys of dTGR, protein levels and AA epoxygenase and AA hydroxylase activities are significantly reduced. NF- κ B DNA binding activity is significantly increased (Figure 4.8).

Alterations in CYP activities alter AA metabolite formation. Pathophysiological CYP2C down-regulation, as found in our dTGRs model, leads to:

- reduced EET levels
- even more pronounced decrease in HEET production
- presumably also to accumulation of 20-HETE levels because of a lower rate of CYP2C-catalyzed 20-HETE epoxidation.

Fenofibrate treatment directly activates PPAR α (Figure 4.8). Activated PPAR α inhibits proinflammatory transcription factors NF- κ B and AP1. At the same time, fenofibrate treatment induces CYP2C23 protein level and even more AA epoxygenase activity, which resulted in increased EET and HEET levels. EETs can also inhibit NF- κ B. Increased levels of HEETs may have resulted in further PPAR α activation. Thus, it appears that exogenous PPAR α activator (fenofibrate) induced the CYP-dependent generation of an endogenous high affinity PPAR α activator (positive feedback loop). PPAR α activation inhibits NF- κ B and AP1 leading to attenuation of the inflammatory reaction and prevention of end-organ damage (Figure 4.8). However, further studies are necessary to prove this hypothesis in detail. In particular it would be important to directly measure the in vivo levels of the different CYP-dependent eicosanoids in the kidney and other tissues and organs of our dTGR model under the different treatment conditions.

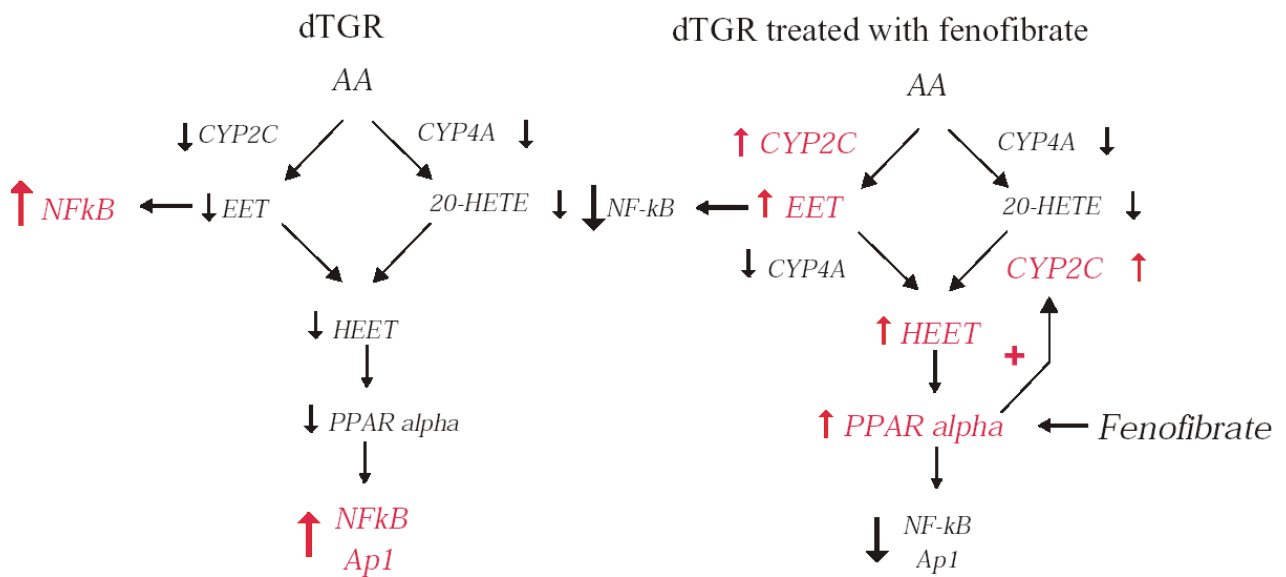


Figure 4.8 CYP-dependent renal metabolism in dTGR and fenofibrate- treated dTGR.

4.3. ω -3 fatty acids as an alternative source for CYP-dependent eicosanoids

4.3.1. CYP-dependent metabolism of ω -3 fatty acids

As already described in Introduction (1.2.2), ω -3 and ω -6 fatty acids are precursors for the synthesis of different eicosanoids. Both classes of fatty acids can be converted by COX, LOX and CYP enzymes producing a wide range of bioactive metabolites. In physiological terms, AA represents the most important ω -6 fatty acid and all three pathways of AA metabolism have been extensively studied in last several decades. COX- and LOX- dependent metabolism of ω -3 fatty acids have been studied in detail whereas, in contrast to AA, CYP-dependent metabolism of ω -3 fatty acids did not attract that much attention. Van Rollins and coworkers described, already in 1984, that rat liver microsomes can metabolize DHA, but till now there are only few published data on CYP-dependent metabolism of ω -3 fatty acids. It has been reported that renal, hepatic, and seminal vesicle microsomes are able to hydroxylate and epoxidize EPA (Van Rollins et al., 1988, Oliw and Sprecher, 1991, Theuer et al., 2005). Knapp et al. (1991) found that humans ingesting ω -3 fatty acids excrete via urine substantial quantities of vicinal diols of EPA that result from CYP-catalyzed EPA epoxidation and subsequent hydrolysis by epoxide hydrolase. Unfortunately, in general the identity and reaction specificity of the individual CYP isoforms involved in ω -3 fatty acid metabolism have been largely unknown.

Therefore, the aim of the present study was to test in detail which of the ω -3 fatty acids can serve as alternative substrates for CYP enzymes. Renal rat, mouse and human and human liver microsomes and individual CYP isoforms were tested. Individual CYP isoforms, which were tested, included two human (CYP2C8 and CYP2C9) and two rat (CYP2C11 and CYP2C23) AA epoxygenases and two human (CYP4A11 and CYP4F2) and two mouse (Cyp4a12a and Cyp4a12b) AA hydroxylases.

Renal microsomes from mouse, rat and human and human liver microsomes and all tested individual CYP isoforms converted all ω -3 fatty acids (EPA, DPA and DHA) with enzymatic activities which were equal or higher of that of AA. All tested CYP

isoforms, except CYP4F2, preferred EPA as the best substrate. DHA the most efficient substrate of CYP4F2 (~170 % of that for AA); Figure 4.9.

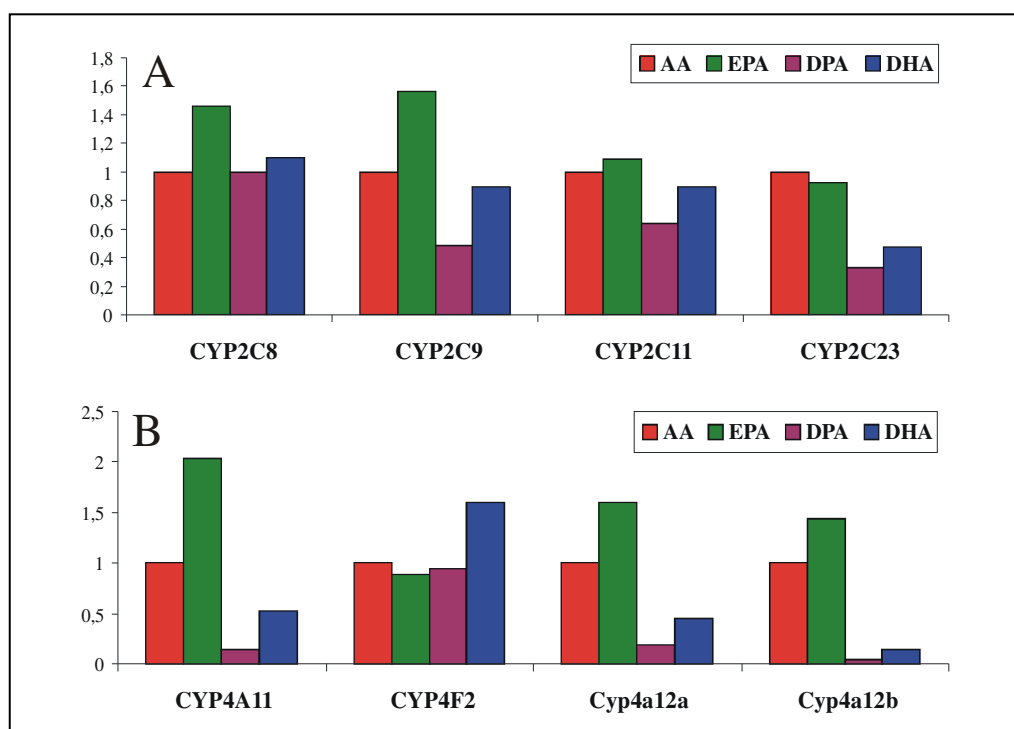


Figure 4.9 Comparison of CYP conversion rates towards AA, EPA, DPA and DHA. AA values are presented as value of 1. Enzymatic activities of other fatty acids are normalized to AA.

Mouse renal and rat renal microsomes and human liver microsomes, metabolized EPA with clearly highest preference. Human renal microsomes preferentially converted DHA as above mentioned for CYP4F2. This analogy can be explained by the fact that human renal microsomes predominantly carry out hydroxylation and CYP4F2 is the major hydroxylase in human kidney (Powell et al., 1998). Therefore preference of human renal microsomes to DHA can be attributed to CYP4F2 activity. Similarly, activities of mouse renal microsomes and Cyp4a12a can be compared. Mouse renal microsomes convert AA: EPA: DPA: DHA in ratio 1: 2: 0.5: 0.6 whereas Cyp4a12a, the major AA-hydroxylase in mouse kidney, converts the same substrates in similar ratio (1: 2: 0.25: 0.5).

Mouse and human renal microsomes metabolized AA mainly to 20-HETE. These microsomes showed clearly enhanced epoxygenase activity when converting ω -3 fatty acids. For example, mouse renal microsomes converted AA to epoxy and

hydroxy in ratio of 1: 2 whereas EPA, DPA and DHA were converted to equal amounts of epoxy and hydroxy metabolites. This clear increase in epoxy product formation can be explained by the fact that Cyp4a12a preferentially epoxidizes ω -3 fatty acids in contrast to an almost exclusive hydroxylation of AA (compare 4.3.2). Thus, reduced regioselectivity of Cyp4a12a when converting ω -3 fatty acids contributes to higher level of epoxy products. In contrast, human renal microsomes predominantly hydroxylate EPA, DPA and DHA. This can be partially explained considering the reaction specificity of the main hydroxylases in human kidney, CYP4F2 and CYP4A11. They have high activities to ω -3 fatty acids but in contrast to Cyp4a12a, they produce only minor quantities of epoxy derivatives therefore, there was no switch of metabolite ratios.

From the data discussed above, it can be concluded that ω -3 fatty acids serve as alternative substrates for CYP enzymes. This conclusion is further confirmed by our results on a direct substrate competition between AA and EPA and AA and DHA. Conversion of mixture of equal amounts of AA and EPA by CYP2C8 yielded preferentially EPA products. A similar result was obtained for the conversion of mixtures of equal amounts of AA and DHA by CYP4F2 where the predominant metabolite produced was 22-OH-DHA (Figure 4.10 and Figure 4.11).

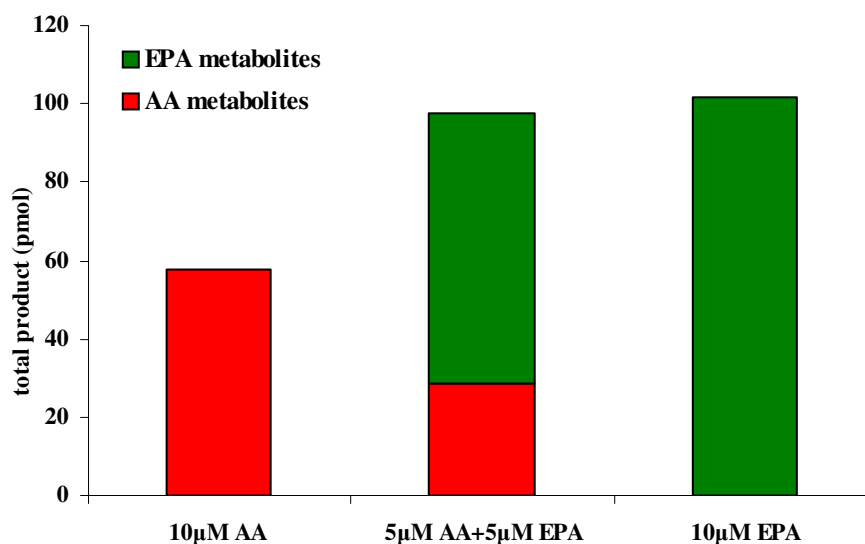


Figure 4.10 Direct competition of AA and EPA for conversion by CYP2C8. For the details compare the Results chapter 3.4.3.2a.

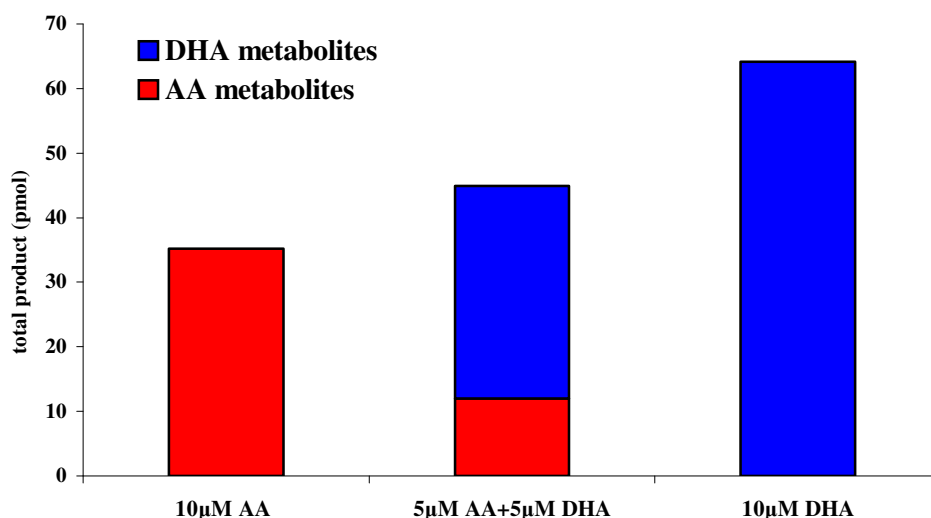


Figure 4.11 Direct competition of AA and DHA for conversion by CYP4F2. . For the details compare the Results chapter 3.4.4.2b.

4.3.2. Profile of CYP-dependent ω -3 metabolites

The results of the present study demonstrate that CYP enzymes produced isoform-specific patterns of regioisomeric derivatives from EPA, DHA and DPA. Moreover the regiospecificity was substrate-dependent.

It has been already described that **AA-epoxygenases** CYP2C8, CYP2C9, CYP2C11 and CYP2C23 convert AA to 8,9-EET, 11,12-EET and 14,15-EET and that the regiospecificity is isoform specific (Dai et al., 2001, Daikh et al., 1994, Holla et al., 1999, Karara et al., 1993). These data were confirmed in the present study (Table 3.9). When converting EPA, DPA and DHA, AA-epoxygenases showed a high preference towards the ω -3 double bond, forming epoxides, which have no “homolog” within the series of the AA-derived epoxides. All except CYP2C9 converted EPA mainly to 17,18-EETeTr. CYP2C23 showed the highest regiospecificity and converted EPA to 17,18-EETeTr reaching 60 % of the total product. CYP2C isoforms converted DHA with high preference for the 19,20-double bond. CYP2C9 was again the only isoform without preference for conversion of the ω -3 double bond of DHA. DPA was not converted with pronounced regiospecificity (Figure 4.12, Table 3.9).

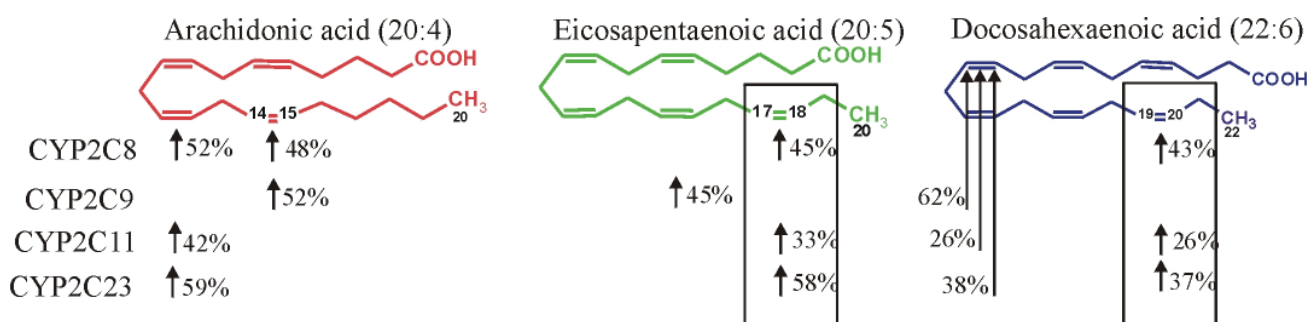


Figure 4.12 Scheme of preferentially attacked double bonds of AA, EPA and DHA by CYP2C isoforms. Double bonds, which were preferentially converted by CYP isoforms, are indicated with arrows. Values represent the percentage of an individual epoxide in relation to total epoxy product.

These data correlate with results from the studies for rat and human AA hydroxylases, CYP4A1 and CYP1A1, which were also conducted in our laboratory (Lauterbach et al., 2002 and Schwarz et al., 2004). CYP4A1 and CYP1A1, in addition to hydroxy products, form high amounts of epoxy products. Furthermore, it has been also described for human isoforms CYP4F8 and CYP4F12 that they metabolize ω -6 and ω -3 fatty acids in different ways. Both isoforms metabolize AA by ω -3 hydroxylation whereas epoxidize DPA and DHA (Stark et al., 2005).

The present study also confirmed already published results from several authors, which show that **AA-hydroxylases** (CYP4A11, CYP4F2, Cyp4a12a and Cyp4a12b) metabolize AA exclusively to 19/20-HETE (Lasker et al., 2000; Powell et al., 1998; Muller et al., 2006). Interestingly, CYP4A11, CYP4F2, Cyp4a12a and Cyp4a12b did not show only hydroxylase activity but also epoxygenase activity towards all tested ω -3 substrates. Cyp4a12a and Cyp4a12b epoxidized all substrates to significant amounts of epoxy products. Surprisingly, Cyp4a12b metabolized all substrates primarily to epoxy product whereas Cyp4a12a metabolized only EPA primarily to an epoxy product. CYP4A11 and CYP4F2 formed only minor quantities of epoxy products (Figure 4.13).

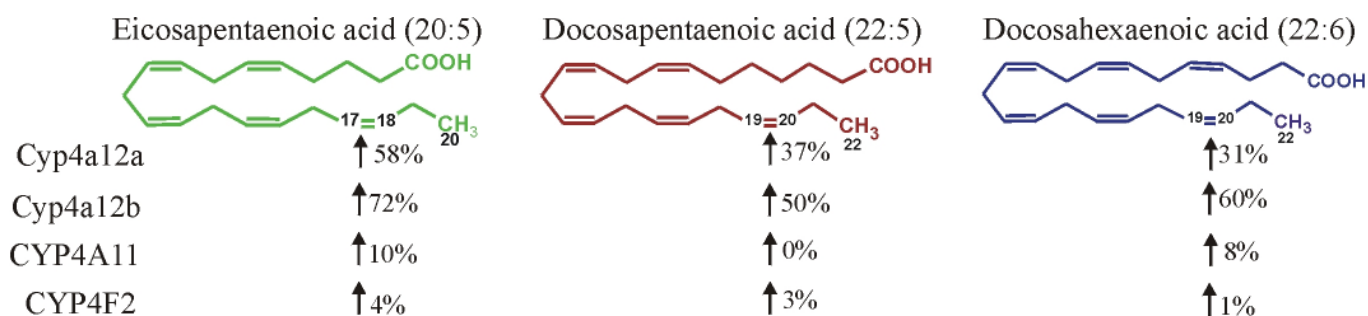


Figure 4.13 Scheme of CYP4A/4F-dependent epoxidation of EPA, DPA and DHA. The ω -3 double bonds, which were epoxidized by CYP isoforms, are indicated with arrows. Values represent the percentage of the epoxide in relation to the total product (epoxy product+ products of ω - and ω -1-hydroxylation). None of the other double bonds were attacked. Using AA as a substrate all CYP isoforms shown produced only hydroxylase products (19/20-HETE).

All CYP4A/4F isoforms epoxidized exclusively double bond at ω -3 position. EPA was epoxidized to 17,18-EETeTr. DPA was epoxidized exclusively to 19,20-EDTeTr and DHA to 19,20-EDP. These data lead to the conclusion that the ω -3 double bond is a crucial factor for the epoxidation activity of AA-hydroxylases when converting ω -3 fatty acids.

All CYP4A/4F isoforms conducted primarily hydroxylation at the ω -carbon atom. When converting AA, the relative amount of ω -hydroxy product (20-HETE), ranges between 78 % for CYP4A11 and 98 % for CYP4F2. Interestingly, hydroxylation of EPA, DPA, and DHA yielded lower ratios of ω - and ω -1 hydroxy products. For example, Cyp4a12b formed 20-HETE to 89 % of total product. In contrast, ω -hydroxylation of EPA and DHA was much less pronounced. 20-OH-EPA: 19-OH-EPA were synthesized in a ratio of 64: 36 and 22-OH-DHA: 21-OH-DHA were synthesized in ratio of 45: 55. CYP4A11, CYP4F2 and Cyp4a12a showed similar substrate dependent shifts of regioselectivities.

4.3.3 Stereospecificity of individual CYP isoforms in 17,18-double bond epoxidation

Epoxides are chiral molecules and they can exist in two enantiomeric forms: R,S and S,R. A number of studies described differences in biological actions of opposite enantiomers. For example, R,S-enantiomer of 11,12-EET activated of BK channel and dilates small renal arteries whereas S,R-enantiomer was not active (Zou et al.,

1996a). Lu et al. (2002) reported that 11(S),12(R)-EET activated the cardiac K_{ATP} channels whereas 11(R),12(S)-EET was totally inactive. Moreover, effects of EPA epoxide enantiomers were also analyzed. 17(R),18(S)-EETeTr activated BK channel in cerebral artery vascular smooth muscle cells. 17(S),18(R)-EETeTr and the remaining four regioisomers were inactive (Lauterbach et al., 2002). 17(R),18(S)-EETeTr can also protect against Ca^{++} overload in cardiac myocytes whereas 17(S),18(R)-EETeTr did not show any effect (G. Wallukat, M. Markovic and W.-H. Schunck, unpublished data).

It can be concluded that the ratio of synthesized enantiomers can determine the biological effect of the metabolite. Therefore, stereoselectivity of CYP2C23 epoxidation of 17,18-double bond of EPA was characterized in the present study. As already described above (3.4.3), CYP2C23 is the major epoxygenase in the rat kidney and showed very high regioselectivity when converting EPA. 17,18-EETeTr represented nearly 60 % of total epoxidation product.

When epoxidizing 17,18 double bond of EPA, CYP2C23 showed high stereoselectivity and predominantly formed 17(R),18(S)-EETeTr (70 % of total 17,18-EETeTr). 17(R),18(S)-EETeTr represented clearly the preferential product of EPA epoxidation by CYP2C23 since it represented 42 % of total epoxy product. The Table 4.3 summarizes the data on stereoselectivities of different isoforms when epoxidizing 11,12-double bond of AA and 17,18-double bond of EPA. 17(R),18(S)-EETeTr is preferentially synthesized by all listed CYP isoforms except CYP2C8. There were no differences in specificity towards R,S-enantiomer between CYP2Cs and CYP4As. Interestingly, human CYP1A1 (Schwarz et al., 2004) and bacterial BM3 (Capdevila et al., 1996), respectively, produced either the R,S or the S,R-enantiomer with nearly absolute optical purity.

Table 4.3 Stereoselectivities of different CYP isoforms in epoxidizing the 17,18 double bond of EPA and the 11,12 double bond of AA. For the details see Results chapter 3.4.3.2d.

	17,18- EETeTr R,S: S,R	11,12- EET R,S: S,R	Reference
CYP1A1	97: 3	-	Schwarz et al., 2004
CYP2C8	28 72	82: 18	Markovic et al., 2005
CYP2C9	68: 32	31: 69	Markovic et al., 2005
CYP2C11	75: 25	79: 21	Markovic et al., 2005
CYP2C23	69: 31	89: 11	This work
CYP2J2	70: 30	49: 51	Schunck et al., unpublished data
CYP4A1	64: 36	-	Lauterbach et al., 2002
Cyp4a12a	72: 28	-	Muller et al., 2006
BM3	2 : 98	-	

4.3.4 Potential biological significance of CYP-dependent ω -3 metabolites

Increased consumption of fish and fish oil or other sources of ω -3 fatty acids can partially replace AA by EPA and DHA in cellular membranes. Several animal studies show that a period of 2-5 weeks of treatment with ω -3 fatty acids, as a dietary supplement, is sufficient for detecting the beneficial effects of ω -3 fatty acids (Theuer et al., 2005; Yu et al., 2006; Sharif et al., 2006). For example, after a period of 3 weeks of dietary supplementation with Omacor, ethylester of EPA and DHA, membrane composition in the heart was significantly changed (Figure 4.14). The cardiac EPA level was increased 27-fold, and that of DHA level was augmented 3-fold. At the same time, the level of AA was diminished to 50 % of control value (unpublished data of a study performed in the laboratory of D. Müller and W-H. Schnuck).

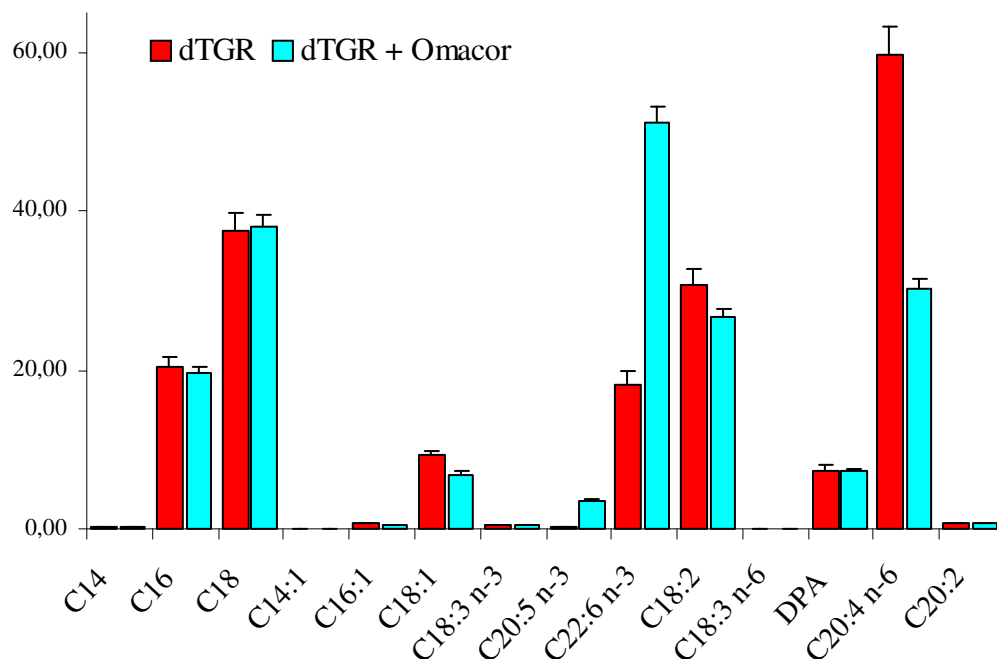


Figure 4.14. Analysis of cardiac fatty acid patterns in untreated and Omacor treated dTGR.

Thus, increased fish oil fatty acid intake increases the level of ω -3 fatty acids in the cell membrane. After releasing by phospholipases, EPA and DHA can compete with AA for binding and conversion with COX and LOX and also with CYP enzymes. Depending on the substrate and reaction specificities of the enzyme involved, this composition may lead to reduced production of AA-derived eicosanoids and will additionally allow formation of alternative EPA- and DHA-derived mediators.

It has been already described that EPA can be converted by COX and LOX enzymes to the 3-series of prostaglandins and tromboxanes and to 5-series of leukotriens which show much less inflammatory effects compared to their AA-derived homologues (Simopoulos, 2002). Moreover, Serhan and Chiang (2002) discovered a new series of EPA- and DHA-derived mediators called resolvins and neuroprotectins, which have very potent anti-inflammatory properties. Resolvins are formed in a two-step reaction, which requires aspirin acetylated COX-2 and LOX enzymes.

As already described in Introduction (1.2.2.1), fish oil fatty acids have beneficial effects on the cardiovascular system. EPA and DHA are described as antihypertensive, antiarrhythmic, anticoagulative, antihypertrophic and

antiinflammatory. Our recent studies with dTGR model revealed moreover remarkable effect on mortality (Theuer et al., 2005). We learned from subsequent studies in collaboration with R. Fisher and A. Schirdewan (Franz Volhard Clinic, Berlin-Buch) that this effect relies mainly on reduction of sudden cardiac death due to antiarrhythmic properties of ω -3 fatty acids.

Although CYP-dependent metabolism of ω -3 fatty acids and effects of their CYP-dependent metabolites are not studied in detail, several reports indicate a potential important biological function of CYP-dependent EPA and DHA derivatives. In particular, they may contribute to the beneficial properties of EPA and DHA, such as

- anticoagulation
- vasodilatation
- antiarrhythmia.

For example, it is known that EPA decreases platelet aggregation (Hashimoto et al., 1984). It is also reported that all the DHA and EPA epoxides have **anticoagulation** properties (VanRollins et al., 1995). Therefore, it can be speculated that CYP-dependent metabolites might be the active forms of EPA and DHA in moderating coagulation process.

Vasodilatatory effect of fish oil fatty acids can be also partially assigned to CYP-dependent metabolites. EETeTrs and EDTs are described to be more effective than EETs in dilating porcine and canine coronary microvessels (Zhang et al., 2001). EET-induced dilation occurs via opening of BK channels of vascular smooth muscle cells. K^+ efflux hyperpolarizes the membrane potential, relaxes smooth muscle cells and dilates vasculature (Hu and Kim, 1993). In contrast, 20-HETE is described as vasoconstrictor and acts in part by inhibiting the opening of BK channel in renal arteriolar VSM (Zou et al., 1996b). Several studies describe that EPA and DHA epoxides also act via activation of BK channels. For example, DHA epoxides potently dilate porcine coronary microvessels by activation of BK channels and they are more effective than EETs. The DHA epoxide, which most potently dilated porcine coronary artery, was 13,14-EDP. This metabolite is also known to activate BK channels in rat coronary smooth muscle cells (Ye et al., 2002). Furthermore, 17,18-EETeTr was also reported to activate BK channels of rat cerebral artery

VSMC. 17(R),18(S)-EETeTr showed more than 2-fold higher effect in comparison to 11(R),12(S)-EET.

K_{ATP} channels are abundant in heart, where they function as biological sensors, regulating membrane potentials and electrical excitability in response to metabolic alterations. It has been found that activation of K_{ATP} channels exerts an **antiarrhythmic** effects. EETs potently activate cardiac K_{ATP} channels by reducing channel sensitivity to ATP (Lu et al., 2001). Moreover, EPA epoxides are also described as very potent activator of cardiac K_{ATP} channels. 11,12-EETeTr reduces channel sensitivity to ATP almost 3-fold more efficient than 11,12-EET, the most potent AA epoxide (Lu et al., 2002).

17,18-EETeTr showed a negative chronotropic effect and prevented the massive increase in the beating rate induced by high concentration of Ca^{2+} in neonatal rat cardiac myocytes. 17,18-EETeTr can act effectively only in presence of active COX enzymes and K_{ATP} channel. (G. Wallukat, M. Markovic and W.-H. Schunck, unpublished data). 17,18-EETeTr belongs together with 20-HETE and 5,6-EET to the few CYP-dependent eicosanoids, which can be further converted by COX enzymes to prostaglandin-analogs (Oliw et al., 1992). Considering these facts, we proposed that a prostaglandin analog of 17,18-EETeTr is the active metabolite and that acts via K_{ATP} channel.

Taken together, diets rich in ω -3 PUFAs do not only modulate the fatty acid pattern but at the same time may lead to a significant shift of physiologically active metabolites produced by CYP enzymes in various tissues and organs. This alteration in CYP-dependent eicosanoid formation may play an important role in mediating the beneficial cardiovascular effects of ω -3 PUFAs.

4.4 Perspectives

The results of the present study provide further substantial evidence for an important role of CYP-dependent eicosanoids in the control and maintenance of various signaling pathways regulating blood pressure, renal, cardiac and vascular function. Taken together with the results of other authors, we propose that CYP-dependent eicosanoid metabolism may become in future a novel target for the treatment of

cardiovascular disease, in particular, of hypertension and associated end-organ damage. The present study demonstrated that both PPAR α activation and ω -3 PUFA supplementation are suitable ways to treat such disease conditions and that alterations in CYP-dependent eicosanoid production contribute to the success of these treatments. Recent efforts in several laboratories are aimed at the translation of the results of animal studies to human cardiovascular disease. This may be a long way since several important mechanisms are still largely unknown of how (1) CYP-dependent eicosanoid production itself is regulated, and (2) the metabolites exert their effects, i.e. via G-protein coupled receptors or other primary targets. However, the development of specific inhibitors of CYP enzymes and of soluble epoxide hydrolase is already in progress. These compounds do not only offer new tool for basic research but may be considered at the same time as first prototypes of drugs to be developed in the future. From the perspective of the present study, the development of sEH inhibitors and of drugs mimicking the action of EETs, HEETs and of 17,18-EETeTr appears particularly promising.

5. Bibliography

- Aguiar, M., R. Masse, and B. F. Gibbs. 2005. Regulation of cytochrome P450 by posttranslational modification. *Drug Metab Rev* 37:379-404.
- Aithal, G. P., C. P. Day, P. J. Kesteven, and A. K. Daly. 1999. Association of polymorphisms in the cytochrome P450 CYP2C9 with warfarin dose requirement and risk of bleeding complications. *Lancet* 353:717-719.
- Aldridge, T. C., J. D. Tugwood, and S. Green. 1995. Identification and characterization of DNA elements implicated in the regulation of CYP4A1 transcription. *Biochem J* 306 (Pt 2):473-479.
- Bang, H. O., J. Dyerberg, and H. M. Sinclair. 1980. The composition of the Eskimo food in north western Greenland. *Am J Clin Nutr* 33:2657-2661.
- Bellamine, A., Y. Wang, M. R. Waterman, J. V. Gainer, 3rd, E. P. Dawson, N. J. Brown, and J. H. Capdevila. 2003. Characterization of the CYP4A11 gene, a second CYP4A gene in humans. *Arch Biochem Biophys* 409:221-227.
- Bornheim, L. M., J. M. Lasker, and J. L. Raucy. 1992. Human hepatic microsomal metabolism of delta 1-tetrahydrocannabinol. *Drug Metab Dispos* 20:241-246.
- Burr, M. L., A. M. Fehily, S. Rogers, E. Welsby, S. King, and S. Sandham. 1989. Diet and reinfarction trial (DART): design, recruitment, and compliance. *Eur Heart J* 10:558-567.
- Calder, P. C. 2004. n-3 fatty acids, inflammation, and immunity--relevance to postsurgical and critically ill patients. *Lipids* 39:1147-1161.
- Campbell, W. B., D. Gebremedhin, P. F. Pratt, and D. R. Harder. 1996. Identification of epoxyeicosatrienoic acids as endothelium-derived hyperpolarizing factors. *Circ Res* 78:415-423.
- Campbell, W. B., and J. R. Falck. 2007. Arachidonic acid metabolites as endothelium-derived hyperpolarizing factors. *Hypertension* 49:590-596.

-
- Capdevila, J., L. Parkhill, N. Chacos, R. Okita, B. S. Masters, and R. W. Estabrook. 1981. The oxidative metabolism of arachidonic acid by purified cytochromes P-450. *Biochem Biophys Res Commun* 101:1357-1363.
- Capdevila, J., N. Chacos, J. R. Falck, S. Manna, A. Negro-Vilar, and S. R. Ojeda. 1983. Novel hypothalamic arachidonate products stimulate somatostatin release from the median eminence. *Endocrinology* 113:421-423.
- Capdevila, J. H., S. Wei, J. Yan, A. Karara, H. R. Jacobson, J. R. Falck, F. P. Guengerich, and R. N. DuBois. 1992. Cytochrome P-450 arachidonic acid epoxygenase. Regulatory control of the renal epoxygenase by dietary salt loading. *J Biol Chem* 267:21720-21726.
- Capdevila, J. H., S. Wei, C. Helvig, J. R. Falck, Y. Belosludtsev, G. Truan, S. E. Graham-Lorence, and J. A. Peterson. 1996. The highly stereoselective oxidation of polyunsaturated fatty acids by cytochrome P450BM-3. *J Biol Chem* 271:22663-22671.
- Capdevila, J. H., J. R. Falck, and R. C. Harris. 2000. Cytochrome P450 and arachidonic acid bioactivation. Molecular and functional properties of the arachidonate monooxygenase. *J Lipid Res* 41:163-181.
- Capdevila, J.H., V.R. Holla, J. R. Falck. 1995. "Cytochrome P450 and the metabolisms and bioactivation of of arachidonic acid and eicosanoids" in *Cytochrome P450: Structure, mechanism, and biochemistry*. Plenum Press New York, sec. ed.: 443-471.
- Carcillo, J. A., K. R. Korzekwa, G. S. Jones, R. A. Parise, D. G. Gillespie, M. J. Whalen, P. M. Kochanek, R. A. Branch, and C. K. Kost, Jr. 1998. The cytochrome P450 suicide inhibitor, 1-aminobenzotriazole, sensitizes rats to zymosan-induced toxicity. *Res Commun Mol Pathol Pharmacol* 102:57-68.
- Caron, M. G., S. Goldstein, K. Savard, and J. M. Marsh. 1975. Protein kinase stimulation of a reconstituted cholesterol side chain cleavage enzyme system in the bovine corpus luteum. *J Biol Chem* 250:5137-5143.
- Carroll, M. A., M. Balazy, P. Margiotta, D. D. Huang, J. R. Falck, and J. C. McGiff. 1996. Cytochrome P-450-dependent HETEs: profile of biological activity and stimulation by vasoactive peptides. *Am J Physiol* 271:R863-869.

-
- Carroll, M. A., and J. C. McGiff. 2000. A new class of lipid mediators: cytochrome P450 arachidonate metabolites. *Thorax* 55 Suppl 2:S13-16.
- Cinti, D. L., and M. B. Feinstein. 1976. Platelet cytochrome P450: a possible role in arachidonate-induced aggregation. *Biochem Biophys Res Commun* 73:171-179.
- Correia, M. A., S. Sadeghi, and E. Mundo-Paredes. 2005. Cytochrome P450 ubiquitination: branding for the proteolytic slaughter? *Annu Rev Pharmacol Toxicol* 45:439-464.
- Cowart, L. A., S. Wei, M. H. Hsu, E. F. Johnson, M. U. Krishna, J. R. Falck, and J. H. Capdevila. 2002. The CYP4A isoforms hydroxylate epoxyeicosatrienoic acids to form high affinity peroxisome proliferator-activated receptor ligands. *J Biol Chem* 277:35105-35112.
- Croft, K. D., J. C. McGiff, A. Sanchez-Mendoza, and M. A. Carroll. 2000. Angiotensin II releases 20-HETE from rat renal microvessels. *Am J Physiol Renal Physiol* 279:F544-551.
- Dai, D., D. C. Zeldin, J. A. Blaisdell, B. Chanas, S. J. Coulter, B. I. Ghanayem, and J. A. Goldstein. 2001. Polymorphisms in human CYP2C8 decrease metabolism of the anticancer drug paclitaxel and arachidonic acid. *Pharmacogenetics* 11:597-607.
- Daikh, B. E., J. M. Lasker, J. L. Raucy, and D. R. Koop. 1994. Regio- and stereoselective epoxidation of arachidonic acid by human cytochromes P450 2C8 and 2C9. *J Pharmacol Exp Ther* 271:1427-1433.
- De Caterina, R., and M. Massaro. 2005. Omega-3 fatty acids and the regulation of expression of endothelial pro-atherogenic and pro-inflammatory genes. *J Membr Biol* 206:103-116.
- Delerive, P., K. De Bosscher, S. Besnard, W. Vanden Berghe, J. M. Peters, F. J. Gonzalez, J. C. Fruchart, A. Tedgui, G. Haegeman, and B. Staels. 1999. Peroxisome proliferator-activated receptor alpha negatively regulates the vascular inflammatory gene response by negative cross-talk with transcription factors NF-kappaB and AP-1. *J Biol Chem* 274:32048-32054.

-
- Delerive, P., P. Gervois, J. C. Fruchart, and B. Staels. 2000. Induction of IkappaBalpha expression as a mechanism contributing to the anti-inflammatory activities of peroxisome proliferator-activated receptor-alpha activators. *J Biol Chem* 275:36703-36707.
- Dos Santos, E. A., A. J. Dahly-Vernon, K. M. Hoagland, and R. J. Roman. 2004. Inhibition of the formation of EETs and 20-HETE with 1-aminobenzotriazole attenuates pressure natriuresis. *Am J Physiol Regul Integr Comp Physiol* 287:R58-68.
- Eliasson, E., I. Johansson, and M. Ingelman-Sundberg. 1988. Ligand-dependent maintenance of ethanol-inducible cytochrome P-450 in primary rat hepatocyte cell cultures. *Biochem Biophys Res Commun* 150:436-443.
- Eliasson, E., I. Johansson, and M. Ingelman-Sundberg. 1990. Substrate-, hormone-, and cAMP-regulated cytochrome P450 degradation. *Proc Natl Acad Sci U S A* 87:3225-3229.
- Elmarakby, A. A., J. E. Quigley, D. M. Pollock, and J. D. Imig. 2006. Tumor necrosis factor alpha blockade increases renal Cyp2c23 expression and slows the progression of renal damage in salt-sensitive hypertension. *Hypertension* 47:557-562.
- Enayattallah, A. E., R. A. French, M. S. Thibodeau, and D. F. Grant. 2004. Distribution of soluble epoxide hydrolase and of cytochrome P450 2C8, 2C9, and 2J2 in human tissues. *J Histochem Cytochem* 52:447-454.
- Escalante, B., D. Erlij, J. R. Falck, and J. C. McGiff. 1991. Effect of cytochrome P450 arachidonate metabolites on ion transport in rabbit kidney loop of Henle. *Science* 251:799-802.
- Falck, J. R., P. Yadagiri, and J. Capdevila. 1990. Synthesis of epoxyeicosatrienoic acids and heteroatom analogs. *Methods Enzymol* 187:357-364.
- Flockhart, D. A. 1995. Drug interactions and the cytochrome P450 system. The role of cytochrome P450 2C19. *Clin Pharmacokinet* 29 Suppl 1:45-52.
- Forman, B. M., J. Chen, and R. M. Evans. 1997. Hypolipidemic drugs, polyunsaturated fatty acids, and eicosanoids are ligands for peroxisome

-
- proliferator-activated receptors alpha and delta. *Proc Natl Acad Sci U S A* 94:4312-4317.
- Fulton, D., J. C. McGiff, and J. Quilley. 1992. Contribution of NO and cytochrome P450 to the vasodilator effect of bradykinin in the rat kidney. *Br J Pharmacol* 107:722-725.
- Gebremedhin, D., A. R. Lange, J. Narayanan, M. R. Aebly, E. R. Jacobs, and D. R. Harder. 1998. Cat cerebral arterial smooth muscle cells express cytochrome P450 4A2 enzyme and produce the vasoconstrictor 20-HETE which enhances L-type Ca²⁺ current. *J Physiol* 507 (Pt 3):771-781.
- Gibson, G. G. 1989. Comparative aspects of the mammalian cytochrome P450 IV gene family. *Xenobiotica* 19:1123-1148.
- Goldstein, J. A. 2001. Clinical relevance of genetic polymorphisms in the human CYP2C subfamily. *Br J Clin Pharmacol* 52:349-355.
- Green, S. 1995. PPAR: a mediator of peroxisome proliferator action. *Mutat Res* 333:101-109.
- Guengerich, F.P. 1993. Cytochrome P450 Enzymes. *American Scientist*, 81:440-447.
- Hardwick, J. P., B. J. Song, E. Huberman, and F. J. Gonzalez. 1987. Isolation, complementary DNA sequence, and regulation of rat hepatic lauric acid omega-hydroxylase (cytochrome P-450LA omega). Identification of a new cytochrome P-450 gene family. *J Biol Chem* 262:801-810.
- Hashimoto, Y., C. Naito, M. Kawamura, and H. Oka. 1984. Effects of the ratio of exogenous eicosapentaenoic acid to arachidonic acid on platelet aggregation and serotonin release. *Thromb Res* 34:439-446.
- Hecker, M., A. T. Bara, J. Bauersachs, and R. Busse. 1994. Characterization of endothelium-derived hyperpolarizing factor as a cytochrome P450-derived arachidonic acid metabolite in mammals. *J Physiol* 481 (Pt 2):407-414.
- Henderson, C. J., T. Bammler, and C. R. Wolf. 1994. Deduced amino acid sequence of a murine cytochrome P-450 Cyp4a protein: developmental and hormonal regulation in liver and kidney. *Biochim Biophys Acta* 1200:182-190.

-
- Heng, Y. M., C. S. Kuo, P. S. Jones, R. Savory, R. M. Schulz, S. R. Tomlinson, T. J. Gray, and D. R. Bell. 1997. A novel murine P-450 gene, Cyp4a14, is part of a cluster of Cyp4a and Cyp4b, but not of CYP4F, genes in mouse and humans. *Biochem J* 325 (Pt 3):741-749.
- Hoagland, K. M., A. K. Flasch, and R. J. Roman. 2003. Inhibitors of 20-HETE formation promote salt-sensitive hypertension in rats. *Hypertension* 42:669-673.
- Holla, V. R., K. Makita, P. G. Zaphiropoulos, and J. H. Capdevila. 1999. The kidney cytochrome P-450 2C23 arachidonic acid epoxygenase is upregulated during dietary salt loading. *J Clin Invest* 104:751-760.
- Holla, V. R., F. Adas, J. D. Imig, X. Zhao, E. Price, Jr., N. Olsen, W. J. Kovacs, M. A. Magnuson, D. S. Keeney, M. D. Breyer, J. R. Falck, M. R. Waterman, and J. H. Capdevila. 2001. Alterations in the regulation of androgen-sensitive Cyp 4a monooxygenases cause hypertension. *Proc Natl Acad Sci U S A* 98:5211-5216.
- Honeck, H., V. Gross, B. Erdmann, E. Kargel, R. Neunaber, A. F. Milia, W. Schneider, F. C. Luft, and W. H. Schunck. 2000. Cytochrome P450-dependent renal arachidonic acid metabolism in desoxycorticosterone acetate-salt hypertensive mice. *Hypertension* 36:610-616.
- Hu, S., and H. S. Kim. 1993. Activation of K⁺ channel in vascular smooth muscles by cytochrome P450 metabolites of arachidonic acid. *Eur J Pharmacol* 230:215-221.
- Iber, H., M. B. Sewer, T. B. Barclay, S. R. Mitchell, T. Li, and E. T. Morgan. 1999. Modulation of drug metabolism in infectious and inflammatory diseases. *Drug Metab Rev* 31:29-41.
- Iber, H., Q. Chen, P. Y. Cheng, and E. T. Morgan. 2000. Suppression of CYP2C11 gene transcription by interleukin-1 mediated by NF-kappaB binding at the transcription start site. *Arch Biochem Biophys* 377:187-194.
- Imaoka, S., P. J. Wedlund, H. Ogawa, S. Kimura, F. J. Gonzalez, and H. Y. Kim. 1993. Identification of CYP2C23 expressed in rat kidney as an arachidonic acid epoxygenase. *J Pharmacol Exp Ther* 267:1012-1016.

-
- Imaoka, S., T. Hashizume, and Y. Funae. 2005. Localization of rat cytochrome P450 in various tissues and comparison of arachidonic acid metabolism by rat P450 with that by human P450 orthologs. *Drug Metab Pharmacokinet* 20:478-484.
- Imig, J. D. 2000. Epoxygenase metabolites. Epithelial and vascular actions. *Mol Biotechnol* 16:233-251.
- Imig, J. D., X. Zhao, J. R. Falck, S. Wei, and J. H. Capdevila. 2001. Enhanced renal microvascular reactivity to angiotensin II in hypertension is ameliorated by the sulfonimide analog of 11,12-epoxyeicosatrienoic acid. *J Hypertens* 19:983-992.
- Imig, J. D., X. Zhao, J. H. Capdevila, C. Morisseau, and B. D. Hammock. 2002. Soluble epoxide hydrolase inhibition lowers arterial blood pressure in angiotensin II hypertension. *Hypertension* 39:690-694.
- Johnson, E. F., C. N. Palmer, K. J. Griffin, and M. H. Hsu. 1996. Role of the peroxisome proliferator-activated receptor in cytochrome P450 4A gene regulation. *Faseb J* 10:1241-1248.
- Kadis, B. 1978. Steroid epoxides in biologic systems: a review. *J Steroid Biochem* 9:75-81.
- Kaergel, E., D. N. Muller, H. Honeck, J. Theuer, E. Shagdarsuren, A. Mullally, F. C. Luft, and W. H. Schunck. 2002. P450-dependent arachidonic acid metabolism and angiotensin II-induced renal damage. *Hypertension* 40:273-279.
- Kaminsky, L. S., S. M. de Moraes, M. B. Faletto, D. A. Dunbar, and J. A. Goldstein. 1993. Correlation of human cytochrome P4502C substrate specificities with primary structure: warfarin as a probe. *Mol Pharmacol* 43:234-239.
- Kang, J. X., and A. Leaf. 1994. Effects of long-chain polyunsaturated fatty acids on the contraction of neonatal rat cardiac myocytes. *Proc Natl Acad Sci U S A* 91:9886-9890.
- Karara, A., K. Makita, H. R. Jacobson, J. R. Falck, F. P. Guengerich, R. N. DuBois, and J. H. Capdevila. 1993. Molecular cloning, expression, and enzymatic

-
- characterization of the rat kidney cytochrome P-450 arachidonic acid epoxygenase. *J Biol Chem* 268:13565-13570.
- Kessler, P., R. Popp, R. Busse, and V. B. Schini-Kerth. 1999. Proinflammatory mediators chronically downregulate the formation of the endothelium-derived hyperpolarizing factor in arteries via a nitric oxide/cyclic GMP-dependent mechanism. *Circulation* 99:1878-1884.
- Kirchheiner, J., J. Brockmoller, I. Meineke, S. Bauer, W. Rohde, C. Meisel, and I. Roots. 2002. Impact of CYP2C9 amino acid polymorphisms on glyburide kinetics and on the insulin and glucose response in healthy volunteers. *Clin Pharmacol Ther* 71:286-296.
- Kirchheiner, J., and J. Brockmoller. 2005. Clinical consequences of cytochrome P450 2C9 polymorphisms. *Clin Pharmacol Ther* 77:1-16.
- Klose, T. S., J. A. Blaisdell, and J. A. Goldstein. 1999. Gene structure of CYP2C8 and extrahepatic distribution of the human CYP2Cs. *J Biochem Mol Toxicol* 13:289-295.
- Knapp, H. R., A. J. Miller, and J. A. Lawson. 1991. Urinary excretion of diols derived from eicosapentaenoic acid during n-3 fatty acid ingestion by man. *Prostaglandins* 42:47-54.
- Korsmeyer, K. K., S. Davoll, M. E. Figueiredo-Pereira, and M. A. Correia. 1999. Proteolytic degradation of heme-modified hepatic cytochromes P450: A role for phosphorylation, ubiquitination, and the 26S proteasome? *Arch Biochem Biophys* 365:31-44.
- Kris-Etherton, P. M., W. S. Harris, and L. J. Appel. 2002. Fish consumption, fish oil, omega-3 fatty acids, and cardiovascular disease. *Circulation* 106:2747-2757.
- Lange, A., D. Gebremedhin, J. Narayanan, and D. Harder. 1997. 20-Hydroxyeicosatetraenoic acid-induced vasoconstriction and inhibition of potassium current in cerebral vascular smooth muscle is dependent on activation of protein kinase C. *J Biol Chem* 272:27345-27352.
- Lasker, J. M., W. B. Chen, I. Wolf, B. P. Bloswick, P. D. Wilson, and P. K. Powell.

-
2000. Formation of 20-hydroxyeicosatetraenoic acid, a vasoactive and natriuretic eicosanoid, in human kidney. Role of Cyp4F2 and Cyp4A11. *J Biol Chem* 275:4118-4126.
- Lauterbach, B., E. Barbosa-Sicard, M. H. Wang, H. Honeck, E. Kargel, J. Theuer, M. L. Schwartzman, H. Haller, F. C. Luft, M. Gollasch, and W. H. Schunck. 2002. Cytochrome P450-dependent eicosapentaenoic acid metabolites are novel BK channel activators. *Hypertension* 39:609-613.
- Leaf, A. 2002. On the reanalysis of the GISSI-Prevenzione. *Circulation* 105:1874-1875.
- Leo, M. A., J. M. Lasker, J. L. Raucy, C. I. Kim, M. Black, and C. S. Lieber. 1989. Metabolism of retinol and retinoic acid by human liver cytochrome P450IIC8. *Arch Biochem Biophys* 269:305-312.
- Lewis, D. F. V., Kap. 3, The P450 catalytic cycle and oxygenation mechanism. *Cytochromes P450: Structure, Function and Mechanism*, (Rubinstein, M.H., Wilson, C.G., eds.).
- Lischke, V., R. Busse, and M. Hecker. 1995. Selective inhibition by barbiturates of the synthesis of endothelium-derived hyperpolarizing factor in the rabbit carotid artery. *Br J Pharmacol* 115:969-974.
- Lu, M., X. Wang, and W. Wang. 1998. Nitric oxide increases the activity of the apical 70-pS K⁺ channel in TAL of rat kidney. *Am J Physiol* 274:F946-950.
- Lu, T., M. VanRollins, and H. C. Lee. 2002. Stereospecific activation of cardiac ATP-sensitive K(+) channels by epoxyeicosatrienoic acids: a structural determinant study. *Mol Pharmacol* 62:1076-1083.
- Luft, F. C., E. Mervaala, D. N. Muller, V. Gross, F. Schmidt, J. K. Park, C. Schmitz, A. Lippoldt, V. Breu, R. Dechend, D. Dragun, W. Schneider, D. Ganten, and H. Haller. 1999. Hypertension-induced end-organ damage : A new transgenic approach to an old problem. *Hypertension* 33:212-218.
- Ma, Y. H., M. L. Schwartzman, and R. J. Roman. 1994. Altered renal P-450 metabolism of arachidonic acid in Dahl salt-sensitive rats. *Am J Physiol* 267:R579-589.

-
- Maier, K. G., and R. J. Roman. 2001. Cytochrome P450 metabolites of arachidonic acid in the control of renal function. *Curr Opin Nephrol Hypertens* 10:81-87.
- Makita, K., K. Takahashi, A. Karara, H. R. Jacobson, J. R. Falck, and J. H. Capdevila. 1994. Experimental and/or genetically controlled alterations of the renal microsomal cytochrome P450 epoxygenase induce hypertension in rats fed a high salt diet. *J Clin Invest* 94:2414-2420.
- McGiff, J. C., and J. Quilley. 1999. 20-HETE and the kidney: resolution of old problems and new beginnings. *Am J Physiol* 277:R607-623.
- McGiff, J. C., and J. Quilley. 2001. 20-hydroxyeicosatetraenoic acid and epoxyeicosatrienoic acids and blood pressure. *Curr Opin Nephrol Hypertens* 10:231-237.
- Mitani, F. 1979. Cytochrome P450 in adrenocortical mitochondria. *Mol Cell Biochem* 24:21-43.
- Morris, M. C., F. Sacks, and B. Rosner. 1993. Does fish oil lower blood pressure? A meta-analysis of controlled trials. *Circulation* 88:523-533.
- Muerhoff, A. S., K. J. Griffin, and E. F. Johnson. 1992. The peroxisome proliferator-activated receptor mediates the induction of CYP4A6, a cytochrome P450 fatty acid omega-hydroxylase, by clofibric acid. *J Biol Chem* 267:19051-19053.
- Muller, D. N., R. Dechend, E. M. Mervaala, J. K. Park, F. Schmidt, A. Fiebeler, J. Theuer, V. Breu, D. Ganten, H. Haller, and F. C. Luft. 2000. NF-kappaB inhibition ameliorates angiotensin II-induced inflammatory damage in rats. *Hypertension* 35:193-201.
- Muller, D. N., V. Heissmeyer, R. Dechend, F. Hampich, J. K. Park, A. Fiebeler, E. Shagdarsuren, J. Theuer, M. Elger, B. Pilz, V. Breu, K. Schroer, D. Ganten, R. Dietz, H. Haller, C. Scheidereit, and F. C. Luft. 2001. Aspirin inhibits NF-kappaB and protects from angiotensin II-induced organ damage. *Faseb J* 15:1822-1824.
- Muller, D. N., E. Shagdarsuren, J. K. Park, R. Dechend, E. Mervaala, F. Hampich, A. Fiebeler, X. Ju, P. Finckenberg, J. Theuer, C. Viedt, J. Kreuzer, H.

-
- Heidecke, H. Haller, M. Zenke, and F. C. Luft. 2002. Immunosuppressive treatment protects against angiotensin II-induced renal damage. *Am J Pathol* 161:1679-1693.
- Muller, D. N., J. Theuer, E. Shagdarsuren, E. Kaergel, H. Honeck, J. K. Park, M. Markovic, E. Barbosa-Sicard, R. Dechend, M. Wellner, T. Kirsch, A. Fiebeler, M. Rothe, H. Haller, F. C. Luft, and W. H. Schunck. 2004. A peroxisome proliferator-activated receptor-alpha activator induces renal CYP2C23 activity and protects from angiotensin II-induced renal injury. *Am J Pathol* 164:521-532.
- Muller, D. N., C. Schmidt, E. Barbosa-Sicard, M. Wellner, V. Gross, H. Hercule, M. Markovic, H. Honeck, F. C. Luft, and W. H. Schunck. 2007. Mouse Cyp4a isoforms: enzymatic properties, gender- and strain-specific expression, and role in renal 20-hydroxyecosatetraenoic acid formation. *Biochem J* 403:109-118.
- Muthalif, M. M., I. F. Benter, N. Karzoun, S. Fatima, J. Harper, M. R. Uddin, and K. U. Malik. 1998. 20-Hydroxyecosatetraenoic acid mediates calcium/calmodulin-dependent protein kinase II-induced mitogen-activated protein kinase activation in vascular smooth muscle cells. *Proc Natl Acad Sci U S A* 95:12701-12706.
- Muthalif, M. M., I. F. Benter, Z. Khandekar, L. Gaber, A. Estes, S. Malik, J. H. Parmentier, V. Manne, and K. U. Malik. 2000. Contribution of Ras GTPase/MAP kinase and cytochrome P450 metabolites to deoxycorticosterone-salt-induced hypertension. *Hypertension* 35:457-463.
- Nelson, D., 2003. Cytochrome P450s in humans. <http://drnelson.utmem.edu/P450lect.html>
- Nelson, D. R., L. Koymans, T. Kamataki, J. J. Stegeman, R. Feyereisen, D. J. Waxman, M. R. Waterman, O. Gotoh, M. J. Coon, R. W. Estabrook, I. C. Gunsalus, and D. W. Nebert. 1996. P450 superfamily: update on new sequences, gene mapping, accession numbers and nomenclature. *Pharmacogenetics* 6:1-42.
- Nelson, D. R., D. C. Zeldin, S. M. Hoffman, L. J. Maltais, H. M. Wain, and D. W.

-
- Nebert. 2004. Comparison of cytochrome P450 (CYP) genes from the mouse and human genomes, including nomenclature recommendations for genes, pseudogenes and alternative-splice variants. *Pharmacogenetics* 14:1-18.
- Nguyen, X., M. H. Wang, K. M. Reddy, J. R. Falck, and M. L. Schwartzman. 1999. Kinetic profile of the rat CYP4A isoforms: arachidonic acid metabolism and isoform-specific inhibitors. *Am J Physiol* 276:R1691-1700.
- Nishimura, M., H. Yaguti, H. Yoshitsugu, S. Naito, and T. Satoh. 2003. Tissue distribution of mRNA expression of human cytochrome P450 isoforms assessed by high-sensitivity real-time reverse transcription PCR. *Yakugaku Zasshi* 123:369-375.
- Node, K., Y. Huo, X. Ruan, B. Yang, M. Spiecker, K. Ley, D. C. Zeldin, and J. K. Liao. 1999. Anti-inflammatory properties of cytochrome P450 epoxygenase-derived eicosanoids. *Science* 285:1276-1279.
- Oesch-Bartlomowicz, B., B. Richter, R. Becker, S. Vogel, P. R. Padma, J. G. Hengstler, and F. Oesch. 2001. cAMP-dependent phosphorylation of CYP2B1 as a functional switch for cyclophosphamide activation and its hormonal control in vitro and in vivo. *Int J Cancer* 94:733-742.
- Ohhira, S., M. Enomoto, and H. Matsui. 2006. In vitro metabolism of tributyltin and triphenyltin by human cytochrome P-450 isoforms. *Toxicology* 228:171-177.
- Okita, R. T., and J. R. Okita. 2001. Cytochrome P450 4A fatty acid omega hydroxylases. *Curr Drug Metab* 2:265-281.
- Oliw, E. H., and H. W. Sprecher. 1991. Metabolism of polyunsaturated (n-3) fatty acids by monkey seminal vesicles: isolation and biosynthesis of omega-3 epoxides. *Biochim Biophys Acta* 1086:287-294.
- Oliw, E. H., S. Okamoto, L. Hornsten, and F. Sato. 1992. Biosynthesis of prostaglandins from 17(18)epoxy-eicosatetraenoic acid, a cytochrome P-450 metabolite of eicosapentaenoic acid. *Biochim Biophys Acta* 1126:261-268.
- Omura, T., and R. Sato. 1964. The Carbon Monoxide-Binding Pigment of Liver

-
- Microsomes. I. Evidence for Its Hemoprotein Nature. *J Biol Chem* 239:2370-2378.
- Oyekan, A., M. Balazy, and J. C. McGiff. 1997. Renal oxygenases: differential contribution to vasoconstriction induced by ET-1 and ANG II. *Am J Physiol* 273:R293-300.
- Oyekan, A. O., K. McAward, J. Conetta, L. Rosenfeld, and J. C. McGiff. 1999. Endothelin-1 and CYP450 arachidonate metabolites interact to promote tissue injury in DOCA-salt hypertension. *Am J Physiol* 276:R766-775.
- Oyekan, A. O., T. Youseff, D. Fulton, J. Quilley, and J. C. McGiff. 1999. Renal cytochrome P450 omega-hydroxylase and epoxygenase activity are differentially modified by nitric oxide and sodium chloride. *J Clin Invest* 104:1131-1137.
- Popp, R., J. Bauersachs, M. Hecker, I. Fleming, and R. Busse. 1996. A transferable, beta-naphthoflavone-inducible, hyperpolarizing factor is synthesized by native and cultured porcine coronary endothelial cells. *J Physiol* 497 (Pt 3):699-709.
- Powell, P. K., I. Wolf, R. Jin, and J. M. Lasker. 1998. Metabolism of arachidonic acid to 20-hydroxy-5,8,11, 14-eicosatetraenoic acid by P450 enzymes in human liver: involvement of CYP4F2 and CYP4A11. *J Pharmacol Exp Ther* 285:1327-1336.
- Quilley, J., D. Fulton, and J. C. McGiff. 1997. Hyperpolarizing factors. *Biochem Pharmacol* 54:1059-1070.
- Randriamboavonjy, V., R. Busse, and I. Fleming. 2003. 20-HETE-induced contraction of small coronary arteries depends on the activation of Rho-kinase. *Hypertension* 41:801-806.
- Rettie, A. E., L. C. Wienkers, F. J. Gonzalez, W. F. Trager, and K. R. Korzekwa. 1994. Impaired (S)-warfarin metabolism catalysed by the R144C allelic variant of CYP2C9. *Pharmacogenetics* 4:39-42.
- Rich, K. J., and A. R. Boobis. 1997. Expression and inducibility of P450 enzymes during liver ontogeny. *Microsc Res Tech* 39:424-435.

-
- Rifkind, A. B., C. Lee, T. K. Chang, and D. J. Waxman. 1995. Arachidonic acid metabolism by human cytochrome P450s 2C8, 2C9, 2E1, and 1A2: regioselective oxygenation and evidence for a role for CYP2C enzymes in arachidonic acid epoxygenation in human liver microsomes. *Arch Biochem Biophys* 320:380-389.
- Roberts, B. J., B. J. Song, Y. Soh, S. S. Park, and S. E. Shoaf. 1995. Ethanol induces CYP2E1 by protein stabilization. Role of ubiquitin conjugation in the rapid degradation of CYP2E1. *J Biol Chem* 270:29632-29635.
- Roman, R. J. 2002. P-450 metabolites of arachidonic acid in the control of cardiovascular function. *Physiol Rev* 82:131-185.
- Romero, M. F., U. Hopfer, Z. T. Madhun, W. Zhou, and J. G. Douglas. 1991. Angiotensin II actions in the rabbit proximal tubule. Angiotensin II mediated signaling mechanisms and electrolyte transport in the rabbit proximal tubule. *Ren Physiol Biochem* 14:199-207.
- Roussel, F., S. Marie, and T. Cresteil. 1995. Gene structure and promoter analysis of the rat constitutive CYP2C23 gene. *DNA Cell Biol* 14:777-788.
- Rushmore, T. H., and A. N. Kong. 2002. Pharmacogenomics, regulation and signaling pathways of phase I and II drug metabolizing enzymes. *Curr Drug Metab* 3:481-490.
- Sato, R., and T. Omura, 1978 *Cytochrome P-450*, pp. 137- 208, Academic Press, New York
- Salen, P., and M. de Lorgeril. 1999. GISSI-Prevenzione trial. *Lancet* 354:1555; author reply 1556-1557.
- Sankaralingam, S., K. M. Desai, H. Glaeser, R. B. Kim, and T. W. Wilson. 2006. Inability to upregulate cytochrome P450 4A and 2C causes salt sensitivity in young Sprague-Dawley rats. *Am J Hypertens* 19:1174-1180.
- Schwartzman, M., N. R. Ferreri, M. A. Carroll, E. Songu-Mize, and J. C. McGiff. 1985. Renal cytochrome P450-related arachidonate metabolite inhibits (Na⁺ + K⁺)ATPase. *Nature* 314:620-622.

-
- Schwarz, U. I. 2003. Clinical relevance of genetic polymorphisms in the human CYP2C9 gene. *Eur J Clin Invest* 33 Suppl 2:23-30.
- Schwarz, D., P. Kisselev, A. Chernogolov, W. H. Schunck, and I. Roots. 2005. Human CYP1A1 variants lead to differential eicosapentaenoic acid metabolite patterns. *Biochem Biophys Res Commun* 336:779-783.
- Seki, T., T. Ishimoto, T. Sakurai, Y. Yasuda, K. Taniguchi, M. Doi, M. Sato, R. J. Roman, and N. Miyata. 2005. Increased excretion of urinary 20-HETE in rats with cyclosporine-induced nephrotoxicity. *J Pharmacol Sci* 97:132-137.
- Serhan, C. N., S. Hong, K. Gronert, S. P. Colgan, P. R. Devchand, G. Mirick, and R. L. Moussignac. 2002. Resolvins: a family of bioactive products of omega-3 fatty acid transformation circuits initiated by aspirin treatment that counter proinflammation signals. *J Exp Med* 196:1025-1037.
- Sharif, S., M. Broman, T. Babcock, E. Ong, D. Jho, M. Rudnicki, W. S. Helton, and N. J. Espat. 2006. A priori dietary omega-3 lipid supplementation results in local pancreatic macrophage and pulmonary inflammatory response attenuation in a model of experimental acute edematous pancreatitis (AEP). *JPEN J Parenter Enteral Nutr* 30:271-276.
- Shataru, R. K., D. W. Quest, and T. W. Wilson. 2000. Fenofibrate lowers blood pressure in two genetic models of hypertension. *Can J Physiol Pharmacol* 78:367-371.
- Shimojo, N., S. Jesmin, S. Zaedi, M. Soma, S. Maeda, I. Yamaguchi, K. Goto, and T. Miyauchi. 2006. Changes in important apoptosis-related molecules in the endothelin-1-induced hypertrophied cardiomyocytes: effect of the pretreatment with eicosapentaenoic Acid. *Exp Biol Med (Maywood)* 231:932-936.
- Siddiqui, R. A., S. R. Shaikh, R. Kovacs, W. Stillwell, and G. Zaloga. 2004. Inhibition of phenylephrine-induced cardiac hypertrophy by docosahexaenoic acid. *J Cell Biochem* 92:1141-1159.
- Simopoulos, A. P. 1999. Essential fatty acids in health and chronic disease. *Am J Clin Nutr* 70:560S-569S.

-
- Simopoulos, A. P. 2002. Omega-3 fatty acids in inflammation and autoimmune diseases. *J Am Coll Nutr* 21:495-505.
- Song, B. J., H. V. Gelboin, S. S. Park, C. S. Yang, and F. J. Gonzalez. 1986. Complementary DNA and protein sequences of ethanol-inducible rat and human cytochrome P-450s. Transcriptional and post-transcriptional regulation of the rat enzyme. *J Biol Chem* 261:16689-16697.
- Song, B. J., T. Matsunaga, J. P. Hardwick, S. S. Park, R. L. Veech, C. S. Yang, H. V. Gelboin, and F. J. Gonzalez. 1987. Stabilization of cytochrome P450j messenger ribonucleic acid in the diabetic rat. *Mol Endocrinol* 1:542-547.
- Sonoda, Y., C. Amano, M. Endo, Y. Sato, Y. Sekigawa, and M. Fukuhara. 1995. Lanosterol 14 alpha-demethylase (cytochrome P-45014DM): modulation of its enzyme activity by cholesterol feeding. *Biol Pharm Bull* 18:1009-1011.
- Spector, A. A., and A. W. Norris. 2007. Action of epoxyeicosatrienoic acids on cellular function. *Am J Physiol Cell Physiol* 292:C996-1012.
- Stark, K., B. Wongsud, R. Burman, and E. H. Oliw. 2005. Oxygenation of polyunsaturated long chain fatty acids by recombinant CYP4F8 and CYP4F12 and catalytic importance of Tyr-125 and Gly-328 of CYP4F8. *Arch Biochem Biophys* 441:174-181.
- Stec, D. E., A. Y. Deng, J. P. Rapp, and R. J. Roman. 1996. Cytochrome P4504A genotype cosegregates with hypertension in Dahl S rats. *Hypertension* 27:564-568.
- Stec, D. E., A. Flasch, R. J. Roman, and J. A. White. 2003. Distribution of cytochrome P-450 4A and 4F isoforms along the nephron in mice. *Am J Physiol Renal Physiol* 284:F95-102.
- Sundseth, S. S., and D. J. Waxman. 1992. Sex-dependent expression and clofibrate inducibility of cytochrome P450 4A fatty acid omega-hydroxylases. Male specificity of liver and kidney CYP4A2 mRNA and tissue-specific regulation by growth hormone and testosterone. *J Biol Chem* 267:3915-3921.
- Theuer, J., E. Shagdarsuren, D. N. Muller, E. Kaergel, H. Honeck, J. K. Park, A.

-
- Fiebeler, R. Dechend, H. Haller, F. C. Luft, and W. H. Schunck. 2005. Inducible NOS inhibition, eicosapentaenoic acid supplementation, and angiotensin II-induced renal damage. *Kidney Int* 67:248-258.
- Tsutsumi, M., J. M. Lasker, T. Takahashi, and C. S. Lieber. 1993. In vivo induction of hepatic P450E1 by ethanol: role of increased enzyme synthesis. *Arch Biochem Biophys* 304:209-218.
- Van Rollins, M., P. D. Frade, and O. A. Carretero. 1988. Oxidation of 5,8,11,14,17-eicosapentaenoic acid by hepatic and renal microsomes. *Biochim Biophys Acta* 966:133-149.
- VanRollins, M., R. C. Baker, H. W. Sprecher, and R. C. Murphy. 1984. Oxidation of docosahexaenoic acid by rat liver microsomes. *J Biol Chem* 259:5776-5783.
- VanRollins, M., P. D. Frade, and O. A. Carretero. 1989. Synthesis of epoxide and vicinal diol regioisomers from docosahexaenoate methyl esters. *J Lipid Res* 30:275-286.
- VanRollins, M. 1995. Epoxygenase metabolites of docosahexaenoic and eicosapentaenoic acids inhibit platelet aggregation at concentrations below those affecting thromboxane synthesis. *J Pharmacol Exp Ther* 274:798-804.
- Vera, T., M. Taylor, Q. Bohman, A. Flasch, R. J. Roman, and D. E. Stec. 2005. Fenofibrate prevents the development of angiotensin II-dependent hypertension in mice. *Hypertension* 45:730-735.
- Veronese, M. E., P. I. Mackenzie, C. J. Doecke, M. E. McManus, J. O. Miners, and D. J. Birkett. 1991. Tolbutamide and phenytoin hydroxylations by cDNA-expressed human liver cytochrome P450C9. *Biochem Biophys Res Commun* 175:1112-1118.
- Vilgrain, I., G. Defaye, and E. M. Chambaz. 1984. Adrenocortical cytochrome P-450 responsible for cholesterol side chain cleavage (P-450scc) is phosphorylated by the calcium-activated, phospholipid-sensitive protein kinase (protein kinase C). *Biochem Biophys Res Commun* 125:554-561.
- Wang, M. H., D. E. Stec, M. Balazy, V. Mastuygin, C. S. Yang, R. J. Roman, and

-
- M. L. Schwartzman. 1996. Cloning, sequencing, and cDNA-directed expression of the rat renal CYP4A2: arachidonic acid omega-hydroxylation and 11,12-epoxidation by CYP4A2 protein. *Arch Biochem Biophys* 336:240-250.
- Wang, H. F., M. E. Figueiredo Pereira, and M. A. Correia. 1999. Cytochrome P450 3A degradation in isolated rat hepatocytes: 26S proteasome inhibitors as probes. *Arch Biochem Biophys* 365:45-53.
- Wang, M. H., A. Smith, Y. Zhou, H. H. Chang, S. Lin, X. Zhao, J. D. Imig, and A. M. Dorrance. 2003. Downregulation of renal CYP-derived eicosanoid synthesis in rats with diet-induced hypertension. *Hypertension* 42:594-599.
- Wang, M. H., A. Smith, Y. Zhou, H. H. Chang, S. Lin, X. Zhao, J. D. Imig, and A. M. Dorrance. 2003. Downregulation of renal CYP-derived eicosanoid synthesis in rats with diet-induced hypertension. *Hypertension* 42:594-599.
- Weber, P., and D. Raederstorff. 2000. Triglyceride-lowering effect of omega-3 LC-polyunsaturated fatty acids--a review. *Nutr Metab Cardiovasc Dis* 10:28-37.
- Wei, Y., D. H. Lin, R. Kemp, G. S. Yaddanapudi, A. Nasjletti, J. R. Falck, and W. H. Wang. 2004. Arachidonic acid inhibits epithelial Na channel via cytochrome P450 (CYP) epoxygenase-dependent metabolic pathways. *J Gen Physiol* 124:719-727.
- Yaghi, A., J. R. Bend, C. D. Webb, D. C. Zeldin, S. Weicker, S. Mehta, and D. G. McCormack. 2004. Excess nitric oxide decreases cytochrome P-450 2J4 content and P-450-dependent arachidonic acid metabolism in lungs of rats with acute pneumonia. *Am J Physiol Lung Cell Mol Physiol* 286:L1260-1267.
- Yamaguchi, Y., S. Kirita, H. Hasegawa, J. Aoyama, S. Imaoka, S. Minamiyama, Y. Funae, T. Baba, and T. Matsubara. 2002. Contribution of CYP4A8 to the formation of 20-hydroxyeicosatetraenoic acid from arachidonic acid in rat kidney. *Drug Metab Pharmacokinet* 17:109-116.
- Ye, D., D. Zhang, C. Oltman, K. Dellsperger, H. C. Lee, and M. VanRollins. 2002. Cytochrome p-450 epoxygenase metabolites of docosahexaenoate potently

-
- dilate coronary arterioles by activating large-conductance calcium-activated potassium channels. *J Pharmacol Exp Ther* 303:768-776.
- Yu, Z., F. Xu, L. M. Huse, C. Morisseau, A. J. Draper, J. W. Newman, C. Parker, L. Graham, M. M. Engler, B. D. Hammock, D. C. Zeldin, and D. L. Kroetz. 2000. Soluble epoxide hydrolase regulates hydrolysis of vasoactive epoxyeicosatrienoic acids. *Circ Res* 87:992-998.
- Yu, Z., V. Y. Ng, P. Su, M. M. Engler, M. B. Engler, Y. Huang, E. Lin, and D. L. Kroetz. 2006. Induction of renal cytochrome P450 arachidonic acid epoxygenase activity by dietary gamma-linolenic acid. *J Pharmacol Exp Ther* 317:732-738.
- Yun, C. H., T. Shimada, and F. P. Guengerich. 1992. Roles of human liver cytochrome P450C and 3A enzymes in the 3-hydroxylation of benzo(a)pyrene. *Cancer Res* 52:1868-1874.
- Zeldin, D. C., R. N. DuBois, J. R. Falck, and J. H. Capdevila. 1995. Molecular cloning, expression and characterization of an endogenous human cytochrome P450 arachidonic acid epoxygenase isoform. *Arch Biochem Biophys* 322:76-86.
- Zhang, L. H., H. Rodriguez, S. Ohno, and W. L. Miller. 1995. Serine phosphorylation of human P450c17 increases 17,20-lyase activity: implications for adrenarcho and the polycystic ovary syndrome. *Proc Natl Acad Sci U S A* 92:10619-10623.
- Zhang, Y., C. L. Oltman, T. Lu, H. C. Lee, K. C. Dellsperger, and M. VanRollins. 2001. EET homologs potently dilate coronary microvessels and activate BK(Ca) channels. *Am J Physiol Heart Circ Physiol* 280:H2430-2440.
- Zhao, X., D. M. Pollock, E. W. Inscho, D. C. Zeldin, and J. D. Imig. 2003. Decreased renal cytochrome P450 2C enzymes and impaired vasodilation are associated with angiotensin salt-sensitive hypertension. *Hypertension* 41:709-714.
- Zhao, X., D. M. Pollock, D. C. Zeldin, and J. D. Imig. 2003. Salt-sensitive hypertension after exposure to angiotensin is associated with inability to

upregulate renal epoxygenases. *Hypertension* 42:775-780.

Zhao, X., T. Yamamoto, J. W. Newman, I. H. Kim, T. Watanabe, B. D. Hammock, J. Stewart, J. S. Pollock, D. M. Pollock, and J. D. Imig. 2004. Soluble epoxide hydrolase inhibition protects the kidney from hypertension-induced damage. *J Am Soc Nephrol* 15:1244-1253.

Zhao, X., J. E. Quigley, J. Yuan, M. H. Wang, Y. Zhou, and J. D. Imig. 2006. PPAR-alpha activator fenofibrate increases renal CYP-derived eicosanoid synthesis and improves endothelial dilator function in obese Zucker rats. *Am J Physiol Heart Circ Physiol* 290:H2187-2195.

Zhou, Y., H. H. Chang, J. Du, C. Y. Wang, Z. Dong, and M. H. Wang. 2005. Renal epoxyeicosatrienoic acid synthesis during pregnancy. *Am J Physiol Renal Physiol* 288:F221-226.

Zhou, Y., H. Huang, H. H. Chang, J. Du, J. F. Wu, C. Y. Wang, and M. H. Wang. 2006. Induction of renal 20-hydroxyeicosatetraenoic acid by clofibrate attenuates high-fat diet-induced hypertension in rats. *J Pharmacol Exp Ther* 317:11-18.

Zou, A. P., J. T. Fleming, J. R. Falck, E. R. Jacobs, D. Gebremedhin, D. R. Harder, and R. J. Roman. 1996. 20-HETE is an endogenous inhibitor of the large-conductance Ca(2+)-activated K⁺ channel in renal arterioles. *Am J Physiol* 270:R228-237.

Zou, A. P., J. T. Fleming, J. R. Falck, E. R. Jacobs, D. Gebremedhin, D. R. Harder, and R. J. Roman. 1996. Stereospecific effects of epoxyeicosatrienoic acids on renal vascular tone and K(+) -channel activity. *Am J Physiol* 270:F822-832.

6. List of publications, awards and conferences

Publications:

- Muller DN, Theuer J, Shagdarsuren E, Kaergel E, Honeck H, Park JK, **Markovic M**, Barbosa-Sicard E, Dechend R, Wellner M, Kirsch T, Fiebeler A, Rothe M, Haller H, Luft FC, Schunck WH: "A *peroxisome proliferator-activated receptor-alpha* activator induces renal CYP2C23 activity and protects from angiotensin II-induced renal injury" Am J Pathol. 2004 Feb; 164(2): 521-32.
- **Markovic M.**¹, Barbosa-Sicard E.¹, Honeck H., Christ B., Muller DN, Schunck WH: "Eicosapentaenoic acid metabolism by Cytochrome P450 enzymes of the CYP2C subfamily " Biochem Biophys Res Commun. 2005 Apr 22; 329(4): 1275-81
- Muller DN¹, Schmidt C¹, Barbosa-Sicard E, Wellner M, Gross V, Hercule H, **Markovic M**, Honeck H, Luft FC, Schunck WH: "Mouse Cyp4a Isoforms: Enzymatic Properties, Gender- and Strain-specific Expression, and Role in Renal 20-Hydroxyeicosatetraenoic Acid Formation" Biochem. J. 2006
- **Markovic M.** et al. " CYP-dependent metabolism of fish oil ω -3 fatty acids" in preparation

Awards:

- **Abstract Award** – National Institute of Environmental Health Sciences (NIEHS) Baltimore 2006
- **New Investigator Award-European Fellows** - Council for High Blood Pressure Research – San Antonio 2006
- **Abstract Award** – National Institute of Environmental Health Sciences (NIEHS) Baltimore 2007

Conferences:

- Barbosa Sicard E., Muller D. N., **Markovic M.**, Honeck H., Shagdarsuren E., Hercule H., Luft F.C., Schunck W-H (2003): " Cooperation of Rat Renal 4A12 & 2C in the Formation of Secunadary Arachidonic Acid Metabolites "Poster #

116, **57th Annual Fall Conference and Scientific Sessions of the Council for High Blood Pressure Research**, Washington; DC, USA

- Muller DN, Barbosa-Sicard E, Wellner M., Schmidt C., Honeck H., Hercule H., **Markovic M.**, Gross V., Luft F.C., Schunck W-H (2004): " Gender and strain - specific expression of Cyp4a isoforms and their role in mouse renal 20 – HETE production" Poster # 176, **58th Annual Fall Conference and Scientific Sessions of the Council for High Blood Pressure Research**, Washington; DC, USA
- **Markovic M.**, Schmidt C., Muller D.N., Luft F.C., Schunck W-H (2005): " Cytochrome P450-dependent Metabolism of Omega-3 Polyunsaturated Fatty Acids" Poster # 93, **59th Annual Fall Conference and Scientific Sessions of the Council for High Blood Pressure Research**, Washington; DC, USA
- **Markovic M.**, Schmidt C., Muller D.N., Luft F.C., Schunck W-H (2006): " Comparison of Omega-6 and Omega-3 Fatty Acids as Substrates for Cytochrome P450 Metabolism" Poster # 14, **8th Annual Winter Eicosanoid Conference**, Baltimore, USA
- **Markovic M.**, Schmidt C., Muller D.N., Luft F.C., Schunck W-H (2006): “ Metabolism of fish oil omega-3 fatty acids by Cytochrome P450 enzymes”, **16th International Symposium on Microsomes and Drug Oxidations**, Budapest, Hungary
- **Markovic M.**, Wallukat G., Schmidt C., Luft F.C., Muller D.N., Schunck W-H (2006): " Role of Cytochrome P450 Enzymes in Mediating Cardioprotective Effects of Omega-3 Fatty Acids" Poster # 93, **60th Annual Fall Conference and Scientific Sessions of the Council for High Blood Pressure Research**, San Antonio; TX, USA
- **Markovic M.**, Wallukat G., Schmidt C., Luft F.C., Muller D.N., Schunck W-H (2007) “Cytochrome P450-mediated anti-arrhythmic effects of omega-3 fatty acids in cardiac myocytes” **9th Annual Winter Eicosanoid Conference**, Baltimore, USA

7. Curriculum vitae

8. Eidesstattliche Erklärung

Berlin, den 08.08.2007

Hiermit versichere ich, die vorliegende Dissertation selbständig und ohne unerlaubte Hilfe angefertigt zu haben.

Bei der Verfassung der Dissertation wurden keine anderen als die im Text aufgeführten Hilfsmittel verwendet.

Ein Promotionsverfahren zu einem früheren Zeitpunkt an einer anderen Hochschule oder bei einem anderen Fachbereich wurde nicht beantragt.

Marija Markovic